CHEMICAL REVIEWS

pubs.acs.org/CR

Review

Root of the Tree: The Significance, Evolution, and Origins of the Ribosome

Jessica C. Bowman, Anton S. Petrov, Moran Frenkel-Pinter, Petar I. Penev, and Loren Dean Williams*

Cite This: https://dx.doi.org/10.1021/acs.chemrev.9b00742

Read Online

ACCESS | Metrics & More | Article Recommendations

ABSTRACT: The ribosome is an ancient molecular fossil that provides a telescope to the origins of life. Made from RNA and protein, the ribosome translates mRNA to coded protein in all living systems. Universality, economy, centrality and antiquity are ingrained in translation. The translation machinery dominates the set of genes that are shared as orthologues across the tree of life. The lineage of the translation system defines the universal tree of life. The function of a ribosome is to build ribosomes; to accomplish this task, ribosomes make ribosomal proteins, polymerases, enzymes, and signaling proteins. Every coded protein ever produced by life on Earth has passed through the exit tunnel, which is the birth canal of biology. During the root phase of the tree of life, before the last common ancestor of life (LUCA), exit tunnel evolution is dominant and unremitting. Protein folding coevolved with evolution of the exit tunnel. The ribosome shows that protein folding initiated with intrinsic disorder, supported through a short, primitive exit tunnel. Folding progressed to thermodynamically stable β-structures and then to kinetically trapped α-structures. The latter were enabled by a long, mature exit tunnel that partially offset the general thermodynamic tendency of all polypeptides to form β-sheets. RNA chaperoned the evolution of protein folding from the very beginning. The universal common core of the ribosome, with a mass of nearly 2 million Daltons, was finalized by LUCA. The ribosome entered stasis after LUCA and remained in that state for billions of years. Bacterial ribosomes never left stasis. Archaeal ribosomes have remained near stasis, except for the superphylum Asgard, which has accreted rRNA post LUCA. Eukaryotic ribosomes in some lineages appear to be logarithmically accreting rRNA over the last billion years. Ribosomal expansion in Asgard and Eukarya has been incremental and iterative, without substantial remodeling of pre-existing basal structures. The ribosome preserves information on its history.

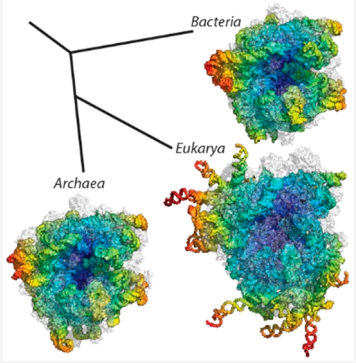

CONTENTS

Special Issue: Chemical Evolution and the Origins of Life

Received: November 18, 2019

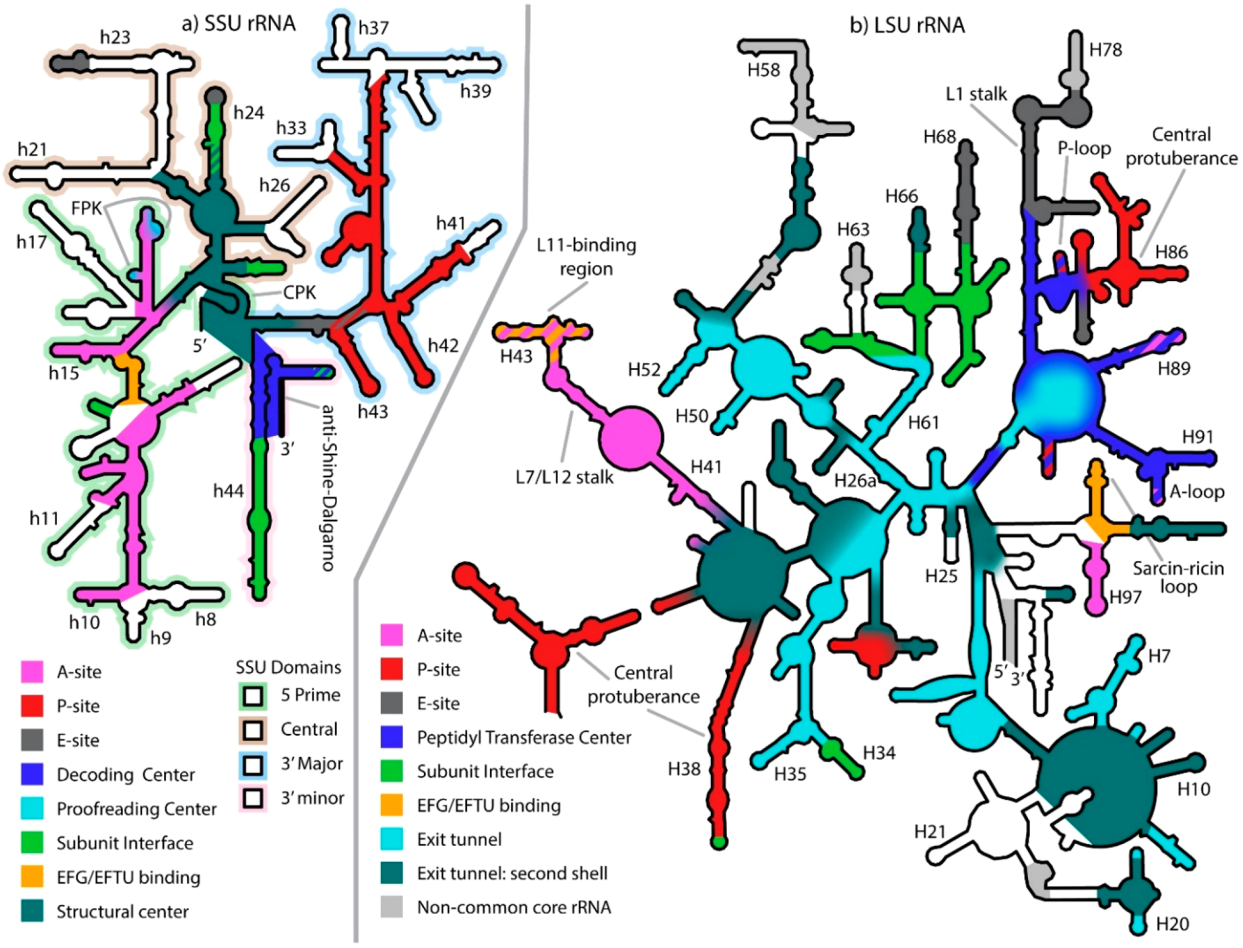

Figure 1. Functional regions of rRNA. (a) Information mapped onto the *E. coli* SSU rRNA secondary structure. CPK indicates the central pseudoknot; FPK is the functional pseudoknot. (b) Information mapped onto the *E. coli* LSU rRNA secondary structure. A plurality of LSU rRNA is assigned to the exit tunnel (cyan), indicating that it performs a principal function of the LSU. The second shell of the exit tunnel provides buttressing for the first shell of the exit tunnel. Regions of multiple function, for example, rRNA that contributes to both the A-site and the PTC, are striped with two colors. Strand termini and select helices are indicated. Domains are indicated on the SSU rRNA. Domains are not indicated on the LSU rRNA where they have no physical significance. Interactions with ribosomal proteins are not included.

1. INTRODUCTION

The partnership between RNA and protein dominates biology. The durability of this ancient partnership is documented in the universal tree of life (TOL), which is the lineage of the translation system. Woese and Fox[1,2] sketched out a universal TOL revealing the blueprint of the common origins and biochemical interrelatedness of all living systems. This TOL contains three primary branches, which are the bacterial, archaeal, and eukaryotic superkingdoms of life. More recent determinations of the TOL, using concatenated sequences of ribosomal proteins (rProteins), increased the resolution and accuracy of the tree.[3,4] TOLs now incorporate reconstructed genomes of unculturable organisms from a variety of environments.[5,6] In the most recent TOLs, eukarya branches from within archaea.[6,7] The last universal common ancestor of life (LUCA) lies at the first branch point of the TOL. Extant biology is the crown. The origin of life occurred within the root of the TOL. As a system to organize and frame vast amounts of information, the TOL is on par with the Periodic Table.

The ribosome, made from RNA and protein, is responsible for synthesizing all protein in living systems. The ribosome is composed of a small ribosomal subunit (SSU) that decodes mRNA and a large ribosomal subunit (LSU) that catalyzes peptidyl transfer. To make a protein, the ribosome initiates, interprets an mRNA codon (decodes), transfers an amino acid from a tRNA to a nascent peptide, translocates, repeats the last three of these steps over and over again, and ultimately

https://dx.doi.org/10.1021/acs.chemrev.9b00742
Chem. Rev. XXXX, XXX, XXX−XXX

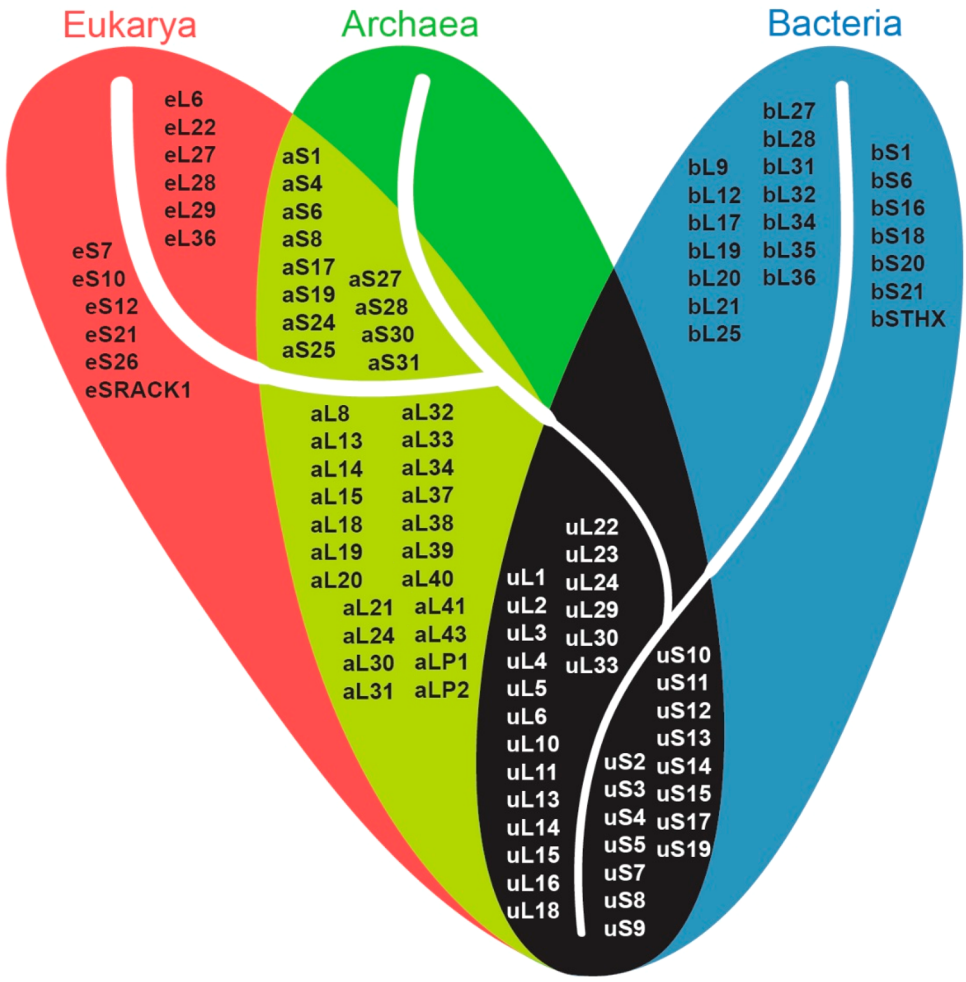

Figure 2. The Tree of Life mapped with universal and superkingdom-specific ribosomal proteins. The line width of the TOL is weighted by the total number of rProteins in a given superkingdom. Universal rProteins are listed in white text in the black region at the bottom. Bacteria-specific rProteins are in the blue region on the right, and Archaea-specific rProteins are in the lime-green region in the center. Eukarya-specific rProteins are in the red region on the left. All Archaea-specific rProteins are found in Eukarya, and thus, no rProteins are unique to Archaea. This rProtein nomenclature is consistent with the TOL; rProteins in Eukarya that are of archaeal ancestry are labeled as archaeal. This rProtein naming scheme, by incorporating evolutionary relationships into rProtein names, is intended to facilitate understanding of the evolution of the translation system. Adapted with permission from ref 16, where a dictionary of various rProtein naming schemes can be found. Copyright 2018 Springer.

terminates synthesis at an mRNA stop codon.[8−12] In Bacteria, new peptide bonds are formed at a rate of ∼20 amino acid additions per second. The functional core of the SSU is the decoding center (DCC) and the functional core of the LSU is the peptidyl transferase center (PTC). The distribution of ribosomal functions within rRNA secondary structures is shown in Figure 1. Aminoacyl-tRNA synthetases (aaRSs) enforce the genetic code by joining amino acids to their cognate tRNAs.

The translation system controls the sequence, amount, time, and place of protein synthesis. The profound significance of translation is indicated by its universality, economy, centrality, antiquity, and complexity. These attributes are explained below.

2. SIGNIFICANCE OF THE RIBOSOME

2.1. Universality of the Ribosome

Genes encoding the translation machinery dominate the universal gene set of life (UGSL),[13−15] which is the set of protein-encoding genes that are shared as orthologues throughout the TOL and are found in essentially every living system. Koonin's version of the UGSL contains around 65 genes.[14] Fifty-three of these are directly involved in translation, including 34 genes for rProteins (Figure 2) and genes for aaRSs and translation factors. The Pace[13] and Doolittle[15] versions of the UGSL are very similar to that of Koonin. The USGL is larger and even more translation-centric if it is expanded to include nontranslated genes such as those encoding rRNAs and tRNAs. A few constituents of the USGL are involved in transcription and even fewer in replication. There are no genes for metabolism, membrane biosynthesis or proton pumps in the UGSL.

The universality of translation across living systems extends beyond sequence homology to three-dimensional structures. Ribosomal and other translational components are universal in three-dimensions for all living systems (Figures 3, 4, and 5).[17−20] The extreme structural conservation of the DCC and the PTC[21−23] is illustrated in Figure 3. All ribosomes, from large bacterial to even larger archaeal ribosomes to gigantic mammalian ribosomes, are built upon the same basal structure, which we call the universal common core. The universal common core has a mass of nearly 2 million Daltons.[18,19]

https://dx.doi.org/10.1021/acs.chemrev.9b00742
Chem. Rev. XXXX, XXX, XXX−XXX

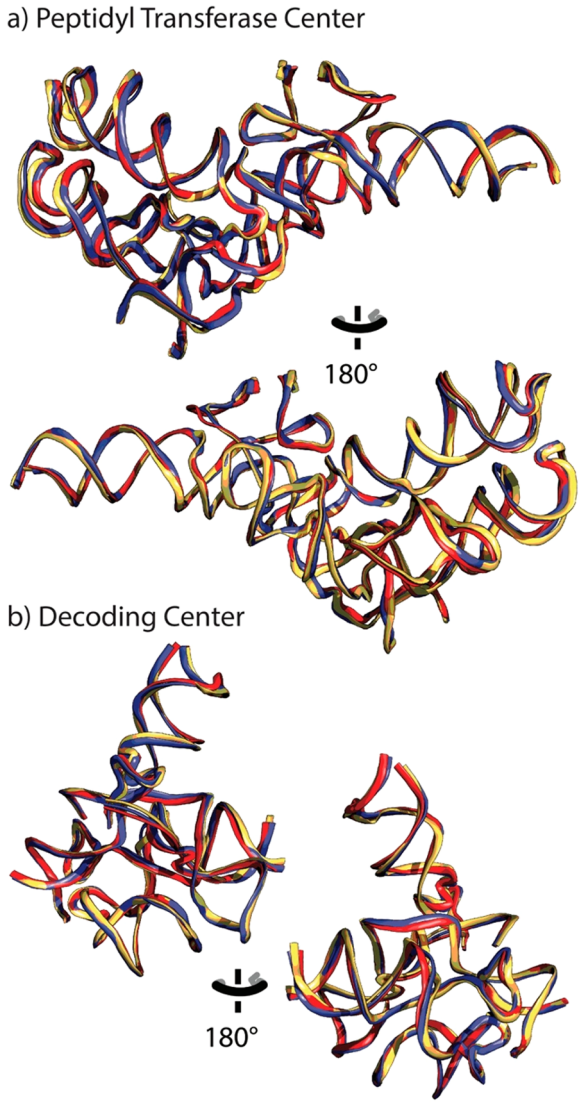

Figure 3. The functional cores of the ribosome are universally conserved in all living systems. rRNA backbone ribbons, extracted from superimposed ribosomes from each of the three superkingdoms of life. The bacterium (*Escherichia coli*) is red, the archaeon (*Pyrococcus furiosus*) is blue, and the eukaryote (*Saccharomyces cerevisiae*) is yellow. rRNAs superimposed are (a) the PTC (of the LSU) and (b) the DCC (of the SSU). Adapted with permission from ref 19. Copyright 2018 Oxford University Press.

The universal common core contains:

(a) 2800 nucleotides,
(b) the PTC,
(c) the exit tunnel excluding the vestibule,
(d) the subunit interfaces,
(e) the A, P, and E sites,
(f) the bulk of the tRNA translocation machinery,
(g) the GTPase-associated region,
(h) 19 LSU proteins,
(i) the DCC,
(j) essentially the entire SSU rRNA, and
(k) 15 SSU proteins, and excludes
(l) the anti-Shine−Dalgarno sequence that has been lost in eukaryotes, and
(m) several exterior helices of the bacterial ribosome.

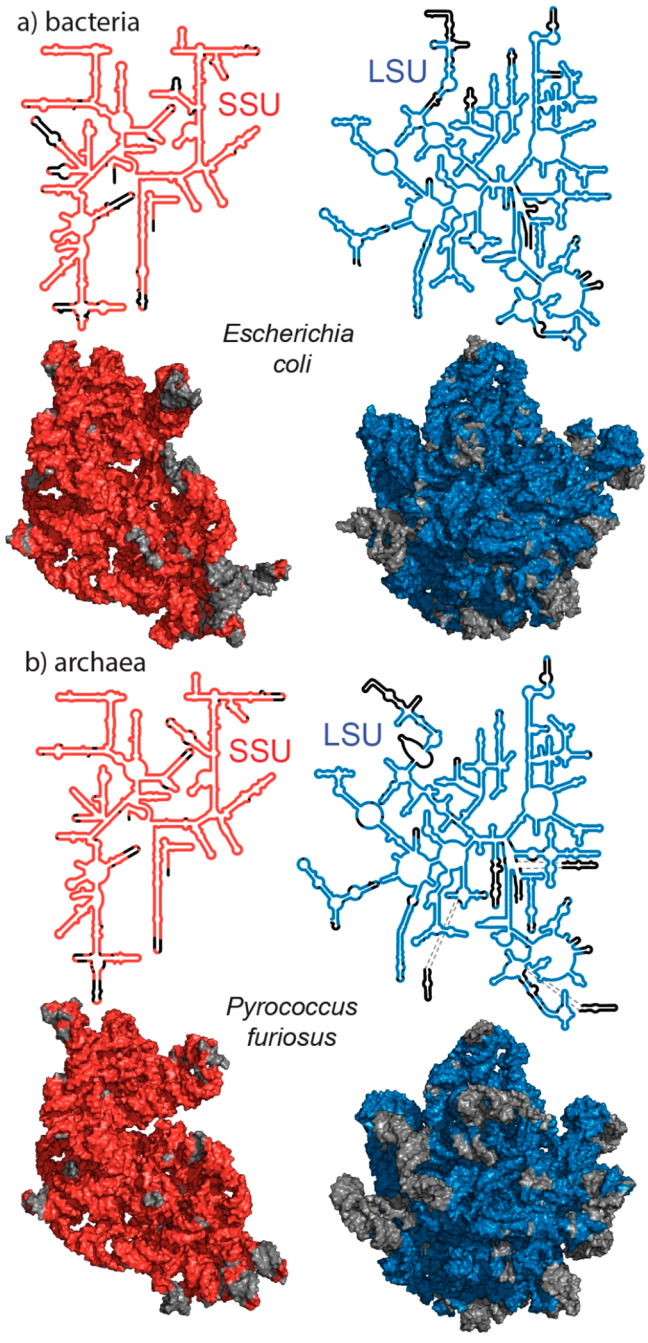

Figure 4. The universal common core of rRNA mapped onto the secondary and three-dimensional structures of rRNAs of a bacterium and an archaeon. The SSU (left) contains the 16S rRNA and the LSU (right) contains the 23S and 5S rRNAs. Red (SSU) and blue (LSU) indicate common core rRNA. Black or gray indicate rRNA that is not part of the common core and is variable in structure or absent from some species. (a) The rRNA of the bacterium *E. coli*. (b) The rRNA of the archaeon *P. furiosus*. Some sites of insertion of microexpansion segments are indicated by dashed lines in the archaeon secondary structure. Each three-dimensional structure is viewed from the solvent exposed surface of the assembled ribosome, with the subunit interface directed into the page. *E. coli*, PDB 4V9D, and *P. furiosus*, PDB 4V6U. Adapted with permission from ref 19. Copyright 2018 Oxford University Press.

Around 90% of bacterial rRNA and 62% of bacterial rProteins are contained within the universal common core. rProteins protect rRNA, provide structural buttressing within

https://dx.doi.org/10.1021/acs.chemrev.9b00742
Chem. Rev. XXXX, XXX, XXX−XXX

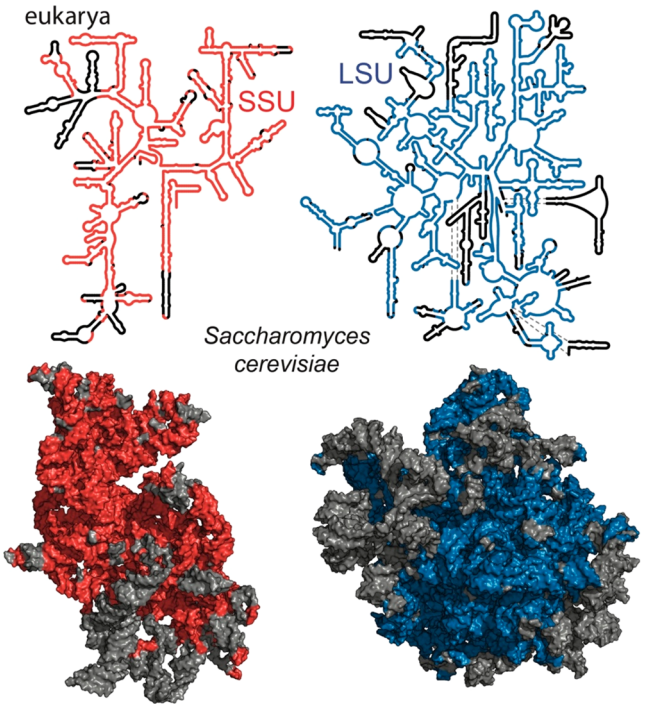

Figure 5. The universal common core mapped onto the secondary and three-dimensional structures of rRNAs of the eukaryote *S. cerevisiae*. The SSU (left) contains the 18S rRNA, and the LSU (right) contains the 26S, 5.8S, and 5S rRNAs. Red (SSU) and blue (LSU) indicate common core rRNA, as in the previous figure. Some sites of insertion of expansion segments are indicated by dashed lines. *S. cerevisiae*: PDB 4V88. Adapted with permission from ref 19. Copyright 2018 Oxford University Press.

the ribosome, and are targets of signaling kinases.[24−26] Some rProteins are essential for ribosomal function and assembly and influence association of the ribosome with mRNA, tRNAs, and translation factors. Bacteria, Archaea, and Eukarya each contain superkingdom-specific rProteins[16,27] in addition to those of the universal common core (Figure 2).

The basics of the translation system are preserved even in organisms with reduced genomes. Genomes were reduced over evolution in some obligate symbiotic and pathogenic Bacteria[28,29] and in obligate eukaryotic parasites.[30] Translation systems in these organisms were reduced in parallel with reduction of genomes.

In organisms with extremely tiny genomes, such as microsporidia, rRNA is reduced beyond the universally conserved core.[30−33] In these eukaryotic parasites, rRNA can be ∼25% smaller than that of *Escherichia coli*. However, microsporidia ribosomes have preserved core functional centers, exit tunnels, subunit interfaces, and most ribosome ligand-binding sites. Reduced genomes retain at least one tRNA gene for each amino acid, even though the total number of tRNA genes is reduced. rProteins are among the last to depart a shrinking genome.[34] Therefore, eukaryotic translation systems regress during genome reduction but reach a hard plateau in size and structure. There appears to be a minimum size of cytosolic ribosomal components, which cannot be violated.

Variability of ribosomes may confer significant adaptive capacity. It is thought that ribosomes in vivo are heterogeneous. "Specialized" ribosomes within a given cell or tissue might contain or lack specific rProteins and/or rRNA paralogues that impact ribosomal function.[35−38] Substoichiometry of nucleotide modifications might cause differential ribosomal function.[39] In zebrafish embryos, down-regulation of various rProteins produces specific brain phenotypes.[40]

The ribosome is robust in structure and resilient in function. The ribosome "idles", in the absence of elongation factors, sampling the conformational trajectory of the elongation cycle.[41,42] The ribosome maintains function after severe reduction by molecular or biochemical methods. Nearly half of bacterial rProteins are dispensable in vivo.[43−45] Only 24 of the 139 rProtein paralogues in the Yeast Genome Database (yeastgenome.org) are essential for survival (Santi Mestre-Fos, personal communication). The LSU can catalyze peptide bond formation in vitro in the absence of the SSU,[46,47] even after treatment with proteases and detergents.[48] Protein synthesis can initiate in vitro without initiation factors.[49] Aminoacyl-tRNAs can bind to the ribosome in the absence of elongation factor EF-Tu.[50] Translocation of tRNA can occur without EF-G and GTP hydrolysis.[51−53] The ribosome is very hard to kill.

2.2. Economy of the Ribosome

The function of a ribosome is to build more ribosomes. Ribosomes make rProteins. Ribosomes make the polymerases that synthesize rRNA, tRNA, and mRNA. Ribosomes make the enzymes that synthesize and import amino acid and nucleotide building blocks of the ribosome. Ribosomes make the enzymes and machines that provide energy for biosynthesis of these building blocks. Ribosomes make the signaling proteins that regulate, coordinate, and otherwise enable all of these systems.

Translation is the largest consumer of cellular resources, defining biological demand and productivity.[54,55] Ribosomal production is limiting.[56,57] The high rRNA/rProtein ratio of ribosomes compared to other enzymatic systems appears to be dictated by faster and energetically cheaper synthesis of RNA than protein.

Bacterial biogenesis of ribosomes requires linkage and synchronization of (i) rRNA transcription, processing, and modification, (ii) rProtein translation and modification, (iii) rRNA and rProtein folding and assembly, and (iv) binding and release of assembly factors (see Nierhaus,[24,58] Nomura,[59] Williamson,[60] and Woodson[61]). The SSU is composed of well-defined domains that can be independently assembled. The LSU is monolithic and entangled and composed of a greater number of components, which is associated with a more complex and demanding assembly processes.

Ribosome biogenesis in eukaryotes, which takes place in the nucleolus, is the most complex task of a replicating cell;[62] cell replication is restrained by the rate and cost of production of ribosomes.[63] The demands of ribosomal biogenesis are high. All three RNA polymerases (I, II, and III) are involved in ribosome production. Rapidly growing *Saccharomyces cerevisiae* devotes 60% of transcription to rRNA and 15% to rProtein.[64] Fifty percent of RNA polymerase II is devoted to transcription of rProteins, which absorb 90% of mRNA splicing activity. Around 30% of RNA polymerase III is dedicated to transcription of 5S rRNA and mitochondrial RNA processing. In *S. cerevisiae*, around 200 different assembly factors and 75 snoRNAs are dedicated to assembling around 200 000 ribosomes per generation at a rate of 40 ribosomes per second.[65] Dedicated and specific chaperones coordinate rProtein folding, import into the nucleus, and incorporation into preribosomes.[66−69] Specific LSU and SSU exporters deliver nearly mature ribosomes to the cytosol.[70]

https://dx.doi.org/10.1021/acs.chemrev.9b00742
Chem. Rev. XXXX, XXX, XXX−XXX

Ribosomal assembly in mammals is far more complex than in protists, requiring nearly twice as many factors,[71,72] generating around 1 million ribosomes per generation per cell.[73] It appears that some ribosomes are remodeled outside the nucleolus. rProteins produced by translation in neuronal axons are incorporated on-site into local ribosomes.[74]

Around 200 000 ribosomes in *S. cerevisiae* are available to translate 15 000 mRNAs.[75] Global levels of transcription by RNA polymerase II are tightly linked to the capacity of the translation system.[75] Around 30% of translation is devoted to rProtein production.[76]

The ribosome content of Bacteria[76,77] and *S. cerevisiae*[78] increases linearly with growth rate under a broad variety of conditions. Ribosome production is precisely coordinated with other cellular functions. Synthesis of excess rProteins can reduce the availability of metabolic proteins and amino acids, negatively impacting the rate of translation and cell growth.[79] In mammalian cells, around 30% of oxygen consumption is used for protein synthesis.[80]

Ribosomes are densely packed in the cytosol. The molecular crowding of bacterial cytosol arises mainly from ribosomal contributions.[81] The density of ribosomes in a small bacterium[82] can be seen in Figure 6. The number of ribosomes

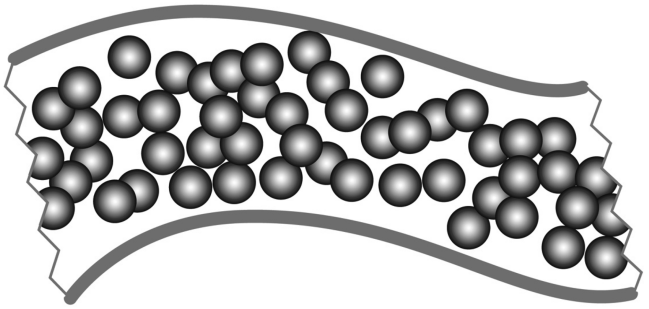

Figure 6. Ribosomes are crowded in the bacterial cytosol. Schematic of ribosomes (spheres) within *Spiroplasma melliferum* as seen by cryo-electron tomography, illustrating the abundance of ribosomal particles in vivo. Adapted with permission from ref 82. Copyright 2006 Elsevier.

in a bacterial cell scales linearly with cell volume over a large range of volumes.[83] An upper volume limit is established by the "ribosome catastrophe", where the required volume of ribosomes exceeds the volume of the cell.

2.3. Centrality of the Ribosome

The universal gene set of life, the antiquity and economy of the ribosome, along with the Central Dogma,[84] suggest that the ribosome is a nexus of biology on several levels. In fact, the 20 000−10 000 000 ribosomes per cell constitute around $^1/_3$ of the dry cellular mass. Around 85% of cellular RNA is rRNA by mass. rRNAs and rProteins are the most abundant biological macromolecules in the biological universe.[82,85,86]

Systems that interact directly with translating ribosomes are *within one degree of separation* from the ribosome. Systems that interact with those within one degree of separation from the ribosome are *within two degrees of separation* from the ribosome. Most biological processes are within one or two degrees of separation from the ribosome (Figure 7). Every aspect of biology is impacted directly or indirectly by translation.

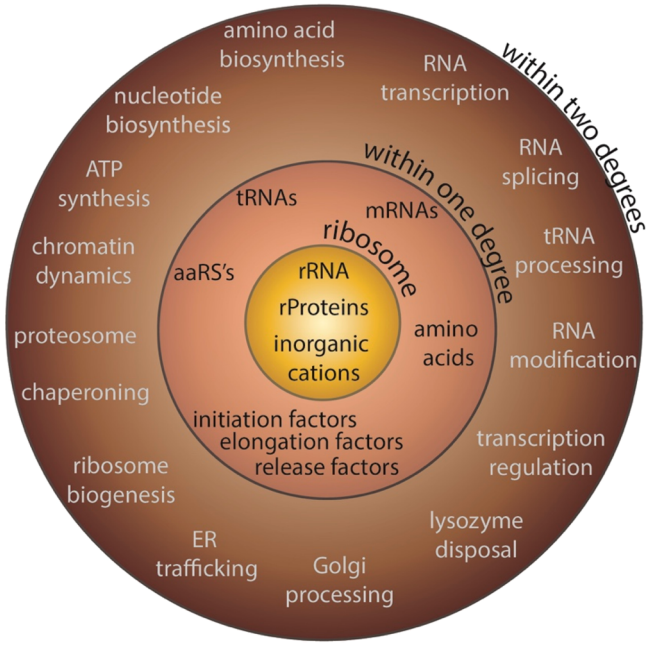

Figure 7. Translation is the hub of life. tRNA, mRNA, and aaRSs are within one degree of separation from the ribosome. A large number of additional cellular systems are within two degrees of separation from the ribosome.

Initiation, elongation and release factors, tRNAs, mRNAs, amino acids, and aaRSs are within one degree of separation from the ribosome. Systems that produce and regulate production of RNA, assemble and evaluate ribosomes and nascent polypeptide, modify or process tRNAs, rRNAs and mRNAs, read RNA modifications, and synthesize amino acids are *within two degrees of separation* from the ribosome. Because translation is a primary consumer of energetic resources, ATP synthases and other metabolic systems are within two degrees of separation from the ribosome.

The centrality of translation is documented in the interactomes of prokaryotes[87,88] and eukaryotes.[89−92] Many types of cytosolic proteins physically interact with one or more components of the translation system.[93] By this measure, first degree of separation components account for 5−15% of all protein−protein interactions. Second degree of separation components account for approximately 35% of additional interactions.[88]

rProteins have important functions outside of the ribosome[94,95] as expected from their abundance, antiquity, universality, and ability to bind to RNA. Many extra-ribosomal functions of rProteins involve regulation of rProtein production or ribosomal quality control. *E. coli* operons encoding rProteins are under autogenous control; one of the rProteins encoded in the operon is a repressor, primarily at the level of translation, of most or all of the genes in the operon.[96,97] rProtein L4 in *E. coli* regulates RNA degradation by allosteric control of RNase E.[98] In eukaryotes, rProteins help regulate cell differentiation[99,100] and proliferation,[101,102] DNA repair,[103,104] and apoptosis.[105−108] If aberrant ribosomal assembly increases levels of free rProteins uL5, uL11, and uL14 above a threshold, they associate with the protein MDM2, inhibiting p53 degradation and causing cell cycle arrest or apoptosis.

https://dx.doi.org/10.1021/acs.chemrev.9b00742
Chem. Rev. XXXX, XXX, XXX−XXX

2.4. Antiquity of the Ribosome

Translation is the oldest existing biological system. The universal common core of the ribosome was finalized around 3.8−4.2 billion years ago.[109,110] The universal common core of the LSU can be modeled as an onion.[17] The central region of the onion, near the PTC, appears older than the surface elements, which are remote from the PTC. This is especially true for rRNA; some ribosomal proteins continue to evolve and diverge even in the central region of the onion.[31,111] The central components of the ribosome predate LUCA[17,21−23,109,110,112−123] and arose during the root phase of the TOL. In robustness and longevity, the ribosome is competitive with the Earth's oldest minerals.[124,125]

2.4.1. The Ribosome at LUCA. Translation was fully mature at LUCA. LUCA was not the first organism or the first cell and does not represent the origin of life. Rather, LUCA was the last type of microbe, or the last diverse population of microbes, before the divergence of Bacteria from Archaea.[126,127] A variety of models of the nature of LUCA have been proposed. Inferences about the ribosome of LUCA here are not dependent on a specific model for LUCA.

The size of the rRNA of LUCA was estimated by two independent methods that give similar results.[19] The first method assumes that LUCA contains all rRNA that is universally conserved in structure, as determined using a carefully curated database that efficiently samples extant phylogeny. A second approach uses an ancestral reconstruction, iteratively stepping back through the TOL, estimating the sizes of ancestral rRNAs at each node using the assumption that the most probable ancestral state contains rRNA whose sequences align in both daughter species. Nonsuperimposing nucleotides are assumed to be nonancestral. This sequence-based method will modestly underestimate sizes of ancestral rRNAs because in some cases ancestral rRNA elements are lost in one daughter. Nevertheless, the ancestral reconstruction gives LUCA rRNA sizes only ∼10% smaller than those estimated by universal conservation.

Our ancestral reconstruction of rRNA incorporates the assumption that the most probable ancestral ribosomes contain only rRNA elements that are common to daughter species; the most conservative changes are considered to be the most likely changes. The universality of ribosomal functional centers deep within the ribosomal onion suggests that rRNA does not remodel once it is established. Foundational rRNAs are structurally conserved during a multibillion-year evolutionary process from the root of the TOL to extant biology. As a general pattern, the more complex daughter organism is, the larger ribosome it contains. The combined data are consistent with a monophyletic origin of life; only one set of rRNAs and one genetic code survived.

Bacteria contain 21 rProteins that are absent from Archaea, which contain 34 proteins that are absent from Bacteria (Figure 2). In some instances, universal rRNA interacts directly with proteins that are not universal. It seems likely that some remodeling of rProteins occurred after rRNA was finalized. A TOL computed from rRNA shows three distinct superkingdoms (Bacteria, Archaea, and Eukarya), whereas a TOL computed from concatenated rProteins shows Eukarya as a sub-branch of Archaea.

2.4.2. Metals in the Ribosome at LUCA. Mg^{2+} appears to be the dominant cofactor for RNA in extant systems. Mg^{2+} interacts with RNA by continuum of modes[17,128−131] that we call condensed, glassy, and chelated.[132] Mg^{2+} ions mediate ribosomal assembly,[133,134] help maintain the reading frame during translation,[135,136] link rProteins to rRNA,[137] stabilize folded tRNA,[138] and are required for catalysis by aaRSs.[139]

Ribosomes originated and matured well before the Great Oxidation Event (GOE), therefore ribosomal origins and evolution were shaped by metal cations under pre-GOE conditions. General anoxia before the GOE would have fostered abundant soluble Fe^{2+} in the biosphere and hydrosphere.[140−142] Pre-GOE conditions would have precluded extant-style precipitation of iron as Fe^{3+} and oxidative damage to ribosomes via Fenton chemistry.[143] Fe^{2+} appears to be a potent all-around cofactor for nucleic acids in the absence of oxygen. It seems unavoidable that pre-GOE ribosomes interacted extensively with Fe^{2+} instead of, or in combination with, Mg^{2+} and other divalent ions. Indeed, recent results indicate that

(a) rRNA folds at lower concentration of Fe^{2+} than Mg^{2+},[144]
(b) the translation system is functional when Fe^{2+} is the dominant divalent cation,[144]
(c) Fe^{2+}, like Mg^{2+}, can form ribosomal microclusters, which contain paired metals bridged by a single phosphate group,[145,146] and
(d) Fe^{2+} confers oxidoreductase catalytic functionality to rRNAs.[145,147]

2.5. Divergence of the Ribosome

Although many features of the translation system are highly conserved among the three superkingdoms of life, there is significant variation in some aspects of the ribosome.[19,113] This divergence includes structure and function. Expansion segments (ESs) are rRNA regions that are especially variable over phylogeny. In eukaryotes, they appear as rRNA helices that have grown well beyond the common core rRNA. Humans have some of the longest ESs. Artificially introduced eukaryotic-like ESs are tolerated in *E. coli*.[148]

Some of the most fundamental differences in ribosome function center on the initiation of translation. To initiate translation in Bacteria or Archaea, most commonly an AUG start codon pairs with the anticodon of a methionyl initiator tRNA (Met-tRNAi),[149,150] but only after the anti-Shine−Dalgarno sequence of the SSU rRNA anneals with the Shine−Dalgarno sequence on mRNA. However, the anti-Shine−Dalgarno sequence is not part of the universal common core and has been lost from eukaryotic lineages. As discovered by Kozac, the start codon on the mRNA in eukaryotes is pinpointed by scanning the 5′ untranslated region for complementarity with the anticodon of Met-tRNAi.[151−153]

2.5.1. rRNA Variation: Rules of the Road.

(a) rRNA size generally tends to increase in the order: eukaryotic obligate pathogens and symbionts < common core < Bacteria < Archaea < protists and plants < Metazoa,[18,19,113]
(b) rRNA size variation is greater among Eukaryotes than among either Bacteria or Archaea,[154−161]
(c) rRNAs of bacterial pathogens are slightly larger (∼100 nucleotides larger) than those of other Bacteria,
(d) rRNA size variability is focused on expansions at few specific sites on common core rRNA,[154−161]
(e) variability of Archaea foreshadows greater variability of eukaryotes; microexpansion segments (μESs) of 5−20 nucleotides in many archaeal rRNAs are observed at sites of larger eukaryotic ESs,

https://dx.doi.org/10.1021/acs.chemrev.9b00742
Chem. Rev. XXXX, XXX, XXX−XXX

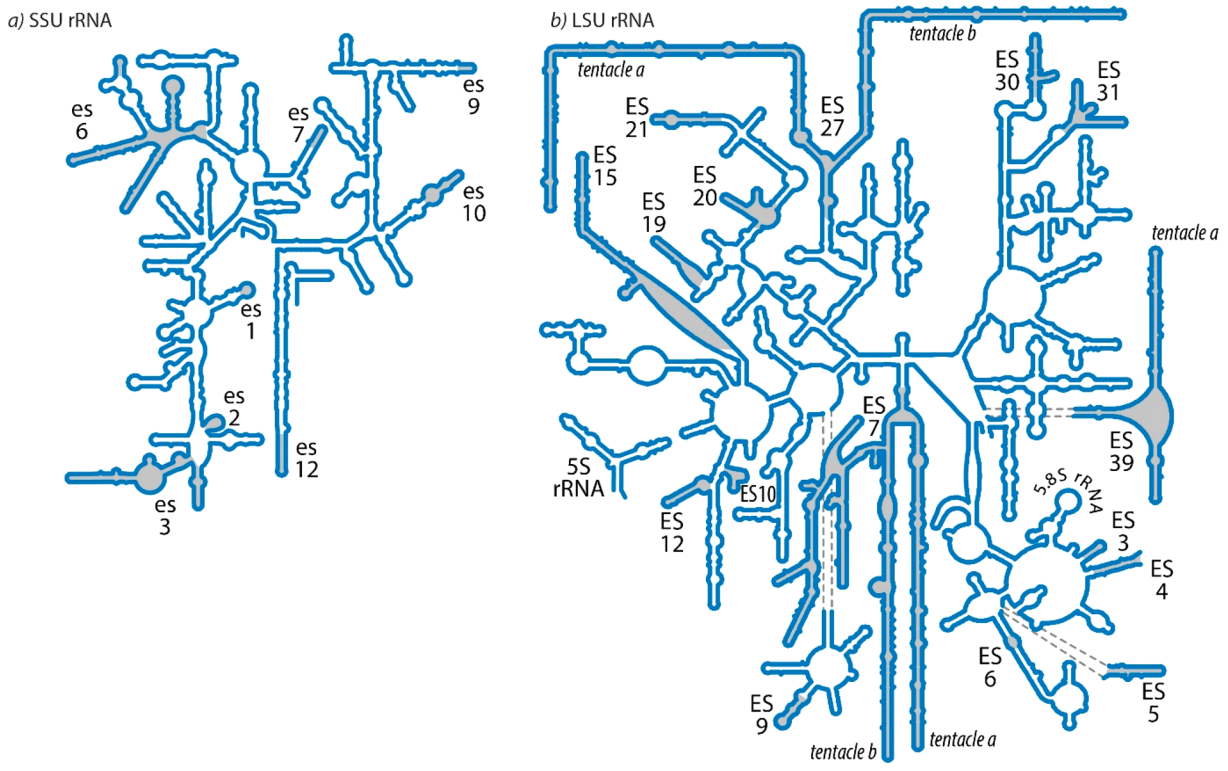

Figure 8. Secondary structures of the SSU (a) and the LSU (b) rRNA of *H. sapiens*. ESs are shaded and numbered. Tentacles, which are seen exclusively on the LSUs of birds and mammals, are labeled *tentacle a* or *tentacle b* in ES7, ES27, and ES39. This figure was created by Petar Penev and Sara Fakhretaha Aval.

(f) some Asgard Archaea have large ESs which rival eukaryotic ESs in size,[162]

(g) ES's of bird and mammal ribosomes contain elongated GC-rich rRNA tentacles[18,163,164] that are hundreds of Ångstroms in length,

(h) SSU rRNA is far more constrained than LSU rRNA and size variation is significantly greater in LSU rRNAs than in SSU rRNAs,[19,155]

(i) ESs are excluded from the subunit interiors and from functional regions of the rRNA such as the PTC, the DCC, the subunit interface, the exit tunnel, and tRNA binding sites,[163,165]

(j) some functional ribosomes contain highly fragmented rRNAs,[166] and

(k) net rRNA size generally increases with organismal complexity.[19,113]

All four classes of introns (group I, group II, spliceosomal, and archaeal) are found in SSU and LSU genes. Introns appear to be focused within the most ancient regions of rRNA transcripts and are seen in all superkingdoms of life. It has been suggested that the evolutionary histories of rRNAs and introns are linked.[167]

Diverse archaeal and eukaryotic tRNA primary transcripts also contain introns.[168] Introns in both rRNA and tRNA transcripts form a secondary RNA structure known as bulge–helix–bulge motif. This motif is excised by a splicing endonuclease in both Archaea and Eukarya.[169] Conservation of intron sequences in different tRNA genes within a given archaeal lineage suggests rapid and specific gain of introns.[170] It has been proposed that introns are remnants of invasions of conjugative plasmids or viruses.[171] Conserved splicing mechanisms suggest a strong evolutionary linkage between archaeal RNAs and processing enzymes.[172,173]

2.5.2. The Ribosome of Bacteria. Bacterial rRNA is on average around 100 nucleotides larger than the common core. For example, the LSU rRNA of *E. coli* is 2904 nucleotides in length (common core is 2800 nucleotides). Lengths of bacterial rRNAs are tightly clustered over phylogeny and, except for pathogens, rarely diverge by more than 150 nucleotides from that of *E. coli*. Bacterial ribosomes are slightly smaller, simpler, and less diverse than archaeal ribosomes, which on average are considerably smaller, simpler, and less diverse than eukaryotic ribosomes (Figures 4 and 5), which are highly variable over phylogeny.

The evolution of the ribosome has been discontinuous. The ribosome gained mass quickly between the origins of life and LUCA, then entered stasis and remained in that state for several billion years. Bacterial ribosomes never left stasis. Archaeal ribosomes have remained near stasis, except for the superphylum Asgard,[174] which has accreted mass post LUCA. Eukaryotic ribosomes of some lineages appear to have been gaining rRNA logarithmically over the last billion years.

2.5.3. The Ribosome of Archaea. Our analysis of rRNAs indicates that the roots of eukarya extend deep into the archaeal superkingdom. Archaeal rRNAs on average are slightly larger than bacterial rRNAs. The LSU rRNA of *P. furiosus* (an archaeon) is 248 nucleotides larger than common core rRNA. The difference in size is centered on archaeal-specific μ-ESs. μ-ESs are stem loops, generally of less than 20 nt, inserted onto the surface of the common core of archaeal rRNA. μ-ES insertion sites in Archaea predict ES insertion sites in Eukarya. μ-ES locations are conserved and exclude regions near functional centers such as the DCC, the PTC and the subunit

https://dx.doi.org/10.1021/acs.chemrev.9b00742
Chem. Rev. XXXX, XXX, XXX–XXX

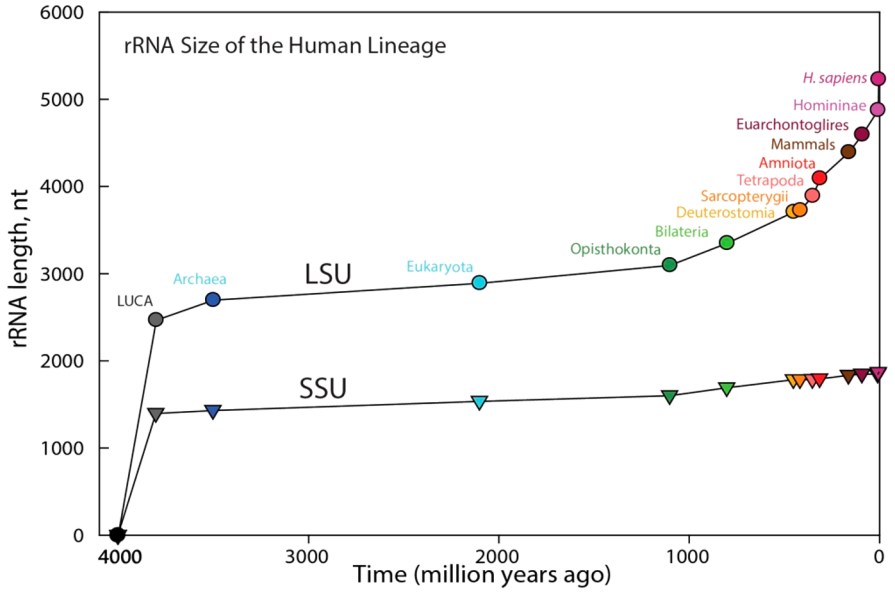

Figure 9. Size-evolution of the LSU and SSU rRNAs of the human lineage. Estimated dates of ancestors are from Hedge.[181] SSU rRNA sizes are nearly constant from LUCA through extant species. Sizes of ancestral rRNAs are estimated using the assumption that the most probable ancestral rRNAs contain rRNAs whose sequences align in daughter species. Nonaligning nucleotides are assumed to be nonancestral. This sequence-based method will modestly underestimate sizes of ancestral rRNAs in part because sequence is less conserved than structure. The origin of the ribosome is around 4000 million years ago. Adapted with permission from ref 19. Copyright 2018 Oxford University Press.

interface. The number of μ-ES insertion sites is small (around 10 on the LSU and 8 on the SSU). μ-ESs on the LSU are generally larger than those on the SSU.

The largest archaeal expansions, and largest archaeal rRNAs, are found in *Lokiarchaeota* and *Heimdallarchaeota* within the Asgard superphylum.[162] In size and complexity, some ESs of *Lokiarchaeota* and *Heimdallarchaeota* exceed those of protists rRNAs and rival those of metazoan rRNAs. Asgard Archaea contain a variety of eukaryotic signature proteins that are involved in cytoskeleton, trafficking, ubiquitination, and translation.[175]

2.5.4. The Ribosome of Eukaryotes. Although the universal common core is shared by essentially all cytosolic ribosomes, eukaryotic ribosomes are much larger than the common core, with more complex structures and functions.[18,176−178] *S. cerevisiae* (a eukaryote) LSU rRNA is 754 nucleotides larger than common core rRNA. *Drosophila melanogaster* LSU rRNA is 1277 nucleotides larger than common core rRNA. *Homo sapiens* LSU rRNA is 2424 nucleotides larger than common core rRNA. Eukaryotic ESs attach at several universally conserved sites on the subunit surfaces.[154−161] Sites of insertion are the same for eukaryotic ESs and archaeal μ-ESs.

Most of the diversity of eukaryotic rRNA is focused on the LSU.[19] The LSU of protists contains a secondary shell of RNA and protein surrounding the common core.[18,163] *H. sapiens* and other endothermic vertebrates contain rRNA "tentacles" (or long ESs), which are helical structures that attach to a protist-like base[18,19,163,164] and extend for hundreds of Ångstroms from the ribosomal surface. As shown in the secondary structure in Figure 8, these rRNA tentacles contain defects such as bulges and mismatches. The tentacles are not integrated into the ribosomal surface and appear to be dynamic and/or positionally disordered within the cytosol. The tentacles of mammals and birds contain repeated G-tracts and have been observed to form extremely stable G-quadruplexes in vitro.[164,179]

Around 2000 million years ago, ribosomes in eukaryotic lineages emerged from stasis and entered a dynamic phase of growth, which remains ongoing and is accelerating in some metazoan lineages.[19] The LSU of the *H. sapiens* lineage is an extreme example of discontinuous growth (Figure 9). In the *H. sapiens* lineage, the ribosome was essentially static from LUCA through the advent of protists, when a secondary shell of rRNA and eukaryotic proteins was acquired by the LSU.[18] From the dawn of multicellularity to the rise of vertebrates, the LSU rRNA in the *H. sapiens* lineage grew by 0.65 nucleotides per million years.[19] With the rise of endothermic vertebrates, the growth rate accelerated to 2.5 nucleotides per million years. Currently the growth rate of the LSU rRNA in the *H. sapiens* lineage appears to be extremely rapid: 62 nucleotides per million years. The ribosome confirms Gould's observation[180] that the upper bound of complexity of life on Earth has been pushed upward as the average complexity has barely increased since LUCA.

Different regions of rRNA evolve at different rates, leaving "islands" of conservation in multiple sequence alignments.[32] In addition, the rates of evolution of the ribosomal subunits differ; SSU rRNAs are among the slowest evolving sequences in biology, making the SSU useful for revealing divergences in the Precambrian (from Earth's origin to 541 million years ago, roughly the start of the Cambrian animal diversification).[32] Similarly, variation in the rates of evolution of the different domains of the LSU make it more useful for divergence events of the Paleozoic and Mesozoic (541−66 million years ago, roughly diversification of early animals through the extinction of dinosaurs), and the rapidly evolving mitochondrial subunit rRNAs are useful for divergences of the Cenozoic (66 Ma to present). While these observations do not imply relative ages of ribosomal subunits, they are consistent with more

https://dx.doi.org/10.1021/acs.chemrev.9b00742
Chem. Rev. XXXX, XXX, XXX−XXX

pronounced size evolution of LSU rRNA than SSU rRNA over the last two billion years (Figure 9).

Why does rRNA grow ever larger in some eukaryotic lineages, especially in endothermic vertebrates? Why is accretion focused almost exclusively on LSU rRNA,[19] while the SSU rRNA is more highly restrained and remains nearly static? We do not know. A natural assumption is that ESs and es's are directly adaptive in complex organisms, conferring immediate advantage in docking, trafficking, quality control, chaperoning, or biogenesis. However, this assumption is unlikely to be correct.[182,183] To paraphrase Lynch, nucleic acid sequences with weakly advantageous or even transiently disadvantageous phenotypes can colonize genomes of species with large cells and small populations.[57] Many eukaryotes are extremely inefficient at eliminating nontranslated sequences.[184] Nonadaptive rRNA ESs and intervening sequences are expected to proliferate in the permissive eukaryotic environment of small populations, slow replication, and large cells; expansions would be eliminated by selection in large, rapidly replicating populations characteristic of protists and prokaryotes. In this model, large eukaryotic ESs and tentacles have been locked in by gain of function subsequent to rRNA expansion. It seems likely that complexity of the ribosome is influenced by the same forces that shape complexity of genome architecture in eukaryotes.

2.5.5. The Ribosome of Organelles. Organellar ribosomes are of bacterial origins but are products of unique evolutionary pressures and biochemical environments.[185−187] Genes for rRNAs are retained in organelle genomes (except for the 5S rRNA in many mitochondria) and exhibit large ranges in size and extent of fragmentation, while genes for organellar rProteins are most commonly encoded in the nucleus.[188−190] Organellar ribosomes can contain reduced rRNAs that are compensated by organelle-specific rProteins.[191,192] The PTC, DCC, and subunit interfaces are conserved in organellar ribosomes, while the central protuberance and the exit tunnel can be remodeled.[193,194] Mitochondrial ribosomes are more derived than plastid ribosomes. Harvey and Gutell generated the first three-dimensional models of mitoribosomal particles.[195] We do not include organellar ribosomes in our comparative analysis of cytosolic ribosomes and exclude them when defining the common core and rRNA rules of the road.

3. EVOLUTION OF THE RIBOSOME: READING THE TAPE OF LIFE

3.1. rRNA Structure in Two Dimensions

It was demonstrated in 1975 that nucleotides in base pairs covary in aligned 5S rRNA sequences.[196] For paired nucleotides, the unit of structure is the base pair. For unpaired nucleotides, the unit of structure is the nucleotide. Thus, base pairs of rRNAs are revealed by sequence alignments. Using this phenomenon, Gutell, Noller, Woese, and co-workers began predicting secondary structures and tertiary interactions of 16S and 23S rRNAs[197−200] in the early 1980s, two decades before the first X-ray structure of a ribosome was published.

As rRNA sequence databases expanded, co-variation methods were refined.[201,202] Once secondary structures were established, comparisons soon revealed the common core of rRNA and elaborations by eukaryotic ESs.[154−161] Comparison with 3D X-ray structures[203,204] demonstrated that covariation is an excellent although not perfect predictor of rRNA secondary structure.[200] Recurrent primary and secondary structures form building block motifs that organize into three-dimensional structure of RNA.[205−207] Most recently, we have published secondary structures of rRNAs based entirely on 3D structures,[208,209] correcting some historical artifacts.

3.2. rRNA Evolution in Three Dimensions

Using comparative methods that incorporate information from two- and three-dimensional structures, we have developed a comprehensive data-driven model of evolution of the ribosome (the accretion model).[17,19,113−115] The availability of X-ray and Cryo-EM ribosomal structures from a variety of species at the atomic level[135,163,165,193,203,204,210−217] enabled our approach, which required new tools for structural comparison and visualization[218] and for sequence comparison.[19]

The combined data support discontinuous accretion of ribosomal structure and function over deep time. By accretion, we mean that, on average, the ribosome has expanded incrementally and iteratively without substantial remodeling pre-existing basal structures.

Systems that accrete record their own history. Oak trees grow by accretion, maintaining historical records of weather, infestation, and fires.[219] Similarly, the ribosome has recorded its long history by accreting rRNA, rProteins, and inorganic cations. Accretion allows inference of key molecular steps in the evolution of rRNA and rProteins and in conformations, interactions, and functions.

The accretion model of the ribosome initiates during the root phase of the TOL, before LUCA, continues through the primary branching nodes of the tree and culminates in the crown, in extant biology. The model links chemical evolution at the dawn of life to Darwinian evolution and the Central Dogma of Molecular Biology. The model has implications for origins of ancillary processes such as replication, transcription, and metabolism but thus far does not incorporate them explicitly. The model is constrained by hard data from the translation system and does not link to conventional origin of life models such as the RNA World.

The model assumes uniformitarianism;[220] the same type of processes have dominated ribosomal evolution over deep time and in extant biology. The forces that shaped the translation system are the same in extant biology as during LUCA; the invention of special or extraordinary processes is not required. This assumption is the simplest and therefore appears to be most probable.

The approach is translation-centric; we favor the idea that coevolution of RNA and protein was accomplished in the context of the ribosome, which we consider to be the cradle of evolution. Protopeptides, then polypeptides and proteins, were created by the ribosome, on the ribosome, and for the ribosome. The model assumes the ribosome was selfish, gaining self-advantage in gradual, incremental, and correlated processes.

The acute modularity of ribosomal structure and function is a useful asset. Functions within the ancestral ribosome are determined by correspondence with their functions in extant ribosomes. Structures formed prior to acquisition of the subunit interface are termed "protoribosomes". The proto-LSU was capable of facilitating the production of noncoded protopeptide and ultimately of catalyzing synthesis of protopeptide. The accretion model is amenable to computational and experimental hypothesis testing and recapitulation of key steps.

https://dx.doi.org/10.1021/acs.chemrev.9b00742
Chem. Rev. XXXX, XXX, XXX−XXX

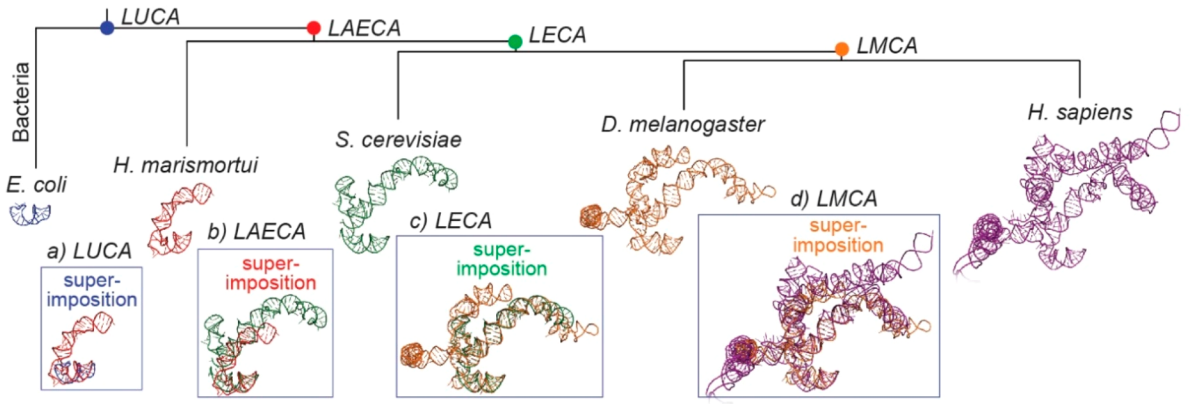

Figure 10. The evolution of ES7 by accretion. We assume that the most probable ancestral state has characteristics common to daughter species; the most conservative elements are most likely to be ancestral. Helix 25 rRNA grew from a small stem-loop in the common core into a large rRNA domain in eukaryotic lineages. (a) Approximation of ancestral Helix 25 of LUCA is obtained by elements conserved between Archaea and Bacteria. Approximation of ancestral ES7 is obtained for (b) the last archaeal and eukaryotic common ancestor (LAECA), (c) the last eukaryotic common ancestor (LECA), and (d) the last metazoan common ancestor (LMCA). Accretion adds to the previous rRNA core but leaves the basal rRNA unaltered. Each structure is experimentally determined by X-ray diffraction or Cryo-EM. Adapted with permission from ref 113. Copyright 2014 U.S. National Academy of Sciences.

3.3. Central Casting

The ribosome contains what we call "molecular casts". In a cast fossil, an object creates an impression in surrounding media then dematerializes. The imprint is filled by new, more persistent material taking the shape of the original object. Traditional cast fossils allow paleontologists to observe the contours of cells, bones, organs, or organisms.[221]

Analogous processes occur at the molecular level over evolution. In a molecular cast, evolutionary processes establish a productive interface between two molecular species. One of the species is replaced by a successor, with retention of conformation and molecular interactions with the partner. Molecular casting depends on selective pressure to maintain basic structure and/or function in the face of changes in bioavailability or other drivers of changes in chemical composition. Molecular casting is common for metals and is known as cambialism.[222] Iron, for example, has been replaced by other metals in a variety of systems. An ancestral di-iron ribonucleotide reductase (RNR) has been converted by casting to iron−manganese and dimanganese RNRs.[223,224] Superoxide dismutase uses a conserved cast to interact with iron, manganese, copper, zinc, or nickel.[225,226]

Molecular casting within the ribosome is seen for both inorganic cations[144,227] and macromolecules.[17,115−117,122,228,229] We have proposed that in the ribosome, conversion of Fe^{2+} to Mg^{2+} by casting[144,145,227] was driven by the Great Oxidation Event 2.4 billion years ago.[230] Divalent metal cation binding sites in rRNA (the media) remain essentially invariant (the impression) as cations changed their identity. Deep within the ribosome, molecular casting extends to biopolymers. It appears that noncoded peptides and/or depsipeptides (see below), synthesized before acquisition of the interface and the establishment of the link between synthesis and coding, interacted with proto-RNA via complementary surfaces (impressions). Noncoded species were ultimately replaced by coded species, retaining basic conformation and molecular interactions. In summary, both rProtein and rRNA segments within the oldest regions of the ribosome appear to contain casts of more ancient species.[17,115−118,122,228,231,232] This casting process of oligomers and ions within the ribosome has preserved information about macromolecules from the deep prehistory of biology.

3.4. Building up

In extant ribosomes of Eukaryotes, ESs in the LSU and es's in the SSU have been built by iterative insertion of small RNA fragments into basal rRNA. Differential insertion into ESs and es's leads to variation in lengths of eukaryotic rRNAs. Here we explain mechanistically how an accretion process takes place, using Helix 25/ES7 as an example (Figures 10 and 11).

One of the most diverse regions of the eukaryotic ribosome[154−161] is LSU expansion segment 7 (ES7, ES indicates LSU, and es indicates SSU, Figures 8, 10, and 11). ES7 illustrates many of the points listed above. We have established a fine-grained trajectory of ES7 evolution, allowing us to assemble frames of a "movie" of rRNA growth in three dimensions. ES7 emerges from Helix 25, a basal stem-loop that is modeled here by 22-nucleotide Helix 25 of *E. coli*. This stem-loop expands to an 80-nucleotide bent helix in the common ancestor of Archaea (approximated by *Haloarcula marismortui*), a branched 210 nucleotide domain in the common ancestor of eukaryotes (approximated by *S. cerevisiae*), and a 342-nucleotide domain in the common ancestor of metazoans (approximated by *Drosophila melanogaster*). In mammalian systems, ES7 has expanded further, exemplified by an 876-nucleotide domain in *Homo sapiens*. ES7 contains long tentacles in humans, chimpanzees, mice, and birds.

In the ES7 trajectory, one observes accretion at a molecular level. Basal rRNA does not remodel during or after expansion. The basal Helix 25 is fully intact in all other rRNAs (Figures 10 and 11) and was structurally conserved during a multibillion-year evolutionary process. The accretion process built the massive mammalian ribosome on a foundation provided by the ribosomes of protists, which were built on the ribosomes of archaea, which were built on the ribosomes of LUCA.

3.5. rRNA Insertion Fingerprints

Insertion of RNA elements into rRNA sometimes leaves distinct structural markers that we call insertion fingerprints. Insertion fingerprints are an important source of information in establishing the accretion model. Insertion fingerprints are historical pointers of chronological relationships between

https://dx.doi.org/10.1021/acs.chemrev.9b00742
Chem. Rev. XXXX, XXX, XXX−XXX

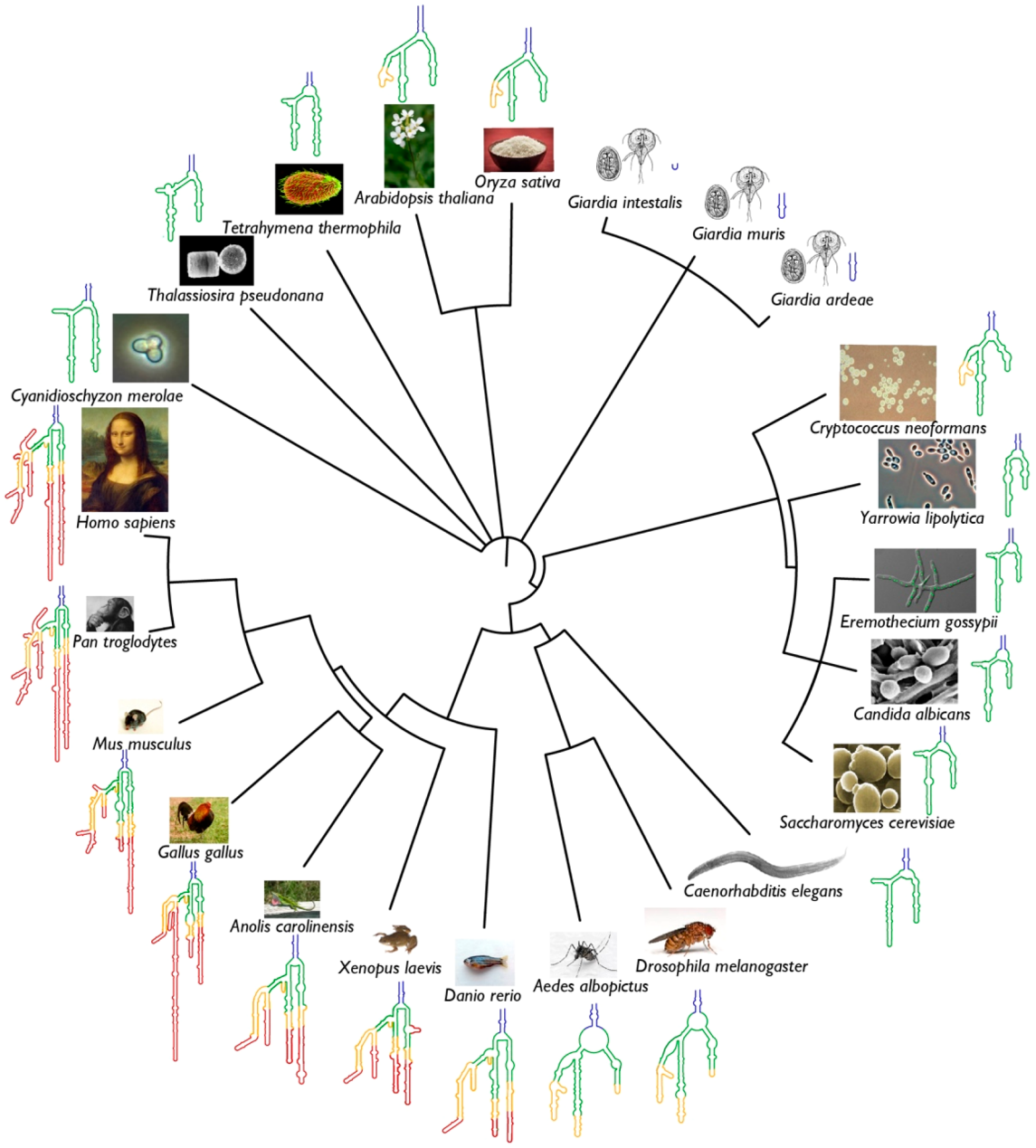

Figure 11. Secondary structures of ES7 mapped onto the canonical eukaryotic TOL. Colors indicate the extent of conservation of ES7 rRNA. Blue is Helix 25, part of the universal common core. Green rRNA is universal to all eukaryotes except those with reduced genomes. Yellow is universal to metazoans. Red is tentacle rRNA. Tentacles reach extreme lengths in birds and mammals.

various elements of the ribosome. The utility of insertion fingerprints is validated by comparisons among ribosomes of various sizes where lineages are well-established. Ribosomal structures with and without ESs, and within ESs, allow us to identify and visualize sites at atomic resolution where new rRNA has been added to basal rRNA. For example, comparison of helix 38 alone (universal, in Bacteria, Archaea, and Eukarya) to helices 38 plus 52 (Eukarya only; Figure 12) shows an expansion of universal to eukaryotic-specific rRNA. We know the temporal sequence of events in the evolution of these rRNAs; universal rRNA is ancestral to eukaryote-specific rRNA.

We have inspected and catalogued rRNA conformation at and around numerous sites where eukaryotic ES branches are inserted into universal trunks. Distinct and recognizable conformations characterize these insertion sites. The ancestral rRNA trunk generally accommodates the daughter insertion without disrupting or unstacking base pairs of the ancestor. Mechanistically, insertion is readily accomplished by (i) strand scission of the trunk helix, (ii) a shift of several backbone atoms by bond rotations, and (iii) ligation of the trunk to the branch. Insertion fingerprints are observed within the LSU rRNA, the SSU rRNA, and the tRNA. An expansion of tRNA, leading ultimately to doubling of the minihelix, is indicated by an insertion fingerprint between the acceptor helix and the T helix (Figure 12d).

Helical elongation is a second mechanism of rRNA accretion. LSU Helix 101 (universal) is elongated in eukaryotic rRNAs. Comparisons of pre- and postexpanded rRNAs (i.e., universal and eukaryotic rRNAs) reveal that helix insertions or

https://dx.doi.org/10.1021/acs.chemrev.9b00742
Chem. Rev. XXXX, XXX, XXX−XXX

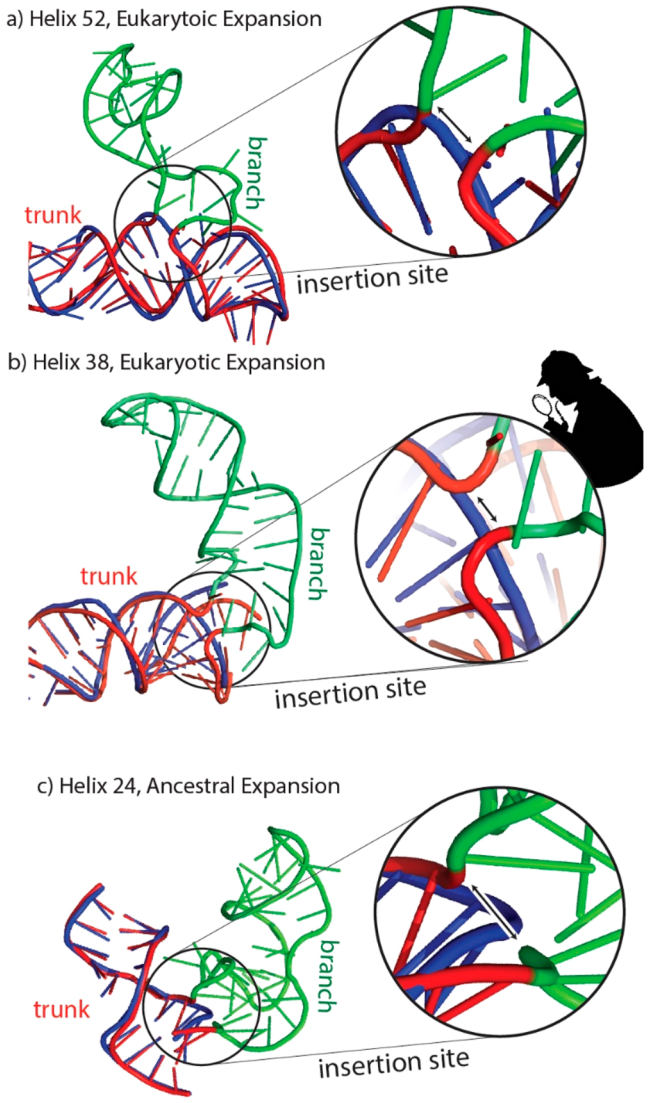

Figure 12. Insertion fingerprints in rRNA and tRNA. (a) Eukaryotic insertion (green) into helix 52 (red is eukaryotic and blue is the prokaryotic ancestor). (b) Eukaryotic insertion into LSU helix 38. (c) Ancestral insertion (green) into LSU helix 24 (red). The preinserted rRNA (blue) is modeled. Adapted with permission from ref 114. Copyright 2015 U.S. National Academy of Sciences.

elongations occurred in helices 25, 30, 38, 52, 54, 63, 79, 98, and 101 of the LSU of eukaryotic rRNA. Helix elongations do not leave distinctive structural fingerprints.

3.6. ESs and AESs: Expansion Segments Before and After LUCA

Inspection of the universal common core reveals numerous insertion fingerprints that appear structurally identical to insertion fingerprints in eukaryotic expansions. These pre-LUCA insertion fingerprints are distributed throughout the common core of both the LSU and SSU (Figure 13a,b). Identification of these insertion fingerprints allows us to demarcate *ancestral expansion segments* (AESs in the LSU and aes's in the SSU), which are small rRNA elements that built up the pre-LUCA ribosome (the universal common core).

Because the evolution of the universal common core can be partially read out by detection of insertion fingerprints and reconstruction of the accretion events, the accretion model extends to pre-LUCA processes. A comprehensive timeline can be established, from initial oligomers to protoribosomes to the common core to large eukaryotic ribosomes.[113−115] The ordering of events is dictated by the iterative nature of AES/aes accumulation and in some cases by the directionalities of A-minor interactions. Bokov and Steinberg reasoned[233] that the donating nucleotides in an A-minor interaction are dependent on the accepting double helix, whereas the accepting helix is independent. Therefore, the donating nucleotides must be the more recent addition.

Temporal correlations can be made between acquisition of rRNA elements (AESs and aes's) and rProtein segments by assuming the age of a given segment of rProtein is the same as that of the rRNA with which it interacts.[115] The accretion model is coherent and self-consistent, and reconciles significant processes in the histories of the LSU, SSU, tRNA, mRNA, rRNA, and rProteins. The accretion model is a chronology of AES/aes acquisition and rProtein evolution. The sections below describe information on the origins and evolution of the ribosome provided by the accretion model.

4. EVOLUTION OF THE RIBOSOME: REWINDING THE TAPE

4.1. Before LUCA: Exhuming the Root

In the accretion model, six phases of ribosomal evolution took place during the root of the TOL (before LUCA, Figures 13, 14, and 15). Each phase consists of a set of AESs and aes's and associated protein segments. The model allows us to "observe" the evolution of pre-LUCA rRNA, rProtein, and interactions with inorganic cations.

4.1.1. LSU: Building the Peptidyl Transferase Center. The PTC (Figures 3a and 14) appears to be among the oldest macromolecular elements[17,21−23,112,121,122] and enzymatic activities[10,11,20,234−238] in the biological universe. The LSU gained mass by iterative incorporation of rRNA stem-loops and other secondary elements as AESs (Figures 13 and 14). Initially, rRNA accreted AESs 1−5 to form the A-site, P-site, and the beginnings of the exit tunnel in the form of a central pore (Figure 14). This structure was rigid, stable, and monolithic. Formation of the PTC occurred before acquisition of the subunit interface and therefore was independent of the DCC. This model is consistent with broad consensus that the early PTC produced noncoded oligomers in isolation of the DCC and that proto-PTC and proto-DCC evolution were not correlated.[22,121,122,233,239,240]

4.1.2. LSU: Chemistry in the Peptidyl Transferase Center. The ribosome forms amide bonds in the PTC. A nascent polypeptide, linked as an ester at the 3′ end of a tRNA, is transferred in the PTC to the α-amino group of an amino acid monomer that is linked as an ester at the 3′ end of another tRNA (Figure 16b). The PTC catalyzes this reaction, then does it again, and again, and again. Ester−amide exchange[241] (an aminolysis reaction), and thioester−amide exchange,[242,243] are broadly employed in biological systems for synthesizing or hydrolyzing peptides. Serine proteases run the reverse reaction, amide-ester exchange, to hydrolyze peptide bonds;[244] the acyl-enzyme intermediate is an ester (Figure 16c).

Ester−amide exchange has a low activation energy, is near equilibrium, and as in the PTC, can be accomplished by wet−dry cycling of mixtures of amino acids and hydroxy acids (Figure 16a) in mild temperatures.[228,231,245−251] The facile nature of ester−amide exchange is a key to understanding the

https://dx.doi.org/10.1021/acs.chemrev.9b00742
Chem. Rev. XXXX, XXX, XXX−XXX

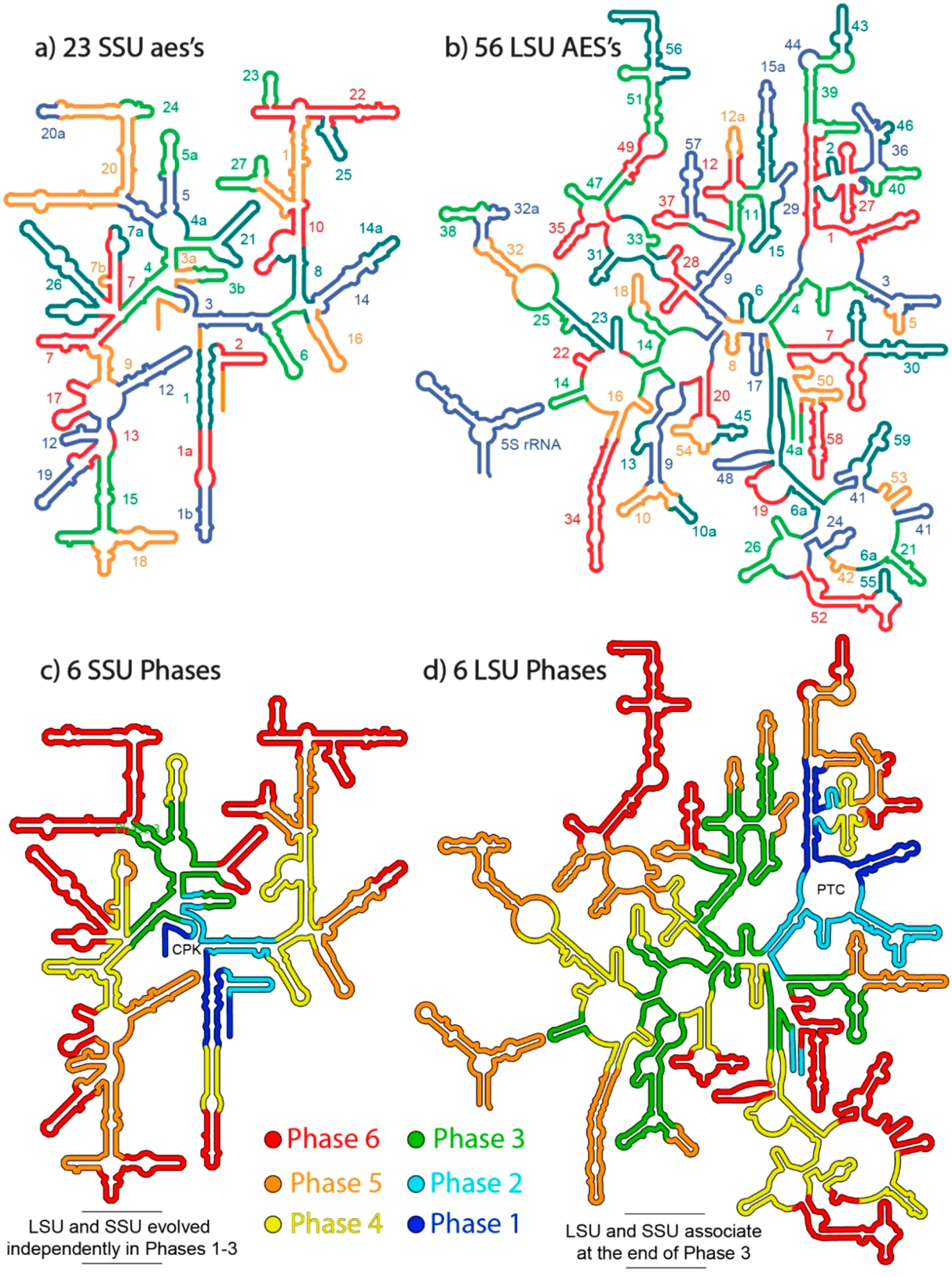

Figure 13. rRNA evolution mapped onto the LSU rRNA secondary structure. The universal common core is built up by stepwise addition of AESs at sites marked by insertion fingerprints. (a) Each AES is in the SSU is individually colored and labeled. AES colors are arbitrary, chosen to distinguish the expansions, such that no AES is the color of its neighbor. (b) Each AES is in the LSU is individually colored and labeled. (c) Accretion of ancestral and eukaryotic ESs in the SSU is distributed into six phases. (d) Accretion of ancestral and eukaryotic ESs in the LSU is distributed into six phases: phase 1, rudimentary binding and catalysis (dark blue); phase 2, maturation of the PTC and exit pore (light blue); phase 3, early tunnel extension (green); phase 4, acquisition of the SSU interface and tunnel extension (yellow); phase 5, acquisition of translocation

https://dx.doi.org/10.1021/acs.chemrev.9b00742
Chem. Rev. XXXX, XXX, XXX−XXX

Figure 13. continued

function and tunnel extension (orange); phase 6, late tunnel extension (red). Some AESs appear to be discontinuous on the secondary structure and so are labeled twice. Adapted with permission from ref 114. Copyright 2015 U.S. National Academy of Sciences.

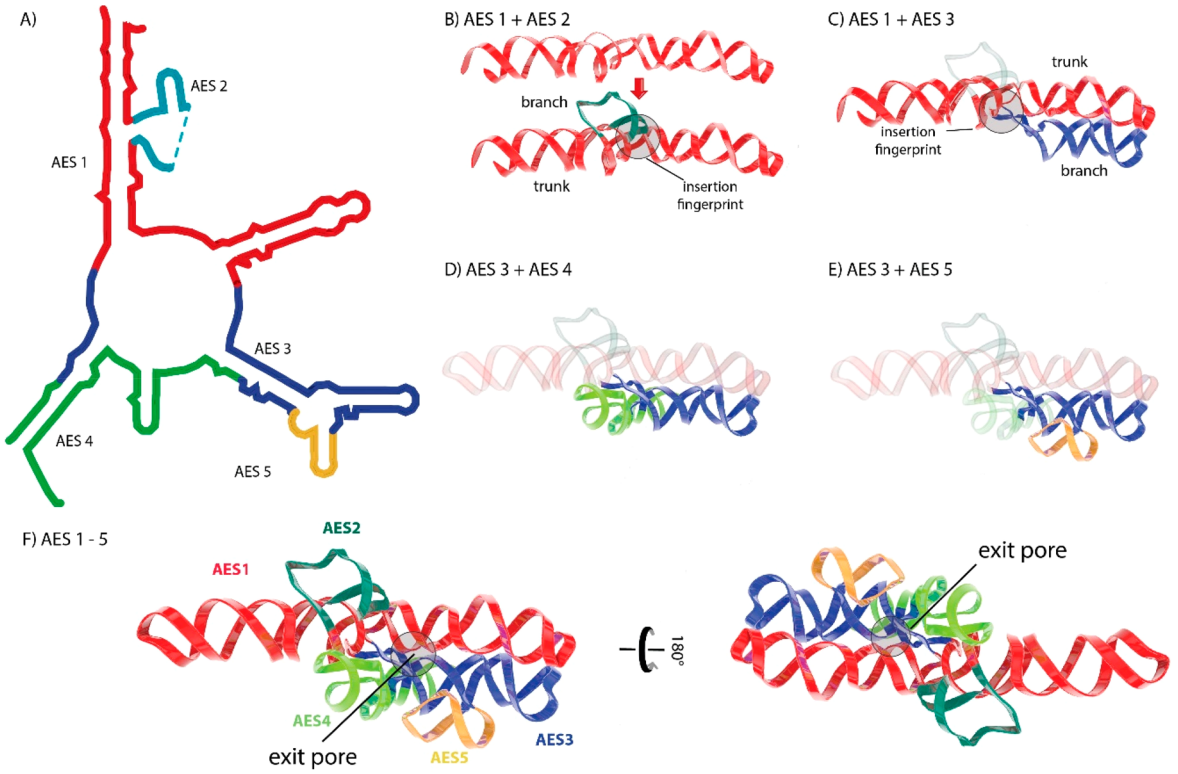

Figure 14. Origins and Evolution of the PTC. Trunk rRNA is shown *before* and *after* insertion of branch helix. (a) The secondary structure of AESs 1−5, which form the PTC and the exit pore (helices 74, 80, 89, 90, 91, 92, and 93). The ends of AES 2 are located in direct proximity to each other in three-dimensions, indicated by a dashed line in the secondary structure. (b) AES 1 (red) is expanded by insertion of AES 2 (teal). (c) AES 1 is expanded by insertion of AES 3 (blue). (d) AES 3 is expanded by insertion of AES 4 (green). (e) AES 3 is expanded by insertion of AES 5 (gold). (f) The three-dimensional structure of AES 1−5, colored as in panels A−E. In each case, the *before* state was computationally modeled by removing the branch helix and sealing the trunk using energy minimization. rRNA is represented by ribbons. Positions of the P-loop, the A-loop, and the exit pore are marked. The color scheme of this figure matches the scheme of Figure 13b. Adapted with permission from ref 113. Copyright 2014 U.S. National Academy of Sciences.

unsophisticated and apparently primordial chemical mechanism utilized by the ribosome. The PTC is not a good enzyme, nor does it have to be. The PTC is a primitive entropy trap[252−254] with minimal mechanistic contributions from chemical catalysis or specific stabilization of the transition state. Even so, this mechanism is sufficient to produce all coded protein in the biological universe at a rate of around 10−20 peptide bonds per second per ribosome.[86]

4.1.3. LSU: The Exit Tunnel. The exit tunnel was initially inferred by the laboratory of Alexander Rich[255] (also see refs 256, 257) and was ultimately revealed in three dimensions by Ada Yonath and co-workers.[20,258] Each protein threads through the exit tunnel N-terminus first, traveling around 100 Å from the PTC, through the center of the LSU, to emerge on the distal surface of the ribosome at the tunnel egress.[259−261] The walls of the tunnel are formed by rRNA and ancient β-hairpin "tails" of ribosomal proteins uL4 and uL22.

In phase 1, the wall of the exit pore is formed by AES 1 (dark blue, (Figures 13c,d, 15, 17−18). In phase 2, the exit pore is completed by AESs 3 and 4 (light blue). In phase 3, the exit pore is extended into a short tunnel by AESs 9−10 and 13 (green). In phase 4, the tunnel is extended and rigidified by AESs 6a, 19, and 28 (yellow). In phase 5, the tunnel is extended by AESs 31, 33, and35 (orange). In phase 6, the tunnel is extended and finalized by AESs 41 48, and 59 (red).

4.1.4. SSU: Building the Decoding Center. The DCC (Figure 3b) is the core functional component of the SSU and is responsible for decoding mRNA in the extant ribosome. As noted above, the late acquisition of the subunit interface is consistent with the consensus that the DCC and PTC originated in isolation of each other.[121,122,233,239,240] The DCC and PTC differ fundamentally in structure, dynamical properties, and function. The PTC can be built simply by ligating stem loops and elongating helices. The core of the DCC contains a pseudoknot, a structure that is not accessible by simple mechanism of PTC evolution. The LSU is monolithic. The dendritic SSU uses the central pseudoknot as a hub and is intrinsically dynamic. The termini are associated in the LSU but are dissociated in the SSU.

The most reasonable mechanism for generation of the central pseudoknot is the sequestration of a transiently unpaired strand of a stem-loop, leaving the complement strand unpaired. The single-stranded region of the central pseudoknot (the anti-Shine−Delgarno sequence), the central pseudoknot,

https://dx.doi.org/10.1021/acs.chemrev.9b00742
Chem. Rev. XXXX, XXX, XXX−XXX

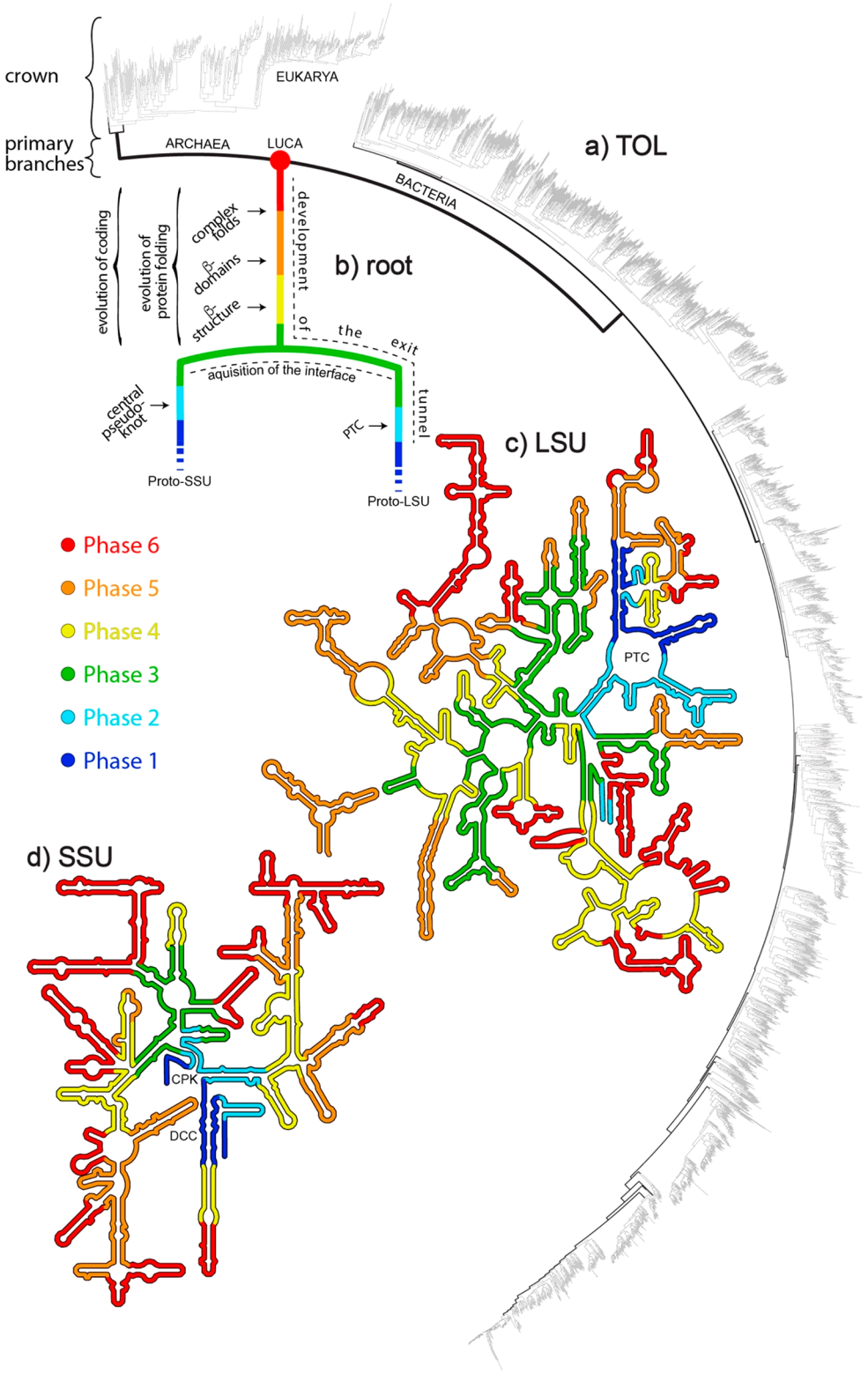

Figure 15. Evolution of the ribosome in the root of the tree of life. (a) The TOL, showing the primary branches and the crown. (b) The root of the TOL, showing the evolution of the ribosome. The root is colored by phase of ribosomal evolution. The figure illustrates the independent origins of the two ribosomal subunits, the acquisition of the intersubunit interface, subunit association, the development of the exit tunnel, the evolution of protein folding, and the evolution of coding. (c) rRNA secondary structure of the ribosomal large subunit. (d) rRNA of the ribosomal small subunit. rRNA is colored by phase as in Figure 13c,d, from oldest (phase 1) to youngest (phase 6). Dark blue (phase 1), light blue (phase 2), green (phase 3), yellow (phase 4), orange (phase 5), and red (phase 6).

the dynamical properties of the SSU, and the dissociation of the strand termini are features of early ancestors of the SSU. The preribosomal function of the SSU is unclear but likely involved a single-stranded binding functionality, probably interacting with other single-stranded RNAs. It seems plausible that an ancestral function of the SSU (Figure 17h), during

https://dx.doi.org/10.1021/acs.chemrev.9b00742
Chem. Rev. XXXX, XXX, XXX−XXX

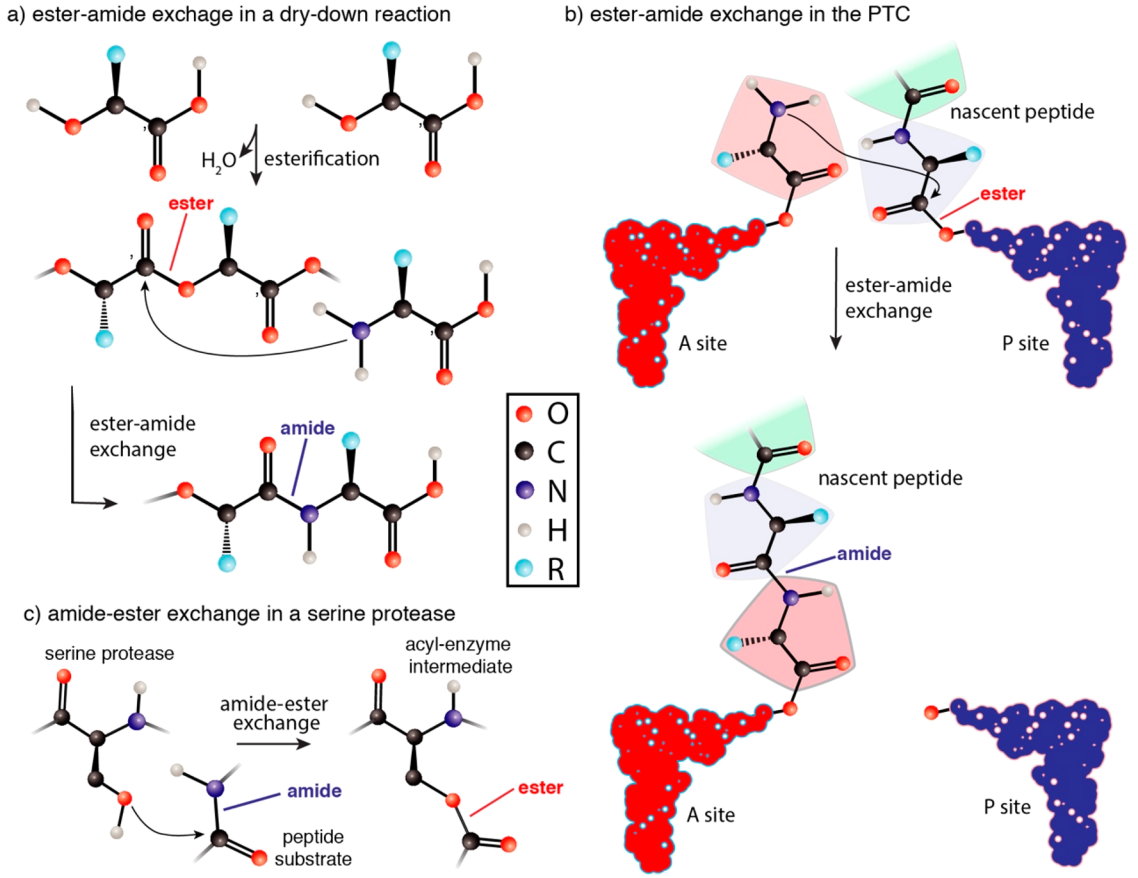

Figure 16. Ester−amide exchange and amide-ester exchange in prebiotic and biochemical reactions. (a) Drying down amino acids and hydroxy acids makes esters that convert to amides under mild conditions. (b) In the PTC of the ribosome, esters are converted to amides, via entropy trapping. (c) In a serine protease, amides are converted to esters. In dry-down reactions, condensation to form the ester is driven by low water activity. In translation, condensation to form the aa-tRNA ester is driven by ATP hydrolysis. In a serine protease, hydrolysis is spontaneous. (a) Adapted with permission from ref 245. Copyright 2019 U.S. National Academy of Science.

early development of the interface, was likely as a cofactor, assisting in the positioning of other RNA molecules at the PTC to optimize the condensation. Upon association of the subunits (Figure 17i), the ribosome would be capable of making short unstructured peptides with greater efficiency than the LSU alone (Figure 17f). This association would also mark the beginning of a transition from a noncoding to a primitive (operational) coding ability. The proto-SSU may have been stabilized by short heterogeneous protopeptides.

4.1.5. LSU-SSU-tRNA: Working Together. tRNA was a central player in driving subunit association and coevolved in concert with the subunit interface. The conversion of the protoribosome (noncoded) to the extant ribosome (coded) involved acquisition of the interface by both subunits and growth of the pre-tRNA mini-helix[262,263] to form the mature L-shaped tRNA molecule. Before minihelix expansion, no functional gain would accrue from association of the two subunits. Before acquisition of the interface, no functional gain would accrue from maturation of tRNA.

4.1.6. LSU-SSU-tRNA: Coding and Energy Transduction. Once tRNA elongates and the subunit interface is acquired, evolution of the two subunits becomes tightly correlated. This correlation of LSU and SSU evolution leads ultimately to a conversion from a Brownian ribozyme (Figure 17j) stabilized by noncoded protopeptides (Figure 17k) to an energy-driven, translocating, ratcheting, decoding machine stabilized by sophisticated folded proteins (Figure 17l). The production of folded rProteins was linked to production of class II aaRSs[264] (Figure 17n), elongation factors, initiation factors,[265] and RNA polymerase. The ribosomal surface incorporates specific binding sites (Figure 17o) for diverse rProteins (Figure 17p). Surface proteinization coincides with the development of highly specific aaRSs (Figure 17q) and marks the maturation of the genetic code.

4.2. Evolution of Protein

4.2.1. Cycling Hydration and the Initiation of Polymer Evolution. One of Nature's greatest accomplishments is the discovery of functional polymers with complex self- and heteroassembly and catalytic behaviors.[266] These discoveries relied on selection for a complex variety of factors. Present models of prebiotic systems suggest that condensation−dehydration chemistry was selected over other linkage chemistries in an environment of cycling water activity.[267,268] Primitive oligomers, produced by condensation, predated the ribosome.

It appears that the Earth's day−night cycle drove this prebiotic phase of chemical evolution. Molecules that linked by condensation−dehydration reactions were chemically selected as building blocks of oligomers. In this scenario, the primitive translation system did not push polymerization thermodynamically uphill but instead took advantage of oscillating reaction directionalities that formed and hydrolyzed ancestors of biopolymers. We believe that the proto-LSU altered the

https://dx.doi.org/10.1021/acs.chemrev.9b00742
Chem. Rev. XXXX, XXX, XXX−XXX

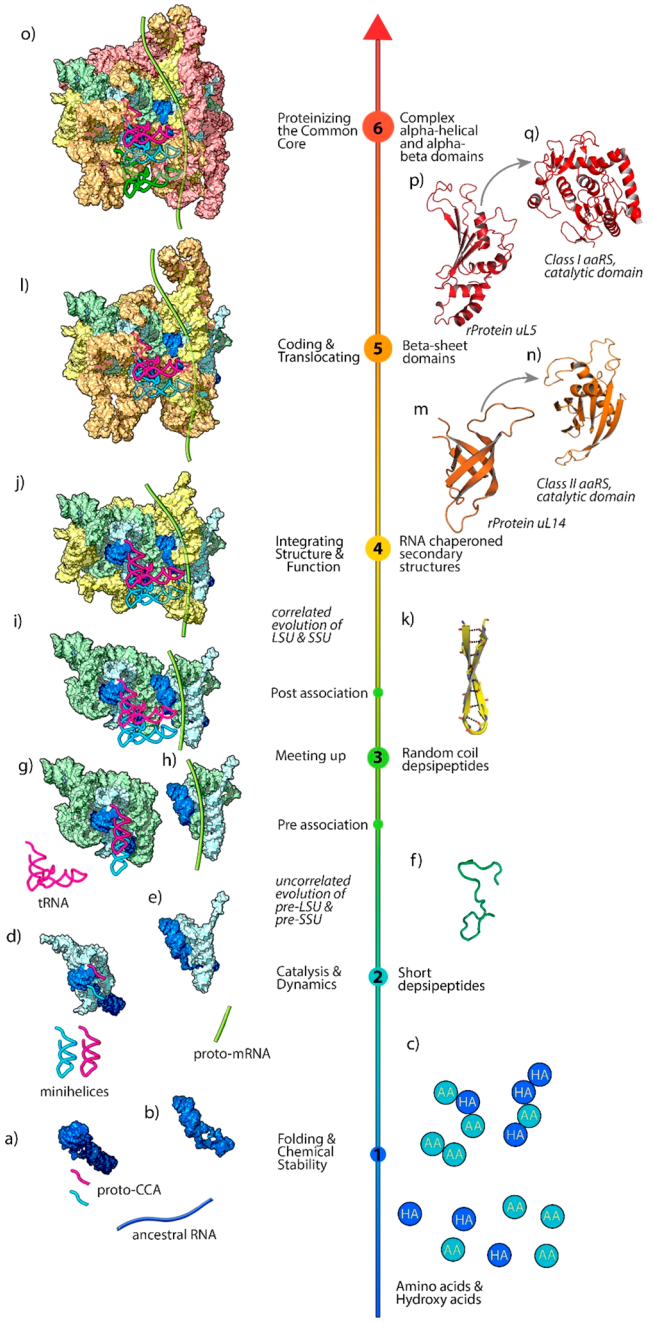

Figure 17. The coevolution of LSU rRNA, SSU rRNA, tRNA, and proteins. Six phases of the accretion model lead to the LUCA ribosome. In phase 1, RNAs form stem-loops and minihelices that begin to accrete. In phase 2, the PTC is formed and catalyzes condensation in the absence of coding. The SSU may have a single-stranded RNA binding function. In phase 3, the subunits gain mass. At the end of phase 3, the interface is acquired and the subunits associate, mediated by the expansion of tRNA from a minihelix to the modern L-shape. LSU and SSU evolution is independent and uncorrelated during phases 1−3. In phase 4, evolution of the subunits is correlated. The ribosome is a noncoding diffusive ribozyme in which proto-mRNA and the SSU act as positioning cofactors. In phase 5, the ribosome expands to an energy-driven, translocating, decoding machine. In phase 6, the ribosome matures, marking completion of the common core with a proteinized surface (the proteins are omitted for clarity). The colors of the rRNA and rProtein phases are the same as in Figures 13c,d, and 15. mRNA is shown in light green. The A-site tRNA is magenta, the P-site tRNA is cyan, and the E-site tRNA is dark green. Adapted with permission from ref 114. Copyright 2015 U.S. National Academy of Sciences.

product distribution of environmentally driven condensation and hydrolysis reactions. Some products of condensation reactions bound to the protoribosome and were protected from hydrolysis[246] and in turn conferred advantage to the protoribosome. Thus, the system gained advantage by discovery of condensation products with affinity for RNA.

During early phases of ribosomal evolution (phases 1−2), the model predicts that the proto-LSU simply influenced short cationic protopeptides whose production was driven by wet−dry cycling.[228,231,245−251] Cationic charge confers the ability to interact strongly with RNA (or proto-RNA), increasing stability of assemblies and chemical lifetimes of both interactors.[246] Noncoded cationic random-coil oligomers could have supported assembly and function of the protoribosome or other ribozymes. Support for this scenario is found in the observation that simple cationic peptides stimulate the activities of several artificial and native ribozymes.[269]

4.2.2. Exaptation and the Discovery of Protein. Protein evolution followed a pathway of exaptation, in which the results of selection for one characteristic formed the basis for selection for other characteristics. Evolution creates by coopting or repurposing; traits that serve one function descend from traits that served a different function that descend from traits that served even different functions and so on.[270] Exaptation explains how the bones of human hands descended from fins of fishes,[271] how the fragile malleus and incus bones of the mammalian ear descended from sturdy jaw bones of reptiles,[272] and how feathers were coopted for flight.[273,274] Without an evolutionary context, one cannot hope to fully understand human hands, structures and functions of the mammalian ear, feathers, or biopolymers.

In the path to discovery of functional proteins, Nature selected

(a) types of building blocks,[275−278]
(b) linkage by condensation−dehydration reactions,[266−268]
(c) amide linkages over esters and other types of condensation linkages,[228,231,245−251]
(d) α-amino-acids over $\beta,\gamma\cdots$-amino acids,
(e) homochiral amino acids over the racemate,
(f) linear over branched polymers,
(g) the 20-proteinaceous side chains over a large pool of alternatives,[277,278] and
(h) specific functional sequences from an immense excess of alternative sequences.[279]

The vast space of possible monomer-types, backbone chemistries, side chain types, polymer topologies, and sequences was not fully explored during the evolution of proteins. The universe lacks sufficient atoms or time to accomplish a random search of even a small subspace of this landscape.[279,280] Instead, the rare suite of features that conferred folding and assembly competence to Nature's functional biopolymers was obtained via repeated exaptation processes. The evolution of proteins was hierarchical and progressive.

4.2.3. The Evolution of Protein Folding, Recorded on the Ribosomal Tape. We presume the evolution of protein,

https://dx.doi.org/10.1021/acs.chemrev.9b00742
Chem. Rev. XXXX, XXX, XXX−XXX

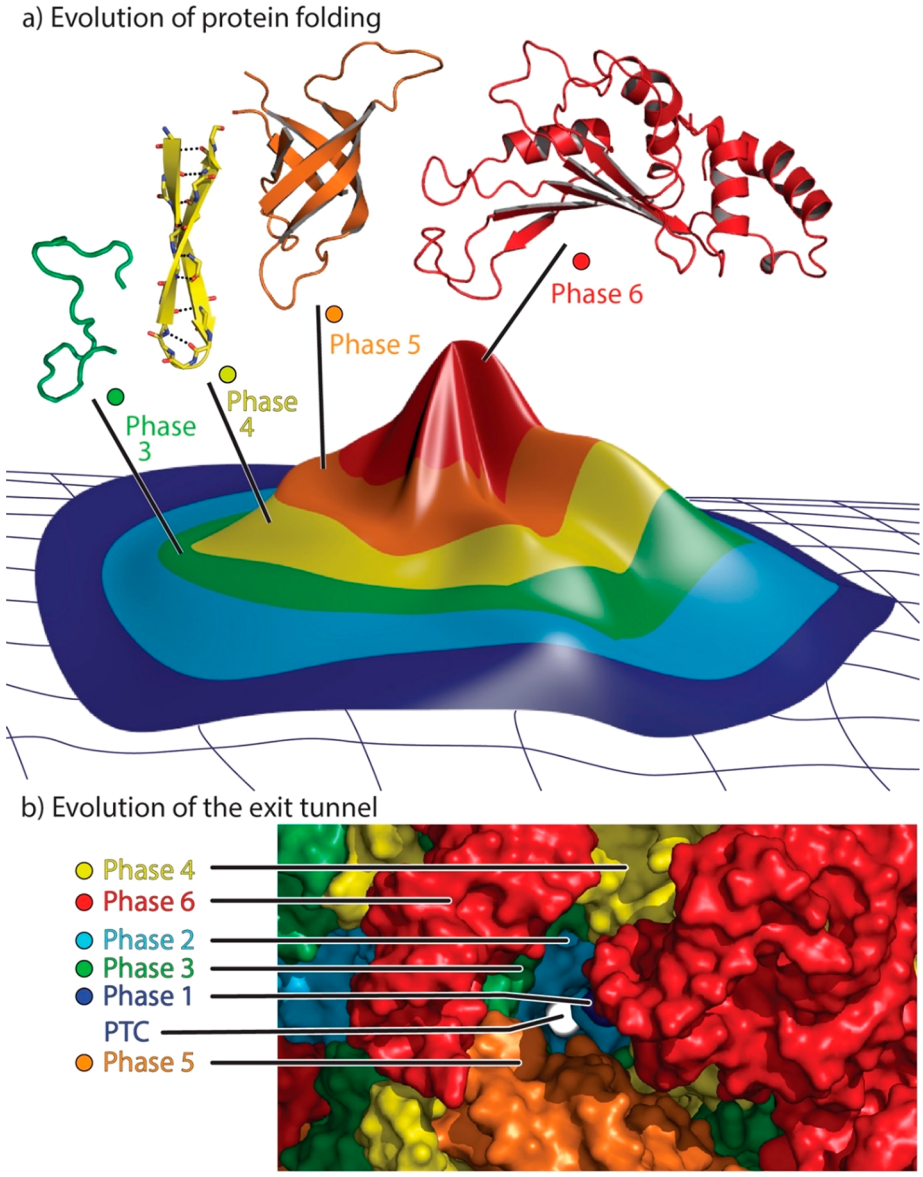

Figure 18. The evolution of protein folding is coupled to the evolution of the ribosome. (a) Development of the ribosome is depicted as a fitness/folding/evolutionary landscape. The evolution of rProtein conformations is shown above the funnel. The metaphorical landscape comes to a peak where modern proteins fold to form complex globular domains. The surface and the rProtein segments are colored by phase of ribosomal evolution (as in Figures 13c,d, 15, and 17). (b) A view directly into the exit tunnel, from the egress (near) to the PTC (far), reveals contributions to the structure of the tunnel from each phase of rRNA evolution. The rProtein segments shown here were extracted from appropriate phases of the *Thermus thermophilus* ribosome. (a) Adapted with permission from ref 115. Copyright 2017 Oxford University Press.

starting with a diverse small molecule inventory and progressing to the elaborate folds of extant biology, to be fine-grained, progressive, and discontinuous; oligomers of successively greater size, ability to fold, increasing backbone homogeneity, sequence specificity, and catalytic functionality conferred ever-increasing advantage.

Incredibly, a reaction coordinate for the evolution of protein folding (Figure 18) appears frozen within the ribosome[115] (also see Lupas[116−118,232] and Hartman[281]). Correlating acquisition of rRNA elements (AESs and aes's) and acquisition of rProtein segments led to a detailed molecular map of the evolution of protein folding.[10] This reaction coordinate was evident once the accretion model was developed and was not assumed or built into the accretion model, nor was it anticipated.

The frozen reaction coordinate within the ribosome suggests that after the maturation of condensation chemistry for the production of oligomers that associated with RNA, the next selection was for oligomers capable of forming of β-hairpins.[115] Here, selection began to favor oligomers with a cohesive and chemically homogeneous backbone. Amino acids were preferred over hydroxy acids, homochirality was preferred over racemates, and α-monomers were preferred over $\beta,\gamma\cdots$-monomers. In a third step, polymers were selected based on formation of globular β-domains. This advance produced a fully cohesive backbone (polypeptide), with correct sequences of hydrophilic and hydrophobic side chains. Globular proteins required at least primitive coding, participation of tRNA and the SSU, and a form of energy currency (ATP). Selection for α-structures lagged selection for β-structures. Once β-only domains were reasonably optimized, selection for complex

https://dx.doi.org/10.1021/acs.chemrev.9b00742
Chem. Rev. XXXX, XXX, XXX−XXX

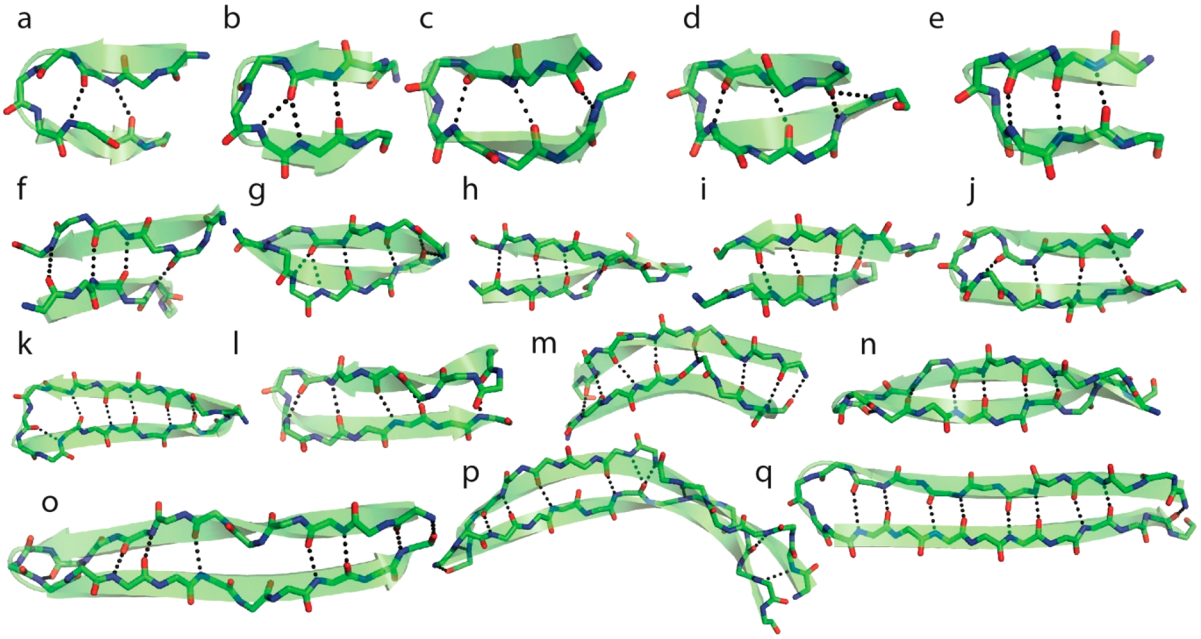

Figure 19. Sixteen β-hairpins are embedded in ancient rRNA in the core of the ribosome. These β-hairpins were computationally excised from the rProteins of a bacterial ribosome. Each is surrounded by rRNA in the LSU (not shown). (a) bL17, (b) bL9, (c) $uL2_c$, (d) $uL2_b$, (e) uL5, (f) $uL2_a$, (g) uL16, (h) $uL24_b$, (i) $uL24_a$, (j) bL25, (k) uL13, (l) uL14, (m) uL3, (n) uL22, (o) uL23, (p) bL28, and (q) bL21. Subscripts a, b, and c indicate multiple rRNA-embedded β-hairpins are observed in a given rProtein. These structures were sorted according to the number of hydrogen bonds linking the two β-strands

folds, containing both β-sheets and α-helices, became dominant.

4.2.3.1. Co-Evolution of Protein Folding and Growth of Exit Tunnel. The ribosomal exit tunnel is the birth canal of biology; every coded protein ever produced by life on Earth has passed through the exit tunnel. The exit tunnel is a unique biological structure, and its evolution was an extraordinary process.

The importance of the exit tunnel in ribosomal function is underscored by the observation that no other structural or functional feature of the ribosome is developed throughout all phases of ribosomal evolution. Exit tunnel evolution is the *only* process in the evolution of the ribosome that we know to be unremitting, taking place throughout all six phases of protoribosomal and ribosomal evolution (Figures 13c,d, 15, 17, and 18). Pore formation, followed by exit tunnel elongation, stabilization, and rigidification, appear to dominate evolution of the ribosome from start to finish (at LUCA). All other aspects of ribosomal evolution, including formation of the PTC and DCC, acquisition of the interface, etc., are punctuated and episodic. The ribosome devotes more rRNA to the exit tunnel than to any other structure/function (Figure 1).

It is not surprising that the accretion model suggests that evolution of the ribosome, specifically the exit tunnel, is linked to evolution of protein folding. Proteins and protein folding evolved in concert with extension, reinforcement, and elaboration of the exit tunnel. Nascent proteins start to fold within the tunnel, as they are synthesized; folding is generally faster than translation.[282] Here we outline a series of exaptation processes the led to mature protein domains.

4.2.3.2. Start with Intrinsic Disordered Proteins. During phases 1 and 2, the exit pore and primitive tunnel are thought to have promoted increased processivity[283] and cationic properties of condensation products[246] by stabilizing ribosomal association with reaction substrates and intermediates. In addition, the exit pore and primitive tunnel may have inhibited formation of dead-end cyclic peptides[284] by maintaining separation of the N and C termini. rProtein segments in phase 3 exclusively form extended and irregular structures consistent with frozen random coil (also known as intrinsically disordered[285]). These segments are constrained by surrounding rRNA and interact extensively with it. The polypeptides that compose these segments in the extant ribosome appear to be cast fossils of ancestral protopeptides.

4.2.3.3. The Ascent of Beta. Protein segments in phase 4 form both secondary structures and frozen random coil. The dominant secondary structural element in phase 4 is antiparallel β-structures (Figure 19), composed of intramolecular β-hairpins or $\beta-\beta$ dimers between amino acids that are remote in primary structure but belong to a common peptide chain. The frequency of secondary structure in polypeptides increases from phase 3 through phase 5 but remains dominated by β-structures.

In phase 5, some of the polypeptide chains form globular domains. These domains, which are composed primarily of antiparallel β-sheets, have hydrophobic cores and hydrophilic surfaces. The β-barrel domains that are common in phase 5 give the appearance of arising from collapse of the isolated $\beta-\beta$ structures observed in phase 4.

4.2.3.4. The Ascent of Alpha. In the final steps of the evolution of the common core, rProteins accumulated and gained complex supersecondary structures composed of mixtures of α-helices and β-strands. The fraction of polypeptide in α-helices increases from phase 5 to phase 6. During phase 6, the tunnel is finalized and rProteins form complex folds composed of both α-helices and β-strands.

4.2.3.5. Kinetics vs Thermodynamics of Protein Folding. The exit tunnel is around 100 Å long and 10−20 Å wide.[259−261] Except near the egress, the geometry is too narrow for β-hairpins, protein aggregates, or "minimal

https://dx.doi.org/10.1021/acs.chemrev.9b00742
Chem. Rev. XXXX, XXX, XXX−XXX

domains".[286] However, the exit tunnel readily accommodates α-helices and has been shown to stabilize and harbor them.[287−291] The length of the tunnel appears critical; while very short peptides in solution can adopt stable β-sheets,[292−298] persistent α-helices require longer fragments, with lengths similar to that of the exit tunnel.[286,299]

Therefore, the exit tunnel is a device to kinetically trap α-helices. The length, width, and electrostatic properties of the exit tunnel appear to be optimized for trapping α-helices. The tunnel partially offsets the general preselected thermodynamic tendency of the polypeptide backbone to form β-sheet structures.[266,300−304] The exit tunnel:

(a) lowers water activity, enthalpically promoting intramolecular H-bonding within the nascent chain,

(b) restricts configurational space, entropically promoting intramolecular H-bonding within the nascent chain, and

(c) sterically disadvantages β-structures over α-structures, facilitating α-helices within the nascent chain.

In this scenario, the tunnel is a mechanism of exaptation. The exit tunnel repurposes a polymer selected for formation of thermodynamically stable β-structures (i.e., polypeptide), facilitating formation of kinetically trapped α-helices.

This model should not be interpreted to mean that the tunnel is the only contributor to α-helix formation. Sequence, post-tunnel chaperons, and environment are additional influences. In addition, it has been shown that β-hairpins can fit within the bacterial vestibule,[305,306] where the tunnel widens near the egress. This region of the tunnel is not universal and narrower and more restricted in Archaea and eukaryotes than in Bacteria.[307]

Our model for the coevolution of protein folding and the exit tunnel explains:

(a) The potent and general chaperoning ability of nucleic acids;[308,309] in this model. rRNA is the ancestral chaperone of all protein.

(b) Why β-structure is the default (thermodynamic) secondary structure of the functional polymer;[266,300−304,310] in this model, the first level of secondary structural selection was for thermodynamically stable β-structures and selection for kinetically trapped α-helices was later.

(c) The adaptability of extant proteins and their high frequency of accidental function;[311] in this model, adaptability was a selection criterion during the evolution of folding.

(d) The observation that extant proteins fold by real-time funnels and do not randomly search conformation space;[312−315] in this model, funneling was intrinsic to the evolution of folding.

4.3. The Genetic Code

Numerous speculations on the origins and evolution of the genetic code have been presented.[281,316−321] There is evidence that the genetic code, along with selection of biopolymer building blocks and linkage chemistries, are products of evolution. The code appears structured to minimize phenotypic effects of mutation and mistranslation.[322] Freeland and Cleaves have made the important observation that random sets of amino acids that cover chemistry space better than the proteinaceous amino acids are rare and energetically costly.[323,324]

We believe fundamental aspects of the origins and evolution of the genetic code will become increasing clear as a molecular level solution to the origins of the translation system is approached. Once the origins and early evolution of the translation system (including tRNA synthetases) are unraveled on a molecular level, the origins of the genetic code and details of the codon assignments can be unveiled.

5. CONJECTURES ON RIBOSOME EVOLUTION

Comparative sequence analysis[325] is a useful tool for ribosome paleontology. "Universally conserved" nucleotides were defined by Gutell as those present more than 95% of the 500+ sequences aligned for the LSU, or 5000+ for the SSU. More recently, we have established a database, which we call the Sparse and Efficient Representation of the Extant Biology (the SEREB database).[19] This database contains complete and cross-validated rRNA sequences and structures of species chosen, as far as possible, to sparsely and efficiently sample all known phyla. Atomic-resolution structures of ribosomes provide data for structural comparison and validation of sequence-based models. This database documents an astounding degree of conservation of the translation system across the tree of life. Gerbi used LSU rRNA alignments to identify 23 "universal sequence elements",[326] which are stretches of 6−18 consecutive nucleotides conserved in three-dimensions and in sequence, in all three superkingdoms of life. As expected, universal sequence elements were found at the PTC, the sarcin-ricin loop, the GTPase center, and the LSU−SSU interface. Three of the most highly conserved sequence elements (in domain I and domain III) could not be linked to known ribosome function. One can speculate that the universal sequence element in domain III could be associated with tertiary structure, protein binding,[327] metal binding, or even novel catalysis.[145,147]

A dimeric protoribosome (DPR) model developed by Agmon and Yonath[21−23,328] describes a proto-PTC that assembled via dimerization of two monomers selected from a pool of random RNAs on the basis of an ability to elongate peptides. The DPR is similar to AESs 1−5 of the accretion model; both contain the A-loop, the P-loop, and the exit pore.

Root-Bernstein hypothesized that rRNAs contain vestiges of an ancient genome encoding translation-associated proteins and tRNAs.[329,330] They aligned rRNAs with tRNAs, sequences encoding protein ligases, phosphatases, polymerases, rProteins, and synthetases. They argue that evolution of mRNAs encoding rProteins and rRNA has not been independent. The Root-Bernstein model is supported by (i) autogenous control of expression of rProtein by its own mRNA, (ii) homologous rProteins binding regions in mRNA and rRNA, (iii) prevalence of arginine in rProtein elements that bind rRNA, and (iv) encoding of some extant proteins by rRNA.

Smith and Hartman are generally supportive of the accretion model. They argue that the proto-PTC was composed of an rRNA stabilized by interactions with short protopeptides,[239,281] that the origins and early evolution of the PTC and DCC were decoupled, and that the proto-PTC synthesized noncoded oligomers (also see Fox,[121,122] Noller,[240] and Steinberg[233]). Smith and Hartman make the important observation that the DCC, unlike the PTC, is not composed of a stable self-folding RNA. In their models, the proto-LSU and proto-SSU were linked by a boomerang-like proto-tRNA.[331,332] Multiple sequence alignments of rProteins led these investigators to suggest that although Bacteria and

https://dx.doi.org/10.1021/acs.chemrev.9b00742
Chem. Rev. XXXX, XXX, XXX−XXX

Archaea have a common ancestor, rProteins acquired additional features after LUCA.[333] Hartman and Smith further extended the analysis of the translational apparatus to initiation and elongation factors,[265] connecting the origins of the translational apparatus with the evolution of tRNA synthetases and the origin of the genetic code.[281]

In a model that has been disputed,[334] Harrish and Caetano-Anolles proposed that rRNAs can be broken into small elements that are related by ancestry.[335] According to this model, evolution was driven exclusively by thermodynamic and dynamical considerations. rRNA secondary structures of the LSU and SSU were cut into small elements that were computationally annealed and melted. Output parameters of the computation were treated as character strings to build phylogenies. The method predicts deep ancestry of long stable helical elements and the late arrival of shorter elements. In this model, the evolution of the ribosome nucleated at the intersubunit interface. The functional elements of the ribosome, such as the PTC, the exit tunnel, DCC, and central pseudoknot appear at later stages of ribosomal evolution.

6. BIOTECHNOLOGY OF THE RIBOSOME

In addition to the effects of natural evolutionary pressures, ribosomes can be modified through various technological processes.[336−338] Several factors impede ribosomal engineering. Most direct changes to the ribosome are lethal because cell viability depends absolutely on ribosome function. In addition, large tandem arrays of rRNA genes in eukaryotes preclude experimental methods such as CRISPR-Cas. Sixty percent of yeast chromosome XII is devoted to approximately 150 tandem repeats of genes that encode rRNAs.[339] In mammalian systems, large arrays of rRNA genes are distributed across multiple chromosomes.[340]

Hecht and colleagues developed a novel strategy for enhanced incorporation of non-natural amino acids, specifically D-amino acids[341,342] and β-amino acids,[343,344] through mutagenesis of the PTC region in 23S rRNAs. These studies expand the repertoire of ribosome substrates and functions have the potential to create novel functional biopolymers in vivo.

Ribosome engineering in vivo has focused on the development of *orthogonal translation systems that operate in parallel to the native* wild-type ribosomes to ensure cell viability.[149,336] Ideally, orthogonal ribosomes exclusively translate only targeted mRNA. Most commonly, orthogonality is engineered only at the bacterial SSU because recognition of the start codon in Bacteria relies on complementary interactions between the Shine-Dalgarno region in mRNA and the anti-Shine−Dalgarno region of the 16S rRNA in the 30S subunit. Recently, covalent linkage between the LSU rRNA and the SSU rRNA was achieved to form a single chimeric engineered ribosome.[338,345] As a complementary approach, ribosome engineering in vitro allows engineering of mutant ribosomes that are not feasible in vivo, such as those selected under varying temperatures, in nonphysiological pH, and at varying redox levels.[346−348]

7. SUMMARY

During the rooting of life, the onset of protein coding led to complex macromolecular structures and functions. Translation of mRNA into protein by the ribosome set the path of biology that has dominated the Earth for over 3.8 billion years. Data derived from ribosomal structures suggest incremental and hierarchical evolution of protein-type polymers in concert with incremental evolution of RNA-type polymers. The extant ribosome exerts profound influence on protein folding.[259,291,349−351] Protein folding and the exit tunnel coevolved. Protein evolution was continuously guided and accelerated by interactions with rRNA. rRNA evolution was guided and accelerated by interactions with peptides and then proteins. RNA and protein, during the rooting of the TOL, established a molecular mutualism.

AUTHOR INFORMATION

Corresponding Author

Loren Dean Williams − *Center for the Origins of Life, School of Chemistry and Biochemistry, Georgia Institute of Technology, Atlanta, Georgia 30332, United States;* orcid.org/0000-0002-7215-4194; Email: loren.williams@chemistry.gatech.edu

Authors

Jessica C. Bowman − *Center for the Origins of Life, School of Chemistry and Biochemistry, Georgia Institute of Technology, Atlanta, Georgia 30332, United States*

Anton S. Petrov − *Center for the Origins of Life, School of Chemistry and Biochemistry, Georgia Institute of Technology, Atlanta, Georgia 30332, United States*

Moran Frenkel-Pinter − *Center for the Origins of Life, School of Chemistry and Biochemistry, Georgia Institute of Technology, Atlanta, Georgia 30332, United States*

Petar I. Penev − *Center for the Origins of Life, School of Chemistry and Biochemistry, Georgia Institute of Technology, Atlanta, Georgia 30332, United States*

Complete contact information is available at: https://pubs.acs.org/10.1021/acs.chemrev.9b00742

Notes

The authors declare no competing financial interest.

Biographies

Jessica C. Bowman received her B.Sc. in Biology from Kennesaw State University. In 2009, she joined Loren Williams' research group at Georgia Tech to work in the area of ribosome origins and evolution. Since 2018, she has worked as a Research Scientist in the same group and is a member of the NASA Center for the Origins of Life. Her research interests focus on early translation and catalysis.

Anton S. Petrov received his M.Sc. in Chemistry from Perm State University (Russia) and Ph.D. in Physical Chemistry from the University of Louisville. He was a Postdoctoral Fellow with Stephen C. Harvey and is currently a Research Scientist with Loren Williams at Georgia Tech and a member of the NASA Center for the Origins of Life. He studies the origins of the ribosome biopolymers and their mutualistic relationships, attempting to answer fundamental questions in the origins of life.

Moran Frenkel-Pinter received her B.Sc., M.Sc., and Ph.D. in Biotechnology from Tel Aviv University in Israel. As a NASA postdoctoral fellow, she worked with Loren Dean Williams, Nick Hud, and Martha Grover in the School of Chemistry and Biochemistry at Georgia Tech. Moran is currently a Research Scientist at Georgia Tech and a member of the NSF/NASA Center for Chemical Evolution as well as the NASA Center for the Origins of Life. Coming from a peptide self-assembly background, Moran is interested in elucidating mechanisms of formation of protopolymers

https://dx.doi.org/10.1021/acs.chemrev.9b00742
Chem. Rev. XXXX, XXX, XXX−XXX

that can spontaneously polymerize, fold, and function under prebiotic conditions.

Petar I. Penev received his B.Sc. in Molecular Biology from Sofia University and was awarded a Fulbright Scholarship and obtained a M.Sc. in bioinformatics at Georgia Tech. He is currently obtaining his Ph.D. in the laboratory of Loren Williams and is a member of the NASA Center for the Origins of Life.

Loren Dean Williams received his B.Sc. in Chemistry from the University of Washington and his Ph.D. in Physical Chemistry from Duke University. He was a graduate student with Barbara Ramsay Shaw at Duke and a Postdoctoral Fellow in the laboratory of Alexander Rich at MIT. He is currently a Professor at Georgia Tech in the School of Chemistry and Biochemistry and is Director of the NASA Center for the Origin of Life (COOL). His research is focused on nucleic acid biophysics and the origins and evolution of the ribosome.

ACKNOWLEDGMENTS

This manuscript is dedicated to the memory of Professor Jonathan R. Warner. We thank Vahab Rajaei and Drs. Claudia Alvarez, George Fox, Jennifer Glass, Robin Gutell, Sergey Melnikov, George Rose, and Ada Yonath for critical review of the manuscript. This work was supported by NASA grant 80NSSC18K1139. M.F.P. acknowledges the NASA Postdoctoral Fellowship program.

ABBREVIATIONS USED

aaRS = amino acyl tRNA synthetase
AES = ancestral expansion segments in the LSU
aes = ancestral expansion segments in the SSU
DCC = decoding center
ES = expansion segment in eukaryotic LSU rRNA
es = expansion segment in eukaryotic SSU rRNA
μ-ES = expansion segment in archaeal LSU rRNA
μ-es = expansion segment in archaeal SSU rRNA
GOE = Great Oxidation Event
LAECA = last archaeal and eukaryotic common ancestor
LECA = last eukaryotic common ancestor
LMCA = last metazoan common ancestor
LUCA = last universal common ancestor
LSU = large ribosomal subunit
PTC = peptidyl transferase center
rProtein = ribosomal protein
rRNA = rRNA
SSU = small ribosomal subunit
TOL = tree of Life

REFERENCES

(1) Woese, C. R.; Fox, G. E. Phylogenetic Structure of the Prokaryotic Domain: The Primary Kingdoms. *Proc. Natl. Acad. Sci. U. S. A.* **1977**, *74*, 5088−5090.
(2) Woese, C. R.; Kandler, O.; Wheelis, M. L. Towards a Natural System of Organisms: Proposal for the Domains Archaea, Bacteria, and Eucarya. *Proc. Natl. Acad. Sci. U. S. A.* **1990**, *87*, 4576−4579.
(3) Ciccarelli, F. D.; Doerks, T.; Von Mering, C.; Creevey, C. J.; Snel, B.; Bork, P. Toward Automatic Reconstruction of a Highly Resolved Tree of Life. *Science* **2006**, *311*, 1283−1287.
(4) Fournier, G. P.; Gogarten, J. P. Rooting the Ribosomal Tree of Life. *Mol. Biol. Evol.* **2010**, *27*, 1792−1801.
(5) Keeling, P. J.; Burki, F. Progress Towards the Tree of Eukaryotes. *Curr. Biol.* **2019**, *29*, R808−R817.
(6) Hug, L. A.; Baker, B. J.; Anantharaman, K.; Brown, C. T.; Probst, A. J.; Castelle, C. J.; Butterfield, C. N.; Hernsdorf, A. W.; Amano, Y.; Ise, K.; Suzuki, Y.; Dudek, N.; Relman, D. A.; Finstad, K. M.; Amundson, R.; Thomas, B. C.; Banfield, J. F. A New View of the Tree of Life. *Nat. Microbiol.* **2016**, *1*, 16048.
(7) Guy, L.; Ettema, T. J. The Archaeal 'Tack'superphylum and the Origin of Eukaryotes. *Trends Microbiol.* **2011**, *19*, 580−587.
(8) Wilson, D. N.; Nierhaus, K. H. The Ribosome through the Looking Glass. *Angew. Chem., Int. Ed.* **2003**, *42*, 3464−3486.
(9) Bashan, A.; Yonath, A. Ribosome Crystallography: Catalysis and Evolution of Peptide-Bond Formation, Nascent Chain Elongation and Its Co-Translational Folding. *Biochem. Soc. Trans.* **2005**, *33*, 488−492.
(10) Steitz, T. A. A Structural Understanding of the Dynamic Ribosome Machine. *Nat. Rev. Mol. Cell Biol.* **2008**, *9*, 242.
(11) Schmeing, T. M.; Ramakrishnan, V. What Recent Ribosome Structures Have Revealed About the Mechanism of Translation. *Nature* **2009**, *461*, 1234.
(12) Moore, P. B.; Steitz, T. A. The Structural Basis of Large Ribosomal Subunit Function. *Annu. Rev. Biochem.* **2003**, *72*, 813−850.
(13) Harris, J. K.; Kelley, S. T.; Spiegelman, G. B.; Pace, N. R. The Genetic Core of the Universal Ancestor. *Genome Res.* **2003**, *13*, 407−412.
(14) Koonin, E. V. Comparative Genomics, Minimal Gene-Sets and the Last Universal Common Ancestor. *Nat. Rev. Microbiol.* **2003**, *1*, 127−136.
(15) Charlebois, R. L.; Doolittle, W. F. Computing Prokaryotic Gene Ubiquity: Rescuing the Core from Extinction. *Genome Res.* **2004**, *14*, 2469−2477.
(16) Kovacs, N. A.; Penev, P. I.; Venapally, A.; Petrov, A. S.; Williams, L. D. Circular Permutation Obscures Universality of a Ribosomal Protein. *J. Mol. Evol.* **2018**, *86*, 581−592.
(17) Hsiao, C.; Mohan, S.; Kalahar, B. K.; Williams, L. D. Peeling the Onion: Ribosomes Are Ancient Molecular Fossils. *Mol. Biol. Evol.* **2009**, *26*, 2415−2425.
(18) Melnikov, S.; Ben-Shem, A.; Garreau de Loubresse, N.; Jenner, L.; Yusupova, G.; Yusupov, M. One Core, Two Shells: Bacterial and Eukaryotic Ribosomes. *Nat. Struct. Mol. Biol.* **2012**, *19*, 560−567.
(19) Bernier, C. R.; Petrov, A. S.; Kovacs, N. A.; Penev, P. I.; Williams, L. D. Translation: The Universal Structural Core of Life. *Mol. Biol. Evol.* **2018**, *35*, 2065−2076.
(20) Wekselman, I.; Davidovich, C.; Agmon, I.; Zimmerman, E.; Rozenberg, H.; Bashan, A.; Berisio, R.; Yonath, A. Ribosome's Mode of Function: Myths, Facts and Recent Results. *J. Pept. Sci.* **2009**, *15*, 122−130.
(21) Agmon, I.; Bashan, A.; Yonath, A. On Ribosome Conservation and Evolution. *Isr. J. Ecol. Evol.* **2006**, *52*, 359−374.
(22) Agmon, I.; Bashan, A.; Zarivach, R.; Yonath, A. Symmetry at the Active Site of the Ribosome: Structural and Functional Implications. *Biol. Chem.* **2005**, *386*, 833−844.
(23) Agmon, I.; Davidovich, C.; Bashan, A.; Yonath, A. Identification of the Prebiotic Translation Apparatus within the Contemporary Ribosome. *Nat. Preced.* **2009**. DOI: 10.1038/npre.2009.2921.1
(24) Wilson, D. N.; Nierhaus, K. H. Ribosomal Proteins in the Spotlight. *Crit. Rev. Biochem. Mol. Biol.* **2005**, *40*, 243−267.
(25) Voorhees, R. M.; Ramakrishnan, V. Structural Basis of the Translational Elongation Cycle. *Annu. Rev. Biochem.* **2013**, *82*, 203−236.
(26) Roux, P. P.; Shahbazian, D.; Vu, H.; Holz, M. K.; Cohen, M. S.; Taunton, J.; Sonenberg, N.; Blenis, J. Ras/Erk Signaling Promotes Site-Specific Ribosomal Protein S6 Phosphorylation Via Rsk and Stimulates Cap-Dependent Translation. *J. Biol. Chem.* **2007**, *282*, 14056−14064.
(27) Ban, N.; Beckmann, R.; Cate, J. H.; Dinman, J. D; Dragon, F.; Ellis, S. R; Lafontaine, D. L.; Lindahl, L.; Liljas, A.; Lipton, J. M; McAlear, M. A; Moore, P. B; Noller, H. F; Ortega, J.; Panse, V. G.; Ramakrishnan, V; Spahn, C. M.; Steitz, T. A; Tchorzewski, M.; Tollervey, D.; Warren, A. J; Williamson, J. R; Wilson, D.; Yonath, A.; Yusupov, M. A New System for Naming Ribosomal Proteins. *Curr. Opin. Struct. Biol.* **2014**, *24*, 165−169.
(28) McCutcheon, J. P.; Moran, N. A. Extreme Genome Reduction in Symbiotic Bacteria. *Nat. Rev. Microbiol.* **2012**, *10*, 13.

https://dx.doi.org/10.1021/acs.chemrev.9b00742
Chem. Rev. XXXX, XXX, XXX−XXX

(29) Moran, N. A. Microbial Minimalism: Genome Reduction in Bacterial Pathogens. *Cell* **2002**, *108*, 583−586.
(30) Peyretaillade, E.; Biderre, C.; Peyret, P.; Duffieux, F.; Méténier, G.; Gouy, M.; Michot, B.; Vivarès, C. P. Microsporidian Encephalitozoon Cuniculi, a Unicellular Eukaryote with an Unusual Chromosomal Dispersion of Ribosomal Genes and a Lsu rRNA Reduced to the Universal Core. *Nucleic Acids Res.* **1998**, *26*, 3513−3520.
(31) Barandun, J.; Hunziker, M.; Vossbrinck, C. R.; Klinge, S. Evolutionary Compaction and Adaptation Visualized by the Structure of the Dormant Microsporidian Ribosome. *Nat. Microbiol.* **2019**, *4*, 1798−1804.
(32) Hillis, D. M.; Dixon, M. T. Ribosomal DNA: Molecular Evolution and Phylogenetic Inference. *Q. Rev. Biol.* **1991**, *66*, 411−453.
(33) Melnikov, S.; Manakongtreecheep, K.; Rivera, K.; Makarenko, A.; Pappin, D.; Söll, D. Muller's Ratchet and Ribosome Degeneration in the Obligate Intracellular Parasites Microsporidia. *Int. J. Mol. Sci.* **2018**, *19*, 4125.
(34) Nikolaeva, D. D.; Gelfand, M. S.; Garushyants, S. K. Simplification of Ribosomes in Bacteria with Tiny Genomes. *bioRxiv* **2019**, 755876.
(35) Haag, E. S.; Dinman, J. D. Still Searching for Specialized Ribosomes. *Dev. Cell* **2019**, *48*, 744−746.
(36) Segev, N.; Gerst, J. E. Specialized Ribosomes and Specific Ribosomal Protein Paralogs Control Translation of Mitochondrial Proteins. *J. Cell Biol.* **2018**, *217*, 117−126.
(37) Shi, Z.; Barna, M. Translating the Genome in Time and Space: Specialized Ribosomes, RNA Regulons, and RNA-Binding Proteins. *Annu. Rev. Cell Dev. Biol.* **2015**, *31*, 31−54.
(38) Xue, S.; Barna, M. Specialized Ribosomes: A New Frontier in Gene Regulation and Organismal Biology. *Nat. Rev. Mol. Cell Biol.* **2012**, *13*, 355.
(39) Sloan, K. E.; Warda, A. S.; Sharma, S.; Entian, K.-D.; Lafontaine, D. L.; Bohnsack, M. T. Tuning the Ribosome: The Influence of rRNA Modification on Eukaryotic Ribosome Biogenesis and Function. *RNA Biol.* **2017**, *14*, 1138−1152.
(40) Uechi, T.; Nakajima, Y.; Nakao, A.; Torihara, H.; Chakraborty, A.; Inoue, K.; Kenmochi, N. Ribosomal Protein Gene Knockdown Causes Developmental Defects in Zebrafish. *PLoS One* **2006**, *1*, No. e37.
(41) Dashti, A.; Schwander, P.; Langlois, R.; Fung, R.; Li, W.; Hosseinizadeh, A.; Liao, H. Y.; Pallesen, J.; Sharma, G.; Stupina, V. A.; Simon, A. E.; Dinman, J. D.; Frank, J.; Ourmazd, A. Trajectories of the Ribosome as a Brownian Nanomachine. *Proc. Natl. Acad. Sci. U. S. A.* **2014**, *111*, 17492−17497.
(42) Whitford, P. C.; Blanchard, S. C.; Cate, J. H.; Sanbonmatsu, K. Y. Connecting the Kinetics and Energy Landscape of tRNA Translocation on the Ribosome. *PLoS Comput. Biol.* **2013**, *9*, No. e1003003.
(43) Dabbs, E. Selection for *Escherichia coli* Mutants with Proteins Missing from the Ribosome. *J. Bacteriol.* **1979**, *140*, 734−737.
(44) Shoji, S.; Dambacher, C. M.; Shajani, Z.; Williamson, J. R.; Schultz, P. G. Systematic Chromosomal Deletion of Bacterial Ribosomal Protein Genes. *J. Mol. Biol.* **2011**, *413*, 751−761.
(45) Baba, T.; Ara, T.; Hasegawa, M.; Takai, Y.; Okumura, Y.; Baba, M.; Datsenko, K. A.; Tomita, M.; Wanner, B. L.; Mori, H. Construction of *Escherichia coli* K-12 in-Frame, Single-Gene Knockout Mutants: The Keio Collection. *Mol. Syst. Biol.* **2006**, *2*, 2006.0008.
(46) Monro, R. E. Catalysis of Peptide Bond Formation by 50S Ribosomal Subunits from *Escherichia coli*. *J. Mol. Biol.* **1967**, *26*, 147−151.
(47) Monro, R. E.: Ribosomal Peptidyltransferase: The Fragment Reaction. In *Methods in Enzymology*; Elsevier, 1971; Vol. *20*; pp 472−481.
(48) Khaitovich, P.; Mankin, A. S.; Green, R.; Lancaster, L.; Noller, H. F. Characterization of Functionally Active Subribosomal Particles from Thermus Aquaticus. *Proc. Natl. Acad. Sci. U. S. A.* **1999**, *96*, 85−90.
(49) Nirenberg, M.; Leder, P. RNA Codewords and Protein Synthesis: The Effect of Trinucleotides Upon the Binding of sRNA to Ribosomes. *Science* **1964**, *145*, 1399−1407.
(50) Lill, R.; Robertson, J. M.; Wintermeyer, W. Affinities of tRNA Binding Sites of Ribosomes from *Escherichia coli*. *Biochemistry* **1986**, *25*, 3245−3255.
(51) Pestka, S. Studies on the Formation of Transfer Ribonucleic Acid-Ribosome Complexes III. The Formation of Peptide Bonds by Ribosomes in the Absence of Supernatant Enzymes. *J. Biol. Chem.* **1968**, *243*, 2810−2820.
(52) Belitsina, N.; Glukhova, M.; Spirin, A. Stepwise Elongation Factor G-Promoted Elongation of Polypeptides on the Ribosome without GTP Cleavage. *J. Mol. Biol.* **1976**, *108*, 609−613.
(53) Gavrilova, L.; Kostiashkina, O.; Koteliansky, V.; Rutkevitch, N.; Spirin, A. Factor-Free ("Non-Enzymic") and Factor-Dependent Systems of Translation of Polyuridylic Acid by *Escherichia coli* Ribosomes. *J. Mol. Biol.* **1976**, *101*, 537−552.
(54) Buttgereit, F.; Brand, M. D. A Hierarchy of ATP-Consuming Processes in Mammalian Cells. *Biochem. J.* **1995**, *312*, 163−167.
(55) Russell, J. B.; Cook, G. M. Energetics of Bacterial Growth: Balance of Anabolic and Catabolic Reactions. *Microbiol. Rev.* **1995**, *59*, 48−62.
(56) Reuveni, S.; Ehrenberg, M.; Paulsson, J. Ribosomes Are Optimized for Autocatalytic Production. *Nature* **2017**, *547*, 293.
(57) Lynch, M.; Marinov, G. K. The Bioenergetic Costs of a Gene. *Proc. Natl. Acad. Sci. U. S. A.* **2015**, *112*, 15690−15695.
(58) Nierhaus, K. H.; Brimacombe, R.; Nowotny, V.; Pon, C. L.; Rheinberger, H.-J.; Wittmann-Liebold, B.; Wittmann, H.-G.: New Aspects of Structure, Assembly, Evolution, and Function of Ribosomes. In *Cold Spring Harbor Symposium in Quantum Biology*; Cold Spring Harbor Laboratory Press, 1987; Vol. *52*; pp 665−674.
(59) Traub, P.; Nomura, i. Structure and Function of E. Coli Ribosomes. V. Reconstitution of Functionally Active 30S Ribosomal Particles from RNA and Proteins. *Proc. Natl. Acad. Sci. U. S. A.* **1968**, *59*, 777.
(60) Shajani, Z.; Sykes, M. T.; Williamson, J. R. Assembly of Bacterial Ribosomes. *Annu. Rev. Biochem.* **2011**, *80*, 501−526.
(61) Woodson, S. A. RNA Folding and Ribosome Assembly. *Curr. Opin. Chem. Biol.* **2008**, *12*, 667−673.
(62) Moss, T.; Langlois, F.; Gagnon-Kugler, T.; Stefanovsky, V. A Housekeeper with Power of Attorney: The rRNA Genes in Ribosome Biogenesis. *Cell. Mol. Life Sci.* **2007**, *64*, 29−49.
(63) Rudra, D.; Warner, J. R. What Better Measure Than Ribosome Synthesis? *Genes Dev.* **2004**, *18*, 2431−2436.
(64) Warner, J. R. The Economics of Ribosome Biosynthesis in Yeast. *Trends Biochem. Sci.* **1999**, *24*, 437−440.
(65) Lafontaine, D. L. Noncoding RNAs in Eukaryotic Ribosome Biogenesis and Function. *Nat. Struct. Mol. Biol.* **2015**, *22*, 11.
(66) Mitterer, V.; Gantenbein, N.; Birner-Gruenberger, R.; Murat, G.; Bergler, H.; Kressler, D.; Pertschy, B. Nuclear Import of Dimerized Ribosomal Protein Rps3 in Complex with Its Chaperone Yar1. *Sci. Rep.* **2016**, *6*, 36714.
(67) Pausch, P.; Singh, U.; Ahmed, Y. L.; Pillet, B.; Murat, G.; Altegoer, F.; Stier, G.; Thoms, M.; Hurt, E.; Sinning, I.; Bange, G.; Kressler, D. Co-Translational Capturing of Nascent Ribosomal Proteins by Their Dedicated Chaperones. *Nat. Commun.* **2015**, *6*, 7494.
(68) Pillet, B.; García-Gómez, J. J.; Pausch, P.; Falquet, L.; Bange, G.; de la Cruz, J.; Kressler, D. The Dedicated Chaperone Acl4 Escorts Ribosomal Protein Rpl4 to Its Nuclear Pre-60S Assembly Site. *PLoS Genet.* **2015**, *11*, No. e1005565.
(69) Stelter, P.; Huber, F. M.; Kunze, R.; Flemming, D.; Hoelz, A.; Hurt, E. Coordinated Ribosomal L4 Protein Assembly into the Pre-Ribosome Is Regulated by Its Eukaryote-Specific Extension. *Mol. Cell* **2015**, *58*, 854−862.
(70) Nerurkar, P.; Altvater, M.; Gerhardy, S.; Schuetz, S.; Fischer, U.; Weirich, C.; Panse, V. G. Eukaryotic Ribosome Assembly and Nuclear Export. *Int. Rev. Cell Mol. Biol.* **2015**, *319*, 107−140.

https://dx.doi.org/10.1021/acs.chemrev.9b00742
Chem. Rev. XXXX, XXX, XXX−XXX

(71) Warner, J. R. Twenty Years of Ribosome Assembly and Ribosomopathies. *RNA* **2015**, *21*, 758−759.
(72) Baßler, J.; Hurt, E. Eukaryotic Ribosome Assembly. *Annu. Rev. Biochem.* **2019**, *88*, 281−306.
(73) Grummt, I. Regulation of Mammalian Ribosomal Gene Transcription by RNA Polymerase I. *Prog. Nucleic Acid Res. Mol. Biol.* **1998**, *62*, 109−154.
(74) Shigeoka, T.; Koppers, M.; Wong, H. H.-W.; Lin, J. Q.; Cagnetta, R.; Dwivedy, A.; de Freitas Nascimento, J.; van Tartwijk, F. W.; Strohl, F.; Cioni, J.-M.; Schaeffer, J.; Carrington, M.; Kaminski, C. F.; Jung, H.; Harris, W. A.; Holt, C. E. On-Site Ribosome Remodeling by Locally Synthesized Ribosomal Proteins in Axons. *Cell Rep.* **2019**, *29*, 3605.
(75) Rudra, D.; Zhao, Y.; Warner, J. R. Central Role of Ifh1p-Fhl1p Interaction in the Synthesis of Yeast Ribosomal Proteins. *EMBO J.* **2005**, *24*, 533−542.
(76) Metzl-Raz, E.; Kafri, M.; Yaakov, G.; Soifer, I.; Gurvich, Y.; Barkai, N. Principles of Cellular Resource Allocation Revealed by Condition-Dependent Proteome Profiling. *eLife* **2017**, *6*, No. e28034.
(77) Bakshi, S.; Siryaporn, A.; Goulian, M.; Weisshaar, J. C. Superresolution Imaging of Ribosomes and RNA Polymerase in Live Escherichia coli Cells. *Mol. Microbiol.* **2012**, *85*, 21−38.
(78) Brauer, M. J.; Huttenhower, C.; Airoldi, E. M.; Rosenstein, R.; Matese, J. C.; Gresham, D.; Boer, V. M.; Troyanskaya, O. G.; Botstein, D. Coordination of Growth Rate, Cell Cycle, Stress Response, and Metabolic Activity in Yeast. *Mol. Biol. Cell* **2008**, *19*, 352−367.
(79) Bosdriesz, E.; Molenaar, D.; Teusink, B.; Bruggeman, F. J. How Fast-Growing Bacteria Robustly Tune Their Ribosome Concentration to Approximate Growth-Rate Maximization. *FEBS J.* **2015**, *282*, 2029−2044.
(80) Rolfe, D.; Brown, G. C. Cellular Energy Utilization and Molecular Origin of Standard Metabolic Rate in Mammals. *Physiol. Rev.* **1997**, *77*, 731−758.
(81) Neidhardt, F. C.; Ingraham, J. L.; Schaechter, M.: *Physiology of the Bacterial Cell: A Molecular Approach*; Sinauer Associates: Sunderland, MA, 1990; Vol. *20*.
(82) Ortiz, J. O.; Förster, F.; Kürner, J.; Linaroudis, A. A.; Baumeister, W. Mapping 70S Ribosomes in Intact Cells by Cryoelectron Tomography and Pattern Recognition. *J. Struct. Biol.* **2006**, *156*, 334−341.
(83) Kempes, C. P.; Wang, L.; Amend, J. P.; Doyle, J.; Hoehler, T. Evolutionary Tradeoffs in Cellular Composition across Diverse Bacteria. *ISME J.* **2016**, *10*, 2145.
(84) Crick, F. Central Dogma of Molecular Biology. *Nature* **1970**, *227*, 561−563.
(85) Bremer, H.; Dennis, P. P. Modulation of Chemical Composition and Other Parameters of the Cell by Growth Rates. *EcoSal Plus* **2008**, *3*, 5.2.3.
(86) Milo, R.; Phillips, R.: *Cell Biology by the Numbers*; Garland Science, 2015.
(87) Hu, P.; Janga, S. C.; Babu, M.; Díaz-Mejía, J. J.; Butland, G.; Yang, W.; Pogoutse, O.; Guo, X.; Phanse, S.; Wong, P.; Chandran, S.; Christopoulos, C.; Nazarians-Armavil, A.; Nasseri, N. K.; Musso, G.; Ali, M.; Nazemof, N.; Eroukova, V.; Golshani, A.; Paccanaro, A.; Greenblatt, J. F.; Moreno-Hagelsieb, G.; Emili, A. Global Functional Atlas of *Escherichia coli* Encompassing Previously Uncharacterized Proteins. *PLoS Biol.* **2009**, *7*, No. e1000096.
(88) Shimoda, Y.; Shinpo, S.; Kohara, M.; Nakamura, Y.; Tabata, S.; Sato, S. A Large Scale Analysis of Protein-Protein Interactions in the Nitrogen-Fixing Bacterium *Mesorhizobium Loti*. *DNA Res.* **2008**, *15*, 13−23.
(89) Guo, J.; Li, H.; Chang, J.-W.; Lei, Y.; Li, S.; Chen, L.-L. Prediction and Characterization of Protein-Protein Interaction Network in *Xanthomonas oryzae* Pv. Oryzae Pxo99a. *Res. Microbiol.* **2013**, *164*, 1035−1044.
(90) Vo, T. V.; Das, J.; Meyer, M. J.; Cordero, N. A.; Akturk, N.; Wei, X.; Fair, B. J.; Degatano, A. G.; Fragoza, R.; Liu, L. G.; Matsuyama, A.; Trickey, M.; Horibata, S.; Grimson, A.; Yamano, H.; Yoshida, M.; Roth, F. P.; Pleiss, J. A.; Xia, Y.; Yu, H. A Proteome-Wide Fission Yeast Interactome Reveals Network Evolution Principles from Yeasts to Human. *Cell* **2016**, *164*, 310−323.
(91) Dominissini, D.; Nachtergaele, S.; Moshitch-Moshkovitz, S.; Peer, E.; Kol, N.; Ben-Haim, M. S.; Dai, Q.; Di Segni, A.; Salmon-Divon, M.; Clark, W. C.; Zheng, G.; Pan, T.; Solomon, O.; Eyal, E.; Hershkovitz, V.; Han, D.; Doré, L. C.; Amariglio, N.; Rechavi, G.; He, C. The Dynamic N1-Methyladenosine Methylome in Eukaryotic Messenger RNA. *Nature* **2016**, *530*, 441.
(92) Wang, Y.-C.; Peterson, S. E.; Loring, J. F. Protein Post-Translational Modifications and Regulation of Pluripotency in Human Stem Cells. *Cell Res.* **2014**, *24*, 143−160.
(93) Butland, G.; Peregrin-Alvarez, J. M.; Li, J.; Yang, W.; Yang, X.; Canadien, V.; Starostine, A.; Richards, D.; Beattie, B.; Krogan, N.; Davey, M.; Parkinson, J.; Greenblatt, J.; Emili, A. Interaction Network Containing Conserved and Essential Protein Complexes in *Escherichia coli*. *Nature* **2005**, *433*, 531.
(94) Lindström, M. S. Emerging Functions of Ribosomal Proteins in Gene-Specific Transcription and Translation. *Biochem. Biophys. Res. Commun.* **2009**, *379*, 167−170.
(95) Warner, J. R.; McIntosh, K. B. How Common Are Extraribosomal Functions of Ribosomal Proteins? *Mol. Cell* **2009**, *34*, 3−11.
(96) Zengel, J. M.; Lindahl, L.: Diverse Mechanisms for Regulating Ribosomal Protein Synthesis in *Escherichia coli*. In *Progress in Nucleic Acid Research and Molecular Biology*; Elsevier, 1994; Vol. *47*; pp 331−370.
(97) Keener, J.; M, N.: Regulation of Ribosome Synthesis. In *Escherichia coli and Salmonella: Cellular and Molecular Biology*; C, N. F., Curtiss, R., III, Ingraham, J. L., Lin, E. C. C., Low, K. B., Magasanik, B., Reznikoff, W. S., Riley, M., Schaechter, M., Umbarger, H. E., Eds.; American Society for Microbiology: Washington, DC, 1996; pp 1417−1431.
(98) Singh, D.; Chang, S.-J.; Lin, P.-H.; Averina, O. V.; Kaberdin, V. R.; Lin-Chao, S. Regulation of Ribonuclease E Activity by the L4 Ribosomal Protein of *Escherichia coli*. *Proc. Natl. Acad. Sci. U. S. A.* **2009**, *106*, 864−869.
(99) Flygare, J.; Kiefer, T.; Miyake, K.; Utsugisawa, T.; Hamaguchi, I.; Da Costa, L.; Richter, J.; Davey, E. J.; Matsson, H.; Dahl, N. Deficiency of Ribosomal Protein S19 in Cd34+ Cells Generated by siRNA Blocks Erythroid Development and Mimics Defects Seen in Diamond-Blackfan Anemia. *Blood* **2005**, *105*, 4627−4634.
(100) Anderson, S. J.; Lauritsen, J. P. H.; Hartman, M. G.; Foushee, A. M. D.; Lefebvre, J. M.; Shinton, S. A.; Gerhardt, B.; Hardy, R. R.; Oravecz, T.; Wiest, D. L. Ablation of Ribosomal Protein L22 Selectively Impairs Aβ T Cell Development by Activation of a P53-Dependent Checkpoint. *Immunity* **2007**, *26*, 759−772.
(101) Lindström, M. S.; Zhang, Y. Ribosomal Protein S9 is a Novel B23/Npm-Binding Protein Required for Normal Cell Proliferation. *J. Biol. Chem.* **2008**, *283*, 15568−15576.
(102) Kim, J. H.; You, K. R.; Kim, I. H.; Cho, B. H.; Kim, C. Y.; Kim, D. G. Over-Expression of the Ribosomal Protein L36a Gene Is Associated with Cellular Proliferation in Hepatocellular Carcinoma. *Hepatology* **2004**, *39*, 129−138.
(103) Hegde, V.; Wang, M.; Deutsch, W. A. Human Ribosomal Protein S3 Interacts with DNA Base Excision Repair Proteins Hape/Ref-1 and Hogg1. *Biochemistry* **2004**, *43*, 14211−14217.
(104) Kim, J.; Chubatsu, L. S.; Admon, A.; Stahl, J.; Fellous, R.; Linn, S. Implication of Mammalian Ribosomal Protein S3 in the Processing of DNA Damage. *J. Biol. Chem.* **1995**, *270*, 13620−13629.
(105) Horn, H.; Vousden, K. Cooperation between the Ribosomal Proteins L5 and L11 in the P53 Pathway. *Oncogene* **2008**, *27*, 5774.
(106) Dai, M.-S.; Lu, H. Inhibition of Mdm2-Mediated P53 Ubiquitination and Degradation by Ribosomal Protein L5. *J. Biol. Chem.* **2004**, *279*, 44475−44482.
(107) Lindström, M. S.; Jin, A.; Deisenroth, C.; White Wolf, G. W.; Zhang, Y. Cancer-Associated Mutations in the Mdm2 Zinc Finger Domain Disrupt Ribosomal Protein Interaction and Attenuate

https://dx.doi.org/10.1021/acs.chemrev.9b00742
Chem. Rev. XXXX, XXX, XXX−XXX

Mdm2-Induced P53 Degradation. *Mol. Cell. Biol.* **2007**, *27*, 1056−1068.
(108) Jin, A.; Itahana, K.; O'Keefe, K.; Zhang, Y. Inhibition of Hdm2 and Activation of P53 by Ribosomal Protein L23. *Mol. Cell. Biol.* **2004**, *24*, 7669−7680.
(109) Woese, C. R. On the Evolution of Cells. *Proc. Natl. Acad. Sci. U. S. A.* **2002**, *99*, 8742−8747.
(110) Olsen, G. J.; Woese, C. R. Lessons from an Archaeal Genome: What Are We Learning from *Methanococcus Jannaschii*? *Trends Genet.* **1996**, *12*, 377−379.
(111) Melnikov, S. V.; Kwok, H. S.; Manakongtreecheep, K.; van den Elzen, A.; Thoreen, C. C.; Soll, D. Archaeal Ribosomal Proteins Possess Nuclear Localization Signal-Type Motifs: Implications for the Origin of the Cell Nucleus. *Mol. Biol. Evol.* **2020**, *37*, 671966.
(112) Hsiao, C.; Lenz, T. K.; Peters, J. K.; Fang, P.-Y.; Schneider, D. M.; Anderson, E. J.; Preeprem, T.; Bowman, J. C.; O'Neill, E. B.; Lie, L.; Athavale, S. S.; Gossett, J. J.; Trippe, C.; Murray, J.; Petrov, A. S.; Wartell, R. M.; Harvey, S. C.; Hud, N. V.; Dean Williams, L. Molecular Paleontology: A Biochemical Model of the Ancestral Ribosome. *Nucleic Acids Res.* **2013**, *41*, 3373−3385.
(113) Petrov, A. S.; Bernier, C. R.; Hsiao, C.; Norris, A. M.; Kovacs, N. A.; Waterbury, C. C.; Stepanov, V. G.; Harvey, S. C.; Fox, G. E.; Wartell, R. M.; Hud, N. V.; Williams, L. D. Evolution of the Ribosome at Atomic Resolution. *Proc. Natl. Acad. Sci. U. S. A.* **2014**, *111*, 10251−10256.
(114) Petrov, A. S.; Gulen, B.; Norris, A. M.; Kovacs, N. A.; Bernier, C. R.; Lanier, K. A.; Fox, G. E.; Harvey, S. C.; Wartell, R. M.; Hud, N. V.; Williams, L. D. History of the Ribosome and the Origin of Translation. *Proc. Natl. Acad. Sci. U. S. A.* **2015**, *112*, 15396−15401.
(115) Kovacs, N. A.; Petrov, A. S.; Lanier, K. A.; Williams, L. D. Frozen in Time: The History of Proteins. *Mol. Biol. Evol.* **2017**, *34*, 1252−1260.
(116) Alva, V.; Söding, J.; Lupas, A. N. A Vocabulary of Ancient Peptides at the Origin of Folded Proteins. *eLife* **2015**, *4*, No. e09410.
(117) Söding, J.; Lupas, A. N. More Than the Sum of Their Parts: On the Evolution of Proteins from Peptides. *BioEssays* **2003**, *25*, 837−846.
(118) Lupas, A. N.; Alva, V. Ribosomal Proteins as Documents of the Transition from Unstructured (Poly) Peptides to Folded Proteins. *J. Struct. Biol.* **2017**, *198*, 74−81.
(119) Roberts, E.; Sethi, A.; Montoya, J.; Woese, C. R.; Luthey-Schulten, Z. Molecular Signatures of Ribosomal Evolution. *Proc. Natl. Acad. Sci. U. S. A.* **2008**, *105*, 13953−13958.
(120) Woese, C. R. Interpreting the Universal Phylogenetic Tree. *Proc. Natl. Acad. Sci. U. S. A.* **2000**, *97*, 8392−8396.
(121) Fox, G. E. Origin and Evolution of the Ribosome. *Cold Spring Harbor Perspect. Biol.* **2010**, *2*, No. a003483.
(122) Fox, G. E.; Naik, A. K.: The Evolutionary History of the Translation Machinery. In *The Genetic Code and the Origin of Life*; de Pouplana, L. R., Ed.; Kluwer Academic/Plenum Publishers, New York, 2004; pp 92−105.
(123) Gray, M. W.; Schnare, M. N.: Evolution of rRNA Gene Organization. In *Ribosomal RNA—Structure, Evolution, Processing, and Function in Protein Synthesis*; Zimmermann, R. A., Dahlberg, A. E., Eds.; CRC Press: Boca Raton, FL, 1996; pp 49−69.
(124) Wilde, S. A.; Valley, J. W.; Peck, W. H.; Graham, C. M. Evidence from Detrital Zircons for the Existence of Continental Crust and Oceans on the Earth 4.4 Gyr Ago. *Nature* **2001**, *409*, 175.
(125) Hoskin, P. W.; Schaltegger, U. The Composition of Zircon and Igneous and Metamorphic Petrogenesis. *Rev. Mineral. Geochem.* **2003**, *53*, 27−62.
(126) Glansdorff, N.; Xu, Y.; Labedan, B. The Last Universal Common Ancestor: Emergence, Constitution and Genetic Legacy of an Elusive Forerunner. *Biol. Direct* **2008**, *3*, 29.
(127) Cornish-Bowden, A.; Cárdenas, M. L. Life before Luca. *J. Theor. Biol.* **2017**, *434*, 68−74.
(128) Klein, D. J.; Moore, P. B.; Steitz, T. A. The Contribution of Metal Ions to the Structural Stability of the Large Ribosomal Subunit. *RNA* **2004**, *10*, 1366−1379.
(129) Hsiao, C.; Tannenbaum, M.; VanDeusen, H.; Hershkovitz, E.; Perng, G.; Tannenbaum, A.; Williams, L. D.: Complexes of Nucleic Acids with Group I and II Cations. In *Nucleic Acid-Metal Ion Interactions*; Hud, N. V., Ed.; The Royal Society of Chemistry: London, 2009; pp 1−35.
(130) Auffinger, P.; Grover, N.; Westhof, E. Metal Ion Binding to RNA. In *Structural and Catalytic Roles of Metal Ions in RNA*; Metal Ions in Life Sciences; Royal Society of Chemistry, 2011; Vol. *9*, p 1, .
(131) Woodson, S. A. Metal Ions and RNA Folding: A Highly Charged Topic with a Dynamic Future. *Curr. Opin. Chem. Biol.* **2005**, *9*, 104−109.
(132) Bowman, J. C.; Lenz, T. K.; Hud, N. V.; Williams, L. D. Cations in Charge: Magnesium Ions in RNA Folding and Catalysis. *Curr. Opin. Struct. Biol.* **2012**, *22*, 262.
(133) Gesteland, R. F. Unfolding of *Escherichia coli* Ribosomes by Removal of Magnesium. *J. Mol. Biol.* **1966**, *18*, 356−371.
(134) Schuwirth, B. S.; Borovinskaya, M. A.; Hau, C. W.; Zhang, W.; Vila-Sanjurjo, A.; Holton, J. M.; Cate, J. H. D. Structures of the Bacterial Ribosome at 3.5 Å Resolution. *Science* **2005**, *310*, 827−834.
(135) Selmer, M.; Dunham, C. M.; Murphy, F. V.; Weixlbaumer, A.; Petry, S.; Kelley, A. C.; Weir, J. R.; Ramakrishnan, V. Structure of the 70S Ribosome Complexed with mRNA and tRNA. *Science* **2006**, *313*, 1935−1942.
(136) Demeshkina, N.; Jenner, L.; Westhof, E.; Yusupov, M.; Yusupova, G. A New Understanding of the Decoding Principle on the Ribosome. *Nature* **2012**, *484*, 256.
(137) Petrov, A. S.; Bernier, C. R.; Hsiao, C.; Okafor, C. D.; Tannenbaum, E.; Stern, J.; Gaucher, E.; Schneider, D.; Hud, N. V.; Harvey, S. C.; Dean Williams, L. RNA-Magnesium-Protein Interactions in Large Ribosomal Subunit. *J. Phys. Chem. B* **2012**, *116*, 8113−8120.
(138) Romer, R.; Hach, R. tRNA Conformation and Magnesium Binding: A Study of Yeast Phenylalanine-Specific tRNA by a Fluorescent Indicator and Differential Melting Curves. *Eur. J. Biochem.* **1975**, *55*, 271−284.
(139) Cusack, S. Aminoacyl-tRNA Synthetases. *Curr. Opin. Struct. Biol.* **1997**, *7*, 881−889.
(140) Anbar, A. D. Elements and Evolution. *Science* **2008**, *322*, 1481−1483.
(141) Holland, H. D. The Oxygenation of the Atmosphere and Oceans. *Philos. Trans. R. Soc., B* **2006**, *361*, 903−915.
(142) Hazen, R. M.; Ferry, J. M. Mineral Evolution: Mineralogy in the Fourth Dimension. *Elements* **2010**, *6*, 9−12.
(143) Winterbourn, C. C. Toxicity of Iron and Hydrogen Peroxide: The Fenton Reaction. *Toxicol. Lett.* **1995**, *82*, 969−974.
(144) Bray, M. S.; Lenz, T. K.; Haynes, J. W.; Bowman, J. C.; Petrov, A. S.; Reddi, A. R.; Hud, N. V.; Williams, L. D.; Glass, J. B. Multiple Prebiotic Metals Mediate Translation. *Proc. Natl. Acad. Sci. U. S. A.* **2018**, *115*, 12164−12169.
(145) Lin, S.-Y.; Wang, Y.-C.; Hsiao, C. Prebiotic Iron Originates the Peptidyl Transfer Origin. *Mol. Biol. Evol.* **2019**, *36*, 999−1007.
(146) Guth-Metzler, R.; Bray, M. S.; Suttapitugsakul, S.; Montllor-Albalate, C.; Bowman, J. C.; Wu, R.; Reddi, A. R.; Okafor, C. D.; Glass, J. B.; Williams, L. D. Cutting In-line with Iron: Ribosomal Function and Non-Oxidative RNA Cleavage. *BiioRxiv* **2019**, DOI: 10.1101/851097.
(147) Hsiao, C.; Chou, I-C.; Okafor, C. D.; Bowman, J. C.; O'Neill, E. B.; Athavale, S. S.; Petrov, A. S.; Hud, N. V.; Wartell, R. M.; Harvey, S. C.; Williams, L. D. RNA with Iron (II) as a Cofactor Catalyses Electron Transfer. *Nat. Chem.* **2013**, *5*, 525.
(148) Yokoyama, T.; Suzuki, T. Ribosomal RNAs Are Tolerant toward Genetic Insertions: Evolutionary Origin of the Expansion Segments. *Nucleic Acids Res.* **2008**, *36*, 3539−3551.
(149) Shine, J.; Dalgarno, L. The 3′-Terminal Sequence of *Escherichia coli* 16S Ribosomal RNA: Complementarity to Nonsense Triplets and Ribosome Binding Sites. *Proc. Natl. Acad. Sci. U. S. A.* **1974**, *71*, 1342−1346.
(150) Gualerzi, C. O.; Pon, C. L. Initiation of mRNA Translation in Prokaryotes. *Biochemistry* **1990**, *29*, 5881−5889.

https://dx.doi.org/10.1021/acs.chemrev.9b00742
Chem. Rev. XXXX, XXX, XXX−XXX

(151) Hinnebusch, A. G. The Scanning Mechanism of Eukaryotic Translation Initiation. *Annu. Rev. Biochem.* **2014**, *83*, 779−812.
(152) Kozak, M. Initiation of Translation in Prokaryotes and Eukaryotes. *Gene* **1999**, *234*, 187−208.
(153) Kozak, M. Point Mutations Define a Sequence Flanking the AUG Initiator Codon That Modulates Translation by Eukaryotic Ribosomes. *Cell* **1986**, *44*, 283−292.
(154) Clark, C. G.; Tague, B. W.; Ware, V. C.; Gerbi, S. A. *Xenopus Laevis* 28S Ribosomal RNA: A Secondary Structure Model and Its Evolutionary and Functional Implications. *Nucleic Acids Res.* **1984**, *12*, 6197−6220.
(155) Gerbi, S. A.: Expansion Segments: Regions of Variable Size that Interrupt the Universal Core Secondary Structure of Ribosomal RNA. In *Ribosomal RNA—Structure, Evolution, Processing, and Function in Protein Synthesis*; Zimmermann, R. A., Dahlberg, A. E., Eds.; CRC Press: Boca Raton, FL, 1996; pp 71−87.
(156) Ware, V. C.; Tague, B. W.; Graham Clark, C.; Gourse, R. L.; Brand, R. C.; Gerbi, S. A. Sequence Analysis of 28S Ribosomal DNA from the Amphibian *Xenopus Laevis*. *Nucleic Acids Res.* **1983**, *11*, 7795−7817.
(157) Bachellerie, J.-P.; Michot, B. Evolution of Large Subunit rRNA Structure. The 3′ Terminal Domain Contains Elements of Secondary Structure Specific to Major Phylogenetic Groups. *Biochimie* **1989**, *71*, 701−709.
(158) Hassouna, N.; Mithot, B.; Bachellerie, J. P. The Complete Nucleotide Sequence of Mouse 28S rRNA Gene. Implications for the Process of Size Increase of the Large Subunit rRNA in Higher Eukaryotes. *Nucleic Acids Res.* **1984**, *12*, 3563−3583.
(159) Lapeyre, B.; Michot, B.; Feliu, J.; Bachellerie, J.-P. Nucleotide Sequence of the *Schizosaccharomyces Pombe* 25S Ribosomal RNA and Its Phylogenetic Implications. *Nucleic Acids Res.* **1993**, *21*, 3322−3322.
(160) Michot, B.; Bachellerie, J. P. Comparisons of Large Subunit rRNAs Reveal Some Eukaryote-Specific Elements of Secondary Structure. *Biochimie* **1987**, *69*, 11−23.
(161) Veldman, G. M.; Klootwijk, J.; de Regt, V. C.; Planta, R. J.; Branlant, C.; Krol, A.; Ebel, J.-P. The Primary and Secondary Structure of Yeast 26S rRNA. *Nucleic Acids Res.* **1981**, *9*, 6935−6952.
(162) Penev, P. I.; Fakhretaha-Aval, S.; Patel, V. J.; Cannone, J. J.; Gutell, R. R.; Petrov, A. S.; Williams, L. D.; Glass, J. B. Eukaryotic-Like Ribosomal RNA Region in Lokiarchaeota. *bioRxiv* **2019**, DOI: 10.1101/2019.12.25.888164
(163) Anger, A. M.; Armache, J.-P.; Berninghausen, O.; Habeck, M.; Subklewe, M.; Wilson, D. N.; Beckmann, R. Structures of the Human and Drosophila 80S Ribosome. *Nature* **2013**, *497*, 80.
(164) Mestre-Fos, S.; Penev, P. I.; Suttapitugsakul, S.; Hu, M.; Ito, C.; Petrov, A. S.; Wartell, R. M.; Wu, R.; Williams, L. D. G-Quadruplexes in Human Ribosomal RNA. *J. Mol. Biol.* **2019**, *431*, 1940−1955.
(165) Ben-Shem, A.; Jenner, L.; Yusupova, G.; Yusupov, M. Crystal Structure of the Eukaryotic Ribosome. *Science* **2010**, *330*, 1203−1209.
(166) Schnare, M. N.; Damberger, S. H.; Gray, M. W.; Gutell, R. R. Comprehensive Comparison of Structural Characteristics in Eukaryotic Cytoplasmic Large Subunit (23 S-Like) Ribosomal RNA. *J. Mol. Biol.* **1996**, *256*, 701−719.
(167) Rogers, S. O. Integrated Evolution of Ribosomal RNAs, Introns, and Intron Nurseries. *Genetica* **2019**, *147*, 103−119.
(168) Yoshihisa, T. Handling tRNA Introns, Archaeal Way and Eukaryotic Way. *Front. Genet.* **2014**, *5*, 213.
(169) Moore, P. B. Structural Motifs in RNA. *Annu. Rev. Biochem.* **1999**, *68*, 287−300.
(170) Fujishima, K.; Sugahara, J.; Tomita, M.; Kanai, A. Large-Scale tRNA Intron Transposition in the Archaeal Order Thermoproteales Represents a Novel Mechanism of Intron Gain. *Mol. Biol. Evol.* **2010**, *27*, 2233−2243.
(171) Sugahara, J.; Fujishima, K.; Nunoura, T.; Takaki, Y.; Takami, H.; Takai, K.; Tomita, M.; Kanai, A. Genomic Heterogeneity in a Natural Archaeal Population Suggests a Model of tRNA Gene Disruption. *PLoS One* **2012**, *7*, e32504.
(172) Tang, T. H.; Rozhdestvensky, T. S.; d'Orval, B. C.; Bortolin, M.-L.; Huber, H.; Charpentier, B.; Branlant, C.; Bachellerie, J.-P.; Brosius, J.; Hüttenhofer, A. RNomics in Archaea Reveals a Further Link between Splicing of Archaeal Introns and rRNA Processing. *Nucleic Acids Res.* **2002**, *30*, 921−930.
(173) Kaneta, A.; Fujishima, K.; Morikazu, W.; Hori, H.; Hirata, A. The RNA-Splicing Endonuclease from the Euryarchaeaon *Methanopyrus Kandleri* Is a Heterotetramer with Constrained Substrate Specificity. *Nucleic Acids Res.* **2018**, *46*, 1958−1972.
(174) Zaremba-Niedzwiedzka, K.; Caceres, E. F.; Saw, J. H.; Backstrom, D.; Juzokaite, L.; Vancaester, E.; Seitz, K. W.; Anantharaman, K.; Starnawski, P.; Kjeldsen, K. U.; Stott, M. B.; Nunoura, T.; Banfield, J. F.; Schramm, A.; Baker, B. J.; Spang, A.; Ettema, T. J. G. Asgard Archaea Illuminate the Origin of Eukaryotic Cellular Complexity. *Nature* **2017**, *541*, 353.
(175) Eme, L.; Spang, A.; Lombard, J.; Stairs, C. W.; Ettema, T. J. Archaea and the Origin of Eukaryotes. *Nat. Rev. Microbiol.* **2017**, *15*, 711.
(176) Wilson, D. N.; Doudna Cate, J. H. D. The Structure and Function of the Eukaryotic Ribosome. *Cold Spring Harbor Perspect. Biol.* **2012**, *4*, No. a011536.
(177) Klinge, S.; Voigts-Hoffmann, F.; Leibundgut, M.; Ban, N. Atomic Structures of the Eukaryotic Ribosome. *Trends Biochem. Sci.* **2012**, *37*, 189−198.
(178) Schuller, A. P.; Green, R. Roadblocks and Resolutions in Eukaryotic Translation. *Nat. Rev. Mol. Cell Biol.* **2018**, *19*, 526−541.
(179) Mestre-Fos, S.; Penev, P. I.; Richards, J. C.; Dean, W. L.; Gray, R. D.; Chaires, J. B.; Williams, L. D. Profusion of G-quadruplexes on Both Subunits of Metazoan Ribosomes. *PLoS One* **2019**, *14*, No. e0226177.
(180) Gould, S. J. *Full House: The Spread of Excellence from Plato to Darwin*; Harvard University Press: Cambridge, MA, 1998.
(181) Hedges, S. B.; Dudley, J.; Kumar, S. Timetree: A Public Knowledge-Base of Divergence Times among Organisms. *Bioinformatics* **2006**, *22*, 2971−2972.
(182) Lynch, M. The Frailty of Adaptive Hypotheses for the Origins of Organismal Complexity. *Proc. Natl. Acad. Sci. U. S. A.* **2007**, *104*, 8597−8604.
(183) Lynch, M.; Conery, J. S. The Origins of Genome Complexity. *Science* **2003**, *302*, 1401−1404.
(184) Koonin, E. V. Energetics and Population Genetics at the Root of Eukaryotic Cellular and Genomic Complexity. *Proc. Natl. Acad. Sci. U. S. A.* **2015**, *112*, 15777−15778.
(185) Allen, J. F. Why Chloroplasts and Mitochondria Retain Their Own Genomes and Genetic Systems: Colocation for Redox Regulation of Gene Expression. *Proc. Natl. Acad. Sci. U. S. A.* **2015**, *112*, 10231−10238.
(186) Gray, M. W. Mitochondrial Evolution. *Cold Spring Harbor Perspect. Biol.* **2012**, *4*, No. a011403.
(187) Gray, M. W. Mosaic Nature of the Mitochondrial Proteome: Implications for the Origin and Evolution of Mitochondria. *Proc. Natl. Acad. Sci. U. S. A.* **2015**, *112*, 10133−10138.
(188) Adams, K. L.; Palmer, J. D. Evolution of Mitochondrial Gene Content: Gene Loss and Transfer to the Nucleus. *Mol. Phylogenet. Evol.* **2003**, *29*, 380−395.
(189) Petrov, A. S.; Wood, E. C.; Bernier, C. R.; Norris, A. M.; Brown, A.; Amunts, A. Structural Patching Fosters Divergence of Mitochondrial Ribosomes. *Mol. Biol. Evol.* **2019**, *36*, 207−219.
(190) Timmis, J. N.; Ayliffe, M. A.; Huang, C. Y.; Martin, W. Endosymbiotic Gene Transfer: Organelle Genomes Forge Eukaryotic Chromosomes. *Nat. Rev. Genet.* **2004**, *5*, 123−135.
(191) Amunts, A.; Brown, A.; Toots, J.; Scheres, S. H. W.; Ramakrishnan, V. The Structure of the Human Mitochondrial Ribosome. *Science* **2015**, *348*, 95−98.
(192) Greber, B. J.; Bieri, P.; Leibundgut, M.; Leitner, A.; Aebersold, R.; Boehringer, D.; Ban, N. The Complete Structure of the 55S Mammalian Mitochondrial Ribosome. *Science* **2015**, *348*, 303−308.
(193) Amunts, A.; Brown, A.; Bai, X. C.; Llacer, J. L.; Hussain, T.; Emsley, P.; Long, F.; Murshudov, G.; Scheres, S. H.; Ramakrishnan,

https://dx.doi.org/10.1021/acs.chemrev.9b00742
Chem. Rev. XXXX, XXX, XXX−XXX

V. Structure of the Yeast Mitochondrial Large Ribosomal Subunit. *Science* **2014**, *343*, 1485−1489.
(194) Desai, N.; Brown, A.; Amunts, A.; Ramakrishnan, V. The Structure of the Yeast Mitochondrial Ribosome. *Science* **2017**, *355*, 528−531.
(195) Mears, J. A.; Cannone, J. J.; Stagg, S. M.; Gutell, R. R.; Agrawal, R. K.; Harvey, S. C. Modeling a Minimal Ribosome Based on Comparative Sequence Analysis. *J. Mol. Biol.* **2002**, *321*, 215−234.
(196) Fox, G. E.; Woese, C. R. 5S RNA Secondary Structure. *Nature* **1975**, *256*, 505−507.
(197) Woese, C.R.; Magrum, L.J.; Gupta, R.; Siegel, R.B.; Stahl, D.A.; Kop, J.; Crawford, N.; Brosius, R.; Gutell, R.; Hogan, J.J.; Noller, H. F. Secondary Structure Model for Bacterial 16S Ribosomal RNA: Phylogenetic, Enzymatic and Chemical Evidence. *Nucleic Acids Res.* **1980**, *8*, 2275−2294.
(198) Noller, H. F.; Kop, J.; Wheaton, V.; Brosius, J.; Gutell, R. R.; Kopylov, A. M.; Dohme, F.; Herr, W.; Stahl, D. A.; Gupta, R.; Woese, C. R. Secondary Structure Model for 23S Ribosomal RNA. *Nucleic Acids Res.* **1981**, *9*, 6167−6189.
(199) Gutell, R. R.; Larsen, N.; Woese, C. R. Lessons from an Evolving rRNA: 16S and 23S rRNA Structures from a Comparative Perspective. *Microbiol. Rev.* **1994**, *58*, 10.
(200) Gutell, R. R.; Lee, J. C.; Cannone, J. J. The Accuracy of Ribosomal RNA Comparative Structure Models. *Curr. Opin. Struct. Biol.* **2002**, *12*, 301−310.
(201) Wang, S.; Gutell, R. R.; Miranker, D. P. Biclustering as a Method for RNA Local Multiple Sequence Alignment. *Bioinformatics* **2007**, *23*, 3289−3296.
(202) Xu, W.; Ozer, S.; Gutell, R. R. Covariant Evolutionary Event Analysis for Base Interaction Prediction Using a Relational Database Management System for RNA In *Scientific and Statistical Database Management*; Springer2009; pp 200−216.
(203) Ban, N.; Nissen, P.; Hansen, J.; Moore, P. B.; Steitz, T. A. The Complete Atomic Structure of the Large Ribosomal Subunit at 2.4 Å Resolution. *Science* **2000**, *289*, 905−920.
(204) Wimberly, B. T.; Brodersen, D. E.; Clemons, W. M., Jr.; Morgan-Warren, R. J.; Carter, A. P.; Vonrhein, C.; Hartsch, T.; Ramakrishnan, V. Structure of the 30S Ribosomal Subunit. *Nature* **2000**, *407*, 327−339.
(205) Leontis, N. B.; Westhof, E. Analysis of RNA Motifs. *Curr. Opin. Struct. Biol.* **2003**, *13*, 300−308.
(206) Leontis, N. B.; Westhof, E. A Common Motif Organizes the Structure of Multi-Helix Loops in 16S and 23S Ribosomal RNAs. *J. Mol. Biol.* **1998**, *283*, 571−583.
(207) Calkins, E. R.; Zakrevsky, P.; Keleshian, V. L.; Aguilar, E. G.; Geary, C.; Jaeger, L. Deducing Putative Ancestral Forms of GNRA/Receptor Interactions from the Ribosome. *Nucleic Acids Res.* **2019**, *47*, 480−494.
(208) Petrov, A. S.; Bernier, C. R.; Gulen, B.; Waterbury, C. C.; Hershkovits, E.; Hsiao, C.; Harvey, S. C.; Hud, N. V.; Fox, G. E.; Wartell, R. M.; Williams, L. D. Secondary Structures of rRNAs from All Three Domains of Life. *PLoS One* **2014**, *9*, No. e88222.
(209) Petrov, A. S.; Bernier, C. R.; Hershkovits, E.; Xue, Y.; Waterbury, C. C.; Hsiao, C.; Stepanov, V. G.; Gaucher, E. A.; Grover, M. A.; Harvey, S. C.; Hud, N. V.; Wartell, R. M.; Fox, G. E.; Williams, L. D. Secondary Structure and Domain Architecture of the 23S and 5S rRNAs. *Nucleic Acids Res.* **2013**, *41*, 7522−7535.
(210) Schluenzen, F.; Tocilj, A.; Zarivach, R.; Harms, J.; Gluehmann, M.; Janell, D.; Bashan, A.; Bartels, H.; Agmon, I.; Franceschi, F.; Yonath, A. Structure of Functionally Activated Small Ribosomal Subunit at 3.3 Å Resolution. *Cell* **2000**, *102*, 615−623.
(211) Harms, J.; Schluenzen, F.; Zarivach, R.; Bashan, A.; Gat, S.; Agmon, I.; Bartels, H.; Franceschi, F.; Yonath, A. High Resolution Structure of the Large Ribosomal Subunit from a Mesophilic Eubacterium. *Cell* **2001**, *107*, 679−688.
(212) Hashem, Y.; des Georges, A.; Fu, J.; Buss, S. N.; Jossinet, F.; Jobe, A.; Zhang, Q.; Liao, H. Y.; Grassucci, R. A.; Bajaj, C.; Westhof, E.; Madison-Antenucci, S.; Frank, J. High-Resolution Cryo-Electron Microscopy Structure of the *Trypanosoma brucei* Ribosome. *Nature* **2013**, *494*, 385−389.
(213) Noeske, J.; Wasserman, M. R.; Terry, D. S.; Altman, R. B.; Blanchard, S. C.; Cate, J. H. High-Resolution Structure of the *Escherichia coli* Ribosome. *Nat. Struct. Mol. Biol.* **2015**, *22*, 336.
(214) Armache, J.-P.; Anger, A. M.; Marquez, V.; Franckenberg, S.; Frohlich, T.; Villa, E.; Berninghausen, O.; Thomm, M.; Arnold, G. J.; Beckmann, R.; Wilson, D. N. Promiscuous Behaviour of Archaeal Ribosomal Proteins: Implications for Eukaryotic Ribosome Evolution. *Nucleic Acids Res.* **2013**, *41*, 1284−1293.
(215) Voorhees, R. M.; Fernández, I. S.; Scheres, S. H.; Hegde, R. S. Structure of the Mammalian Ribosome-Sec61 Complex to 3.4 Å Resolution. *Cell* **2014**, *157*, 1632−1643.
(216) Rabl, J.; Leibundgut, M.; Ataide, S. F.; Haag, A.; Ban, N. Crystal Structure of the Eukaryotic 40S Ribosomal Subunit in Complex with Initiation Factor 1. *Science* **2011**, *331*, 730−736.
(217) Jobe, A.; Liu, Z.; Gutierrez-Vargas, C.; Frank, J. New Insights into Ribosome Structure and Function. *Cold Spring Harbor Perspect. Biol.* **2019**, *11*, No. a032615.
(218) Bernier, C. R.; Petrov, A. S.; Waterbury, C. C.; Jett, J.; Li, F.; Freil, L. E.; Xiong, X.; Wang, L.; Migliozzi, B. L. R.; Hershkovits, E.; Xue, Y.; Hsiao, C.; Bowman, J. C.; Harvey, S. C.; Grover, M. A.; Wartell, Z. J.; Williams, L. D. Ribovision: Visualization and Analysis of Ribosomes. *Faraday Discuss.* **2014**, *169*, 195−207.
(219) Schweingruber, F. H.: *Tree Rings: Basics and Applications of Dendrochronology*; Springer Science & Business Media, 2012.
(220) Gould, S. J.: *Time's Arrow, Time's Cycle: Myth and Metaphor in the Discovery of Geological Time*; Harvard University Press: Cambridge, MA, 1987.
(221) Schopf, J. M. Modes of Fossil Preservation. *Rev. Palaeobot. Palynol.* **1975**, *20*, 27−53.
(222) Glass, J. B. Microbes That Meddle with Metals. *Microbe Mag* **2015**, *10*, 197−202.
(223) Stubbe, J.; Ge, J.; Yee, C. S. The Evolution of Ribonucleotide Reduction Revisited. *Trends Biochem. Sci.* **2001**, *26*, 93−99.
(224) Torrents, E. Ribonucleotide Reductases: Essential Enzymes for Bacterial Life. *Front. Cell. Infect. Microbiol.* **2014**, *4*, 52.
(225) Wolfe-Simon, F.; Grzebyk, D.; Schofield, O.; Falkowski, P. G. The Role and Evolution of Superoxide Dismutases in Algae. *J. Phycol.* **2005**, *41*, 453−465.
(226) Culotta, V. C.; Yang, M.; O'Halloran, T. V. Activation of Superoxide Dismutases: Putting the Metal to the Pedal. *Biochim. Biophys. Acta, Mol. Cell Res.* **2006**, *1763*, 747−758.
(227) Okafor, C. D.; Lanier, K. A.; Petrov, A. S.; Athavale, S. S.; Bowman, J. C.; Hud, N. V.; Williams, L. D. Iron Mediates Catalysis of Nucleic Acid Processing Enzymes: Support for Fe(II) as a Cofactor before the Great Oxidation Event. *Nucleic Acids Res.* **2017**, *45*, 3634−3642.
(228) Rich, A.: The Possible Participation of Esters as Well as Amides in Prebiotic Polymers. In *Chemical Evolution and the Origin of Life*; Buvet, R., Ponnamperuma, C., Eds.; North-Holland Publishing Company: Amsterdam, 1971.
(229) Forsythe, J. G.; Yu, S. S.; Mamajanov, I.; Grover, M. A.; Krishnamurthy, R.; Fernandez, F. M.; Hud, N. V. Ester-Mediated Amide Bond Formation Driven by Wet-Dry Cycles: A Possible Path to Polypeptides on the Prebiotic Earth. *Angew. Chem., Int. Ed.* **2015**, *54*, 9871−9875.
(230) Holland, H. D.: *The Chemical Evolution of the Atmosphere and Oceans*; Princeton University Press, 1984.
(231) Forsythe, J. G.; Yu, S. S.; Mamajanov, I.; Grover, M. A.; Krishnamurthy, R.; Fernández, F. M.; Hud, N. V. Ester-Mediated Amide Bond Formation Driven by Wet-Dry Cycles: A Possible Path to Polypeptides on the Prebiotic Earth. *Angew. Chem., Int. Ed.* **2015**, *54*, 9871−9875.
(232) Lupas, A.; Koretke, K.: Evolution of Protein Folds. In *Computational Structural Biology: Methods and Applications*; Schwede, T., Peitsch, M. C., Eds.; World Scientific: Singapore, 2008; pp 131−151.

https://dx.doi.org/10.1021/acs.chemrev.9b00742
Chem. Rev. XXXX, XXX, XXX−XXX

(233) Bokov, K.; Steinberg, S. V. A Hierarchical Model for Evolution of 23S Ribosomal RNA. *Nature* **2009**, *457*, 977−980.
(234) Davidovich, C.; Belousoff, M.; Bashan, A.; Yonath, A. The Evolving Ribosome: From Non-Coded Peptide Bond Formation to Sophisticated Translation Machinery. *Res. Microbiol.* **2009**, *160*, 487−492.
(235) Zhang, B.; Cech, T. R. Peptidyl-Transferase Ribozymes: Trans Reactions, Structural Characterization and Ribosomal RNA-Like Features. *Chem. Biol.* **1998**, *5*, 539−553.
(236) Zhang, B.; Cech, T. R. Peptide Bond Formation by in Vitro Selected Ribozymes. *Nature* **1997**, *390*, 96.
(237) Polacek, N.; Mankin, A. S. The Ribosomal Peptidyl Transferase Center: Structure, Function, Evolution, Inhibition. *Crit. Rev. Biochem. Mol. Biol.* **2005**, *40*, 285−311.
(238) Beringer, M.; Rodnina, M. V. The Ribosomal Peptidyl Transferase. *Mol. Cell* **2007**, *26*, 311−321.
(239) Smith, T. F.; Lee, J. C.; Gutell, R. R.; Hartman, H. The Origin and Evolution of the Ribosome. *Biol. Direct* **2008**, *3*, 16.
(240) Noller, H. F. Evolution of Protein Synthesis from an RNA World. *Cold Spring Harbor Perspect. Biol.* **2012**, *4*, No. a003681.
(241) Jencks, W. P.; Gilchrist, M. Nonlinear Structure-Reactivity Correlations. The Reactivity of Nucleophilic Reagents toward Esters. *J. Am. Chem. Soc.* **1968**, *90*, 2622−2637.
(242) Marahiel, M. A. Working Outside the Protein-Synthesis Rules: Insights into Non-Ribosomal Peptide Synthesis. *J. Pept. Sci.* **2009**, *15*, 799−807.
(243) Siklos, M.; BenAissa, M.; Thatcher, G. R. Cysteine Proteases as Therapeutic Targets: Does Selectivity Matter? A Systematic Review of Calpain and Cathepsin Inhibitors. *Acta Pharm. Sin. B* **2015**, *5*, 506−519.
(244) Hedstrom, L. Serine Protease Mechanism and Specificity. *Chem. Rev.* **2002**, *102*, 4501−4524.
(245) Frenkel-Pinter, M.; Haynes, J. W.; C, M.; Petrov, A. S.; Burcar, B. T.; Krishnamurthy, R.; Hud, N. V.; Leman, L. J.; Williams, L. D. Selective Incorporation of Proteinaceous over Nonproteinaceous Cationic Amino Acids in Model Prebiotic Oligomerization Reactions. *Proc. Natl. Acad. Sci. U. S. A.* **2019**, *116*, 16338−16346.
(246) Frenkel-Pinter, M.; Haynes, J. W.; Mohyeldinm, A. M.; C, M.; Sargon, A. B.; Petrov, A. S.; Krishnamurthy, R.; Hud, N. V.; Williams, L. D.; Leman, L. J. Mutually Beneficial Interactions between Proto-Peptides and RNA. 2019, submitted for publication.
(247) Doran, D.; Abul-Haija, Y.; Cronin, L. Emergence of Function and Selection from Recursively Programmed Polymerisation Reactions in Mineral Environments. *Angew. Chem., Int. Ed.* **2019**, *58*, 11253−11256.
(248) Forsythe, J. G.; Petrov, A. S.; Millar, W. C.; Yu, S.-S.; Krishnamurthy, R.; Grover, M. A.; Hud, N. V.; Fernández, F. M. Surveying the Sequence Diversity of Model Prebiotic Peptides by Mass Spectrometry. *Proc. Natl. Acad. Sci. U. S. A.* **2017**, *114*, E7652.
(249) Mamajanov, I.; MacDonald, P. J.; Ying, J.; Duncanson, D. M.; Dowdy, G. R.; Walker, C. A.; Engelhart, A. E.; Fernandez, F. M.; Grover, M. A.; Hud, N. V.; Schork, F. J. Ester Formation and Hydrolysis During Wet-Dry Cycles: Generation of Far-from-Equilibrium Polymers in a Model Prebiotic Reaction. *Macromolecules* **2014**, *47*, 1334−1343.
(250) Sawai, H.; Lohrmann, R.; Orgel, L. Prebiotic Peptide-Formation in the Solid State. *J. Mol. Evol.* **1975**, *6*, 165−184.
(251) Ross, D.; Deamer, D. Dry/Wet Cycling and the Thermodynamics and Kinetics of Prebiotic Polymer Synthesis. *Life* **2016**, *6*, 28.
(252) Sievers, A.; Beringer, M.; Rodnina, M. V.; Wolfenden, R. The Ribosome as an Entropy Trap. *Proc. Natl. Acad. Sci. U. S. A.* **2004**, *101*, 7897−7901.
(253) Bashan, A.; Agmon, I.; Zarivach, R.; Schluenzen, F.; Harms, J.; Berisio, R.; Bartels, H.; Franceschi, F.; Auerbach, T.; Hansen, H. A. S.; Kossoy, E.; Kessler, M.; Yonath, A. Structural Basis of the Ribosomal Machinery for Peptide Bond Formation, Translocation, and Nascent Chain Progression. *Mol. Cell* **2003**, *11*, 91−102.
(254) Bieling, P.; Beringer, M.; Adio, S.; Rodnina, M. V. Peptide Bond Formation Does Not Involve Acid-Base Catalysis by Ribosomal Residues. *Nat. Struct. Mol. Biol.* **2006**, *13*, 423.
(255) Malkin, L. I.; Rich, A. Partial Resistance of Nascent Polypeptide Chains to Proteolytic Digestion Due to Ribosomal Shielding. *J. Mol. Biol.* **1967**, *26*, 329−346.
(256) Blobel, G.; Sabatini, D. Controlled Proteolysis of Nascent Polypeptides in Rat Liver Cell Fractions: I. Location of the Polypeptides within Ribosomes. *J. Cell Biol.* **1970**, *45*, 130−145.
(257) Bernabeu, C.; Lake, J. A. Nascent Polypeptide Chains Emerge from the Exit Domain of the Large Ribosomal Subunit: Immune Mapping of the Nascent Chain. *Proc. Natl. Acad. Sci. U. S. A.* **1982**, *79*, 3111−3115.
(258) Yonath, A.; Leonard, K.; Wittmann, H. A Tunnel in the Large Ribosomal Subunit Revealed by Three-Dimensional Image Reconstruction. *Science* **1987**, *236*, 813−816.
(259) Fedyukina, D. V.; Cavagnero, S. Protein Folding at the Exit Tunnel. *Annu. Rev. Biophys.* **2011**, *40*, 337−359.
(260) Fulle, S.; Gohlke, H. Statics of the Ribosomal Exit Tunnel: Implications for Cotranslational Peptide Folding, Elongation Regulation, and Antibiotics Binding. *J. Mol. Biol.* **2009**, *387*, 502−517.
(261) Voss, N.; Gerstein, M.; Steitz, T.; Moore, P. The Geometry of the Ribosomal Polypeptide Exit Tunnel. *J. Mol. Biol.* **2006**, *360*, 893−906.
(262) Francklyn, C.; Schimmel, P. Aminoacylation of RNA Minihelices with Alanine. *Nature* **1989**, *337*, 478−481.
(263) Schimmel, P.; de Pouplana, L. R. Transfer RNA: From Minihelix to Genetic Code. *Cell* **1995**, *81*, 983−986.
(264) Smith, T. F.; Hartman, H. The Evolution of Class II Aminoacyl-tRNA Synthetases and the First Code. *FEBS Lett.* **2015**, *589*, 3499−3507.
(265) Hartman, H.; Smith, T. F. GTPases and the Origin of the Ribosome. *Biol. Direct* **2010**, *5*, 36.
(266) Runnels, C. M.; Lanier, K. A.; Williams, J. K.; Bowman, J. C.; Petrov, A. S.; Hud, N. V.; Williams, L. D. Folding, Assembly, and Persistence: The Essential Nature and Origins of Biopolymers. *J. Mol. Evol.* **2018**, *86*, 598−610.
(267) Hud, N. V.; Cafferty, B. J.; Krishnamurthy, R.; Williams, L. D. The Origin of RNA and "My Grandfather's Axe. *Chem. Biol.* **2013**, *20*, 466−474.
(268) Hud, N. V.; Anet, F. A. Intercalation-Mediated Synthesis and Replication: A New Approach to the Origin of Life. *J. Theor. Biol.* **2000**, *205*, 543−562.
(269) Tagami, S.; Attwater, J.; Holliger, P. Simple Peptides Derived from the Ribosomal Core Potentiate RNA Polymerase Ribozyme Function. *Nat. Chem.* **2017**, *9*, 325.
(270) Gould, S. J.; Vrba, E. S. Exaptation—a Missing Term in the Science of Form. *Paleobiology* **1982**, *8*, 4−15.
(271) Schneider, I.; Shubin, N. H. The Origin of the Tetrapod Limb: From Expeditions to Enhancers. *Trends Genet.* **2013**, *29*, 419−426.
(272) Anthwal, N.; Joshi, L.; Tucker, A. S. Evolution of the Mammalian Middle Ear and Jaw: Adaptations and Novel Structures. *J. Anat.* **2013**, *222*, 147−160.
(273) Prum, R. O.; Torres, R.; Williamson, S.; Dyck, J. Two-Dimensional Fourier Analysis of the Spongy Medullary Keratin of Structurally Coloured Feather Barbs. *Proc. R. Soc. London, Ser. B* **1999**, *266*, 13−22.
(274) Dhouailly, D.; Godefroit, P.; Martin, T.; Nonchev, S.; Caraguel, F.; Oftedal, O. Getting to the Root of Scales, Feather and Hair: As Deep as Odontodes? *Exp. Dermatol.* **2019**, *28*, 503−508.
(275) Cleaves, H. J.; Butch, C.; Burger, P. B.; Goodwin, J.; Meringer, M. One among Millions: The Chemical Space of Nucleic Acid-Like Molecules. *J. Chem. Inf. Model.* **2019**, *59*, 4266.
(276) Cleaves, H. J.; Meringer, M.; Goodwin, J. Views of RNA: Is RNA Unique in Its Chemical Isomer Space? *Astrobiology* **2015**, *15*, 538−558.
(277) Cleaves, H. J. The Origin of the Biologically Coded Amino Acids. *J. Theor. Biol.* **2010**, *263*, 490−498.

https://dx.doi.org/10.1021/acs.chemrev.9b00742
Chem. Rev. XXXX, XXX, XXX−XXX

(278) Meringer, M.; Cleaves, H. J. Exploring Astrobiology Using in Silico Molecular Structure Generation. *Philos. Trans. R. Soc., A* **2017**, *375*, 20160344.
(279) Keefe, A. D.; Szostak, J. W. Functional Proteins from a Random-Sequence Library. *Nature* **2001**, *410*, 715.
(280) Karas, C.; Hecht, M. A Strategy for Combinatorial Cavity Design in De Novo Proteins. *Life* **2020**, *10*, 9.
(281) Hartman, H.; Smith, T. The Evolution of the Ribosome and the Genetic Code. *Life* **2014**, *4*, 227−249.
(282) Cabrita, L. D.; Dobson, C. M.; Christodoulou, J. Protein Folding on the Ribosome. *Curr. Opin. Struct. Biol.* **2010**, *20*, 33−45.
(283) Fox, G. E.; Tran, Q.; Yonath, A. An Exit Cavity Was Crucial to the Polymerase Activity of the Early Ribosome. *Astrobiology* **2012**, *12*, 57−60.
(284) Orgel, L. E. The Origin of Polynucleotide-Directed Protein Synthesis. *J. Mol. Evol.* **1989**, *29*, 465−474.
(285) Dunker, A. K.; Brown, C. J.; Lawson, J. D.; Iakoucheva, L. M.; Obradović, Z. Intrinsic Disorder and Protein Function. *Biochemistry* **2002**, *41*, 6573−6582.
(286) Baker, E. G.; Bartlett, G. J.; Porter Goff, K. L.; Woolfson, D. N. Miniprotein Design: Past, Present, and Prospects. *Acc. Chem. Res.* **2017**, *50*, 2085−2092.
(287) Bhushan, S.; Gartmann, M.; Halic, M.; Armache, J.-P.; Jarasch, A.; Mielke, T.; Berninghausen, O.; Wilson, D. N.; Beckmann, R. A-Helical Nascent Polypeptide Chains Visualized within Distinct Regions of the Ribosomal Exit Tunnel. *Nat. Struct. Mol. Biol.* **2010**, *17*, 313.
(288) Ziv, G.; Haran, G.; Thirumalai, D. Ribosome Exit Tunnel Can Entropically Stabilize α-Helices. *Proc. Natl. Acad. Sci. U. S. A.* **2005**, *102*, 18956−18961.
(289) Woolhead, C. A.; McCormick, P. J.; Johnson, A. E. Nascent Membrane and Secretory Proteins Differ in Fret-Detected Folding Far inside the Ribosome and in Their Exposure to Ribosomal Proteins. *Cell* **2004**, *116*, 725−736.
(290) Nissley, D. A.; O'Brien, E. P. Structural Origins of Fret-Observed Nascent Chain Compaction on the Ribosome. *J. Phys. Chem. B* **2018**, *122*, 9927−9937.
(291) Liutkute, M.; Samatova, E.; Rodnina, M. V. Cotranslational Folding of Proteins on the Ribosome. *Biomolecules* **2020**, *10*, 97.
(292) Mazor, Y.; Gilead, S.; Benhar, I.; Gazit, E. Identification and Characterization of a Novel Molecular-Recognition and Self-Assembly Domain within the Islet Amyloid Polypeptide. *J. Mol. Biol.* **2002**, *322*, 1013−1024.
(293) Reches, M.; Porat, Y.; Gazit, E. Amyloid Fibril Formation by Pentapeptide and Tetrapeptide Fragments of Human Calcitonin. *J. Biol. Chem.* **2002**, *277*, 35475−35480.
(294) Frederix, P. W.; Scott, G. G.; Abul-Haija, Y. M.; Kalafatovic, D.; Pappas, C. G.; Javid, N.; Hunt, N. T.; Ulijn, R. V.; Tuttle, T. Exploring the Sequence Space for (Tri-) Peptide Self-Assembly to Design and Discover New Hydrogels. *Nat. Chem.* **2015**, *7*, 30.
(295) Reches, M.; Gazit, E. Casting Metal Nanowires within Discrete Self-Assembled Peptide Nanotubes. *Science* **2003**, *300*, 625−627.
(296) Reches, M.; Gazit, E. Formation of Closed-Cage Nanostructures by Self-Assembly of Aromatic Dipeptides. *Nano Lett.* **2004**, *4*, 581−585.
(297) Reches, M.; Gazit, E. Designed Aromatic Homo-Dipeptides: Formation of Ordered Nanostructures and Potential Nanotechnological Applications. *Phys. Biol.* **2006**, *3*, S10.
(298) Xiong, Q.; Jiang, Y.; Cai, X.; Yang, F.; Li, Z.; Han, W. Conformation Dependence of Diphenylalanine Self-Assembly Structures and Dynamics: Insights from Hybrid-Resolution Simulations. *ACS Nano* **2019**, *13*, 4455−4468.
(299) Counterman, A. E.; Clemmer, D. E. Gas Phase Polyalanine: Assessment of I' I+ 3 and I' I+ 4 Helical Turns in [Ala N+ 4h] 4+(N= 29- 49) Ion. *J. Phys. Chem. B* **2002**, *106*, 12045−12051.
(300) Rose, G. D.; Fleming, P. J.; Banavar, J. R.; Maritan, A. A Backbone-Based Theory of Protein Folding. *Proc. Natl. Acad. Sci. U. S. A.* **2006**, *103*, 16623−16633.
(301) Chiti, F.; Webster, P.; Taddei, N.; Clark, A.; Stefani, M.; Ramponi, G.; Dobson, C. M. Designing Conditions for in Vitro Formation of Amyloid Protofilaments and Fibrils. *Proc. Natl. Acad. Sci. U. S. A.* **1999**, *96*, 3590−3594.
(302) Knowles, T. P.; Vendruscolo, M.; Dobson, C. M. The Amyloid State and Its Association with Protein Misfolding Diseases. *Nat. Rev. Mol. Cell Biol.* **2014**, *15*, 384−396.
(303) Diaz-Villanueva, J. F.; Diaz-Molina, R.; Garcia-Gonzalez, V. Protein Folding and Mechanisms of Proteostasis. *Int. J. Mol. Sci.* **2015**, *16*, 17193−17230.
(304) Ma, J.; Wang, F. Prion Disease and the 'Protein-Only Hypothesis'. *Essays Biochem.* **2014**, *56*, 181−191.
(305) Nilsson, O. B.; Hedman, R.; Marino, J.; Wickles, S.; Bischoff, L.; Johansson, M.; Muller-Lucks, A.; Trovato, F.; Puglisi, J. D.; O'Brien, E. P.; Beckmann, R.; von Heijne, G. Cotranslational Protein Folding inside the Ribosome Exit Tunnel. *Cell Rep.* **2015**, *12*, 1533−1540.
(306) Kosolapov, A.; Deutsch, C. Tertiary Interactions within the Ribosomal Exit Tunnel. *Nat. Struct. Mol. Biol.* **2009**, *16*, 405.
(307) Dao Duc, K.; Batra, S. S.; Bhattacharya, N.; Cate, J. H.; Song, Y. S. Differences in the Path to Exit the Ribosome across the Three Domains of Life. *Nucleic Acids Res.* **2019**, *47*, 4198−4210.
(308) Docter, B. E.; Horowitz, S.; Gray, M. J.; Jakob, U.; Bardwell, J. C. Do Nucleic Acids Moonlight as Molecular Chaperones? *Nucleic Acids Res.* **2016**, *44*, 4835−4845.
(309) Patel, A.; Malinovska, L.; Saha, S.; Wang, J.; Alberti, S.; Krishnan, Y.; Hyman, A. A. ATP as a Biological Hydrotrope. *Science* **2017**, *356*, 753−756.
(310) Brack, A.; Orgel, L. E. B Structures of Alternating Polypeptides and Their Possible Prebiotic Significance. *Nature* **1975**, *256*, 383.
(311) Aharoni, A.; Gaidukov, L.; Khersonsky, O.; Gould, S. M.; Roodveldt, C.; Tawfik, D. S. The'evolvability'of Promiscuous Protein Functions. *Nat. Genet.* **2005**, *37*, 73.
(312) Levinthal, C. Are There Pathways for Protein Folding? *J. Chim. Phys. Phys.-Chim. Biol.* **1968**, *65*, 44−45.
(313) Bryngelson, J. D.; Onuchic, J. N.; Socci, N. D.; Wolynes, P. G. Funnels, Pathways, and the Energy Landscape of Protein Folding: A Synthesis. *Proteins: Struct., Funct., Genet.* **1995**, *21*, 167−195.
(314) Dill, K. A.; Bromberg, S.; Yue, K.; Chan, H. S.; Ftebig, K. M.; Yee, D. P.; Thomas, P. D. Principles of Protein Folding—a Perspective from Simple Exact Models. *Protein Sci.* **1995**, *4*, 561−602.
(315) Wolynes, P. G. Evolution, Energy Landscapes and the Paradoxes of Protein Folding. *Biochimie* **2015**, *119*, 218−230.
(316) Crick, F. H. The Origin of the Genetic Code. *J. Mol. Biol.* **1968**, *38*, 367−379.
(317) Ikehara, K.; Omori, Y.; Arai, R.; Hirose, A. A Novel Theory on the Origin of the Genetic Code: A GNC-SNS Hypothesis. *J. Mol. Evol.* **2002**, *54*, 530−538.
(318) Trifonov, E. N. The Triplet Code from First Principles. *J. Biomol. Struct. Dyn.* **2004**, *22*, 1−11.
(319) Trifonov, E. N. The Origin of the Genetic Code and of the Earliest Oligopeptides. *Res. Microbiol.* **2009**, *160*, 481−486.
(320) Wong, J. T.-F. A Co-Evolution Theory of the Genetic Code. *Proc. Natl. Acad. Sci. U. S. A.* **1975**, *72*, 1909.
(321) Wolf, Y. I.; Koonin, E. V. On the Origin of the Translation System and the Genetic Code in the RNA World by Means of Natural Selection, Exaptation, and Subfunctionalization. *Biol. Direct* **2007**, *2*, 14.
(322) Freeland, S. J.; Hurst, L. D. The Genetic Code Is One in a Million. *J. Mol. Evol.* **1998**, *47*, 238−248.
(323) Ilardo, M.; Meringer, M.; Freeland, S.; Rasulev, B.; Cleaves, H. J., II Extraordinarily Adaptive Properties of the Genetically Encoded Amino Acids. *Sci. Rep.* **2015**, *5*, 9414.
(324) Meringer, M.; Cleaves, H. J.; Freeland, S. J. Beyond Terrestrial Biology: Charting the Chemical Universe of α-Amino Acid Structures. *J. Chem. Inf. Model.* **2013**, *53*, 2851−2862.
(325) Cannone, J. J.; Subramanian, S.; Schnare, M. N.; Collett, J. R.; D'Souza, L. M.; Du, Y.; Feng, B.; Lin, N.; Madabusi, L. V.; Muller, K.

https://dx.doi.org/10.1021/acs.chemrev.9b00742
Chem. Rev. XXXX, XXX, XXX−XXX

M.; Pande, N.; Shang, Z.; Yu, N.; Gutell, R. R. The Comparative RNA Web (CRW) Site: An Online Database of Comparative Sequence and Structure Information for Ribosomal, Intron, and Other RNAs. *BMC Bioinf.* **2002**, *3*, 2.

(326) Doris, S. M.; Smith, D. R.; Beamesderfer, J. N.; Raphael, B. J.; Nathanson, J. A.; Gerbi, S. A. Universal and Domain-Specific Sequences in 23S-28S Ribosomal RNA Identified by Computational Phylogenetics. *RNA* **2015**, *21*, 1719−1730.

(327) Kooi, E. A.; Rutgers, C. A.; Mulder, A.; Van't Riet, J.; Venema, J.; Raue, H. A. The Phylogenetically Conserved Doublet Tertiary Interaction in Domain III of the Large Subunit rRNA Is Crucial for Ribosomal Protein Binding. *Proc. Natl. Acad. Sci. U. S. A.* **1993**, *90*, 213.

(328) Agmon, I. The Dimeric Proto-Ribosome: Structural Details and Possible Implications on the Origin of Life. *Int. J. Mol. Sci.* **2009**, *10*, 2921−2934.

(329) Root-Bernstein, M.; Root-Bernstein, R. The Ribosome as a Missing Link in the Evolution of Life. *J. Theor. Biol.* **2015**, *367*, 130−158.

(330) Root-Bernstein, R.; Root-Bernstein, M. The Ribosome as a Missing Link in Prebiotic Evolution III: Over-Representation of tRNA- and rRNA-Like Sequences and Plieofunctionality of Ribosome-Related Molecules Argues for the Evolution of Primitive Genomes from Ribosomal RNA Modules. *Int. J. Mol. Sci.* **2019**, *20*, 140.

(331) Hartman, H.; Smith, T. F. Origin of the Genetic Code is Found at the Transition between a Thioester World of Peptides and the Phosphoester World of Polynucleotides. *Life* **2019**, *9*, 69.

(332) Fournier, G. P.; Neumann, J. E.; Gogarten, J. P. Inferring the Ancient History of the Translation Machinery and Genetic Code Via Recapitulation of Ribosomal Subunit Assembly Orders. *PLoS One* **2010**, *5*, No. e9437.

(333) Vishwanath, P.; Favaretto, P.; Hartman, H.; Mohr, S. C.; Smith, T. F. Ribosomal Protein-Sequence Block Structure Suggests Complex Prokaryotic Evolution with Implications for the Origin of Eukaryotes. *Mol. Phylogenet. Evol.* **2004**, *33*, 615−625.

(334) Petrov, A. S.; Williams, L. D. The Ancient Heart of the Ribosomal Large Subunit: A Response to Caetano-Anolles. *J. Mol. Evol.* **2015**, *80*, 166−170.

(335) Harish, A.; Caetano-Anollés, G. Ribosomal History Reveals Origins of Modern Protein Synthesis. *PLoS One* **2012**, *7*, No. e32776.

(336) Young, D. D.; Schultz, P. G. Playing with the Molecules of Life. *ACS Chem. Biol.* **2018**, *13*, 854−870.

(337) Liu, Y.; Kim, D. S.; Jewett, M. C Repurposing Ribosomes for Synthetic Biology. *Curr. Opin. Chem. Biol.* **2017**, *40*, 87−94.

(338) Orelle, C.; Carlson, E. D.; Szal, T.; Florin, T.; Jewett, M. C.; Mankin, A. S. Protein Synthesis by Ribosomes with Tethered Subunits. *Nature* **2015**, *524*, 119.

(339) Kobayashi, T. Strategies to Maintain the Stability of the Ribosomal RNA Gene Repeats. *Genes Genet. Syst.* **2006**, *81*, 155−161.

(340) Gibbons, J. G.; Branco, A. T.; Godinho, S. A.; Yu, S.; Lemos, B. Concerted Copy Number Variation Balances Ribosomal DNA Dosage in Human and Mouse Genomes. *Proc. Natl. Acad. Sci. U. S. A.* **2015**, *112*, 2485−2490.

(341) Dedkova, L. M.; Fahmi, N. E.; Golovine, S. Y.; Hecht, S. M. Enhanced D-Amino Acid Incorporation into Protein by Modified Ribosomes. *J. Am. Chem. Soc.* **2003**, *125*, 6616−6617.

(342) Dedkova, L. M.; Fahmi, N. E.; Golovine, S. Y.; Hecht, S. M. Construction of Modified Ribosomes for Incorporation of α-Amino Acids into Proteins. *Biochemistry* **2006**, *45*, 15541−15551.

(343) Maini, R.; Nguyen, D. T.; Chen, S.; Dedkova, L. M.; Chowdhury, S. R.; Alcala-Torano, R.; Hecht, S. M. Incorporation of B-Amino Acids into Dihydrofolate Reductase by Ribosomes Having Modifications in the Peptidyltransferase Center. *Bioorg. Med. Chem.* **2013**, *21*, 1088−1096.

(344) Maini, R.; Chowdhury, S. R.; Dedkova, L. M.; Roy, B.; Daskalova, S. M.; Paul, R.; Chen, S.; Hecht, S. M. Protein Synthesis with Ribosomes Selected for the Incorporation of β-Amino Acids. *Biochemistry* **2015**, *54*, 3694−3706.

(345) Carlson, E. D.; d'Aquino, A. E.; Kim, D. S.; Fulk, E. M.; Hoang, K.; Szal, T.; Mankin, A. S.; Jewett, M. C. Engineered Ribosomes with Tethered Subunits for Expanding Biological Function. *Nat. Commun.* **2019**, *10*, 3920.

(346) Jewett, M. C.; Fritz, B. R.; Timmerman, L. E.; Church, G. M. In Vitro Integration of Ribosomal RNA Synthesis, Ribosome Assembly, and Translation. *Mol. Syst. Biol.* **2013**, *9*, 678.

(347) Cochella, L.; Green, R. Isolation of Antibiotic Resistance Mutations in the rRNA by Using an in Vitro Selection System. *Proc. Natl. Acad. Sci. U. S. A.* **2004**, *101*, 3786−3791.

(348) Terasaka, N.; Hayashi, G.; Katoh, T.; Suga, H. An Orthogonal Ribosome-tRNA Pair Via Engineering of the Peptidyl Transferase Center. *Nat. Chem. Biol.* **2014**, *10*, 555.

(349) Samelson, A. J.; Jensen, M. K.; Soto, R. A.; Cate, J. H.; Marqusee, S. Quantitative Determination of Ribosome Nascent Chain Stability. *Proc. Natl. Acad. Sci. U. S. A.* **2016**, *113*, 13402−13407.

(350) Zhang, G.; Ignatova, Z. Folding at the Birth of the Nascent Chain: Coordinating Translation with Co-Translational Folding. *Curr. Opin. Struct. Biol.* **2011**, *21*, 25−31.

(351) Kramer, G.; Boehringer, D.; Ban, N.; Bukau, B. The Ribosome as a Platform for Co-Translational Processing, Folding and Targeting of Newly Synthesized Proteins. *Nat. Struct. Mol. Biol.* **2009**, *16*, 589.

https://dx.doi.org/10.1021/acs.chemrev.9b00742
Chem. Rev. XXXX, XXX, XXX−XXX